Aus der Abteilung für Neurochirurgie der Klinik und

Poliklinik für Chirurgie

der Universitätsmedizin Rostock

(Prof. em. Dr. med. Dr. h.c. Jürgen Piek)

Wertigkeit der volumetrischen Tumorsegmentation des Glioblastoms im Kontext klinischer Forschung

Kumulative Habilitationsschrift

zur Erlangung des akademischen Grades

doctor medicinae habilitatus (Dr. med. habil.)

der Universitätsmedizin Rostock

Vorgelegt von Dr. med. Christian Henker

geboren am 05.10.1980 in Dresden

Wohnhaft in Rostock

Rostock, den 15.01.2020

https://doi.org/10.18453/rosdok_id00002825

Gutachter der Habilitationsschrift:

Prof. em. Dr. med. Dr. h.c. Jürgen Piek – Universitätsmedizin Rostock

Prof. Dr. med. Jürgen Meixensberger – Universitätsklinikum Leipzig

Prof. Dr. med. Joachim Oertel – Universitätsklinikum des Saarlandes

Tag der öffentlichen Habilitationsverteidigung:

31.08.2020

Tag der öffentlichen Lehrprobe:

23.10.2020

Inhaltsverzeichnis

Einleitung 4

Prätherapeutische Diagnostik des Glioblastoms 5

Fragestellung, Methodik und Ergebnisse der Originalarbeiten 10

OA 1 - Volumetrische Erfassung des Glioblastoms: Erfahrungen mit verschiedenen Messmethoden und deren Einfluss auf das Überleben. 11

OA 2 – Die volumetrische Tumorsegmentation des Glioblastoms und ihre Wertigkeit als Prädiktor des Überlebens. 14

OA 3 – Korrelation des Ki-67 Index mit den Ergebnissen der Tumor-segmentation des Glioblastoms und die Wertigkeit als prognostischer Marker. 16

OA 4 – Einfluss von zehn verschiedenen Polymorphismen auf die präoperative Volumetrie bei Glioblastompatienten. 18

OA 5 – Assoziation zwischen volumetrisch erfassten Tumorkompartimenten des Glioblastoms, dem Auftreten von Krampfanfällen und protektive Effekte einer Statinmedikation. 20

Diskussion 23

Zusammenfassung und Ausblick 28

Danksagung 30

Curriculum vitae 32

Publikationsliste 34

Literaturverzeichnis 36

Selbständigkeitserklärung 44

Originalarbeiten 45

Einleitung

Das Glioblastom (GBM) gehört zu den bösartigen Hirntumoren des Menschen. Im Vergleich zu anderen Erkrankungen ist die Inzidenz des Glioblastoms mit 3,20 pro Jahr und 100.000 Einwohnern verhältnismäßig gering [1] und gehört *per definitionem* zur Gruppe der Seltenen Erkrankungen [1–3]. Leider stellt es aber auch die häufigste bösartige Tumorentität und insgesamt die dritthäufigste Tumorerkrankung des Zentralnervensystem (ZNS) dar [1]. Trotz multimodaler Therapie liegt das mediane Überleben nach „vollständiger" Resektion, gefolgt von einer kombinierten Radio- und Chemotherapie lediglich bei 18,8 Monaten [4], die 5-Jahres-Überlebensrate liegt bei 5,6 % [5]. Die den Tumor verursachenden Zelle, die sogenannte *cell-of-origin*, ist noch immer nicht eindeutig identifiziert. Jüngste Forschungsergebnisse lassen Stammzellen als ursächlichen Zellpool vermuten [6]; da sich im Vergleich zu anderen Organsystemen hiervon nur sehr wenige im ZNS befinden, würde sich die geringere Tumorinzidenz im Vergleich zu anderen Malignomen erklären.

Die erste histologische Beschreibung von Gliomen erfolgte 1865 durch Rudolf Virchow [7, 8]. Hierauf aufbauend bildeten 1926 Percival Baley und Harvey Cushing die Grundlage der heutig noch verwendeten WHO-Klassifikation: sie benannten erstmalig das GBM als *Spongioblastoma multiforme* in Abgrenzung zu den sonstigen Astrozytomen [9]. Der beschreibende Terminus *multiforme* befindet sich noch heute in der gebräuchlichen Abkürzung des Glioblastoms, GBM. Ursprünglich bezieht sich diese semantische Beschreibung auf das bunte histologische Schnittbild und die atypischen und pleomorphen Zellen des Tumors, ohne sichtbaren morphologischen Bezug zur ursprünglichen Zelllinie. Die umfassendste histopathologische Aufarbeitung des Glioblastoms erfolgte zwischen 1934 und 1941 durch Hans-Joachim Scherer [10]. Dieser beschrieb erstmals den Unterschied zwischen *de novo* entstandenen, also primären GBMs, und den sekundären Glioblastomen, welche sich durch Malignisierung eines bereits bestehenden Astrozytom entwickeln. Darüber hinaus beschrieb Scherer

die pathognomonischen Kennzeichen dieses Tumors im histologischen Schnitt: die atypische Neovaskularisierung des Tumors mit glomerulärem Aussehen und die nekrotischen Areale mit den typischen in Pseudopallisaden ausgerichteten Zellen, welche die Nekrose umgreifend, der sogenannten Scherer-Formation. Die großen Weiterentwicklungen im Bereich der Immunhistochemie und Genetik ließen schließlich eine detailliere Charakterisierung des Tumors zu und der histologisch geprägte Begriffszusatz *multiforme* wurde wieder verlassen; wenngleich er eine Vielzahl von Eigenschaften des Glioblastoms sehr treffend beschreibt.

Nicht nur das Aussehen des Tumors ist vielgestaltig, auch genetisch besitzt der Tumor eine hohe Diversität: zahlreiche Aberration wie Deletionen oder Amplifikation konnten bereits innerhalb des GBMs nachgewiesen werden. Die hauptsächlich betroffenen Signalkaskaden betreffen den Tyrosinkinase-Rezeptor-(RAS)–PI3K – Signalweg, den p53- und den Retinoblastom (RB)-Signalweg [11, 12]. Bemerkenswert ist hierbei auch, dass nicht alle diese Aberration gleichmäßig innerhalb des Tumors nachweisbar sind, vielmehr finden sich Subpopulation von Tumorzellklonen in diesem [13]. Die für die Diagnostik zunächst wichtigste genetische Entdeckung war die einer Mutation im *Isocitratdehydrogenase* (*IDH*) – Gen [14–17]. Diese führt zu einer veränderten Neutralisation von Sauerstoffradikalen und somit zu einer Akkumulation von Onkometaboliten [18]. In Verbindung mit anderen genetischen Aberration findet sich diese Mutation fast ausschließlich bei sekundären Glioblastomen und *low-grade* Astrozytomen [19]. Diese Beobachtungen führten schließlich zur aktuellen Revision der WHO-Klassifikation der Hirntumore aus dem Jahr 2016 [20].

Prätherapeutische Diagnostik des Glioblastoms

Der Goldstandard zum bildmorphologischen Tumornachweis ist die Magnetresonanztomographie (MRT). Der große Vorteil dieser Modalität besteht in der mittlerweile flächendeckenden Verfügbarkeit in Verbindung mit einer hohen Ortsauflösung und sehr guten Darstellung des Hirnparenchyms. Es gibt nur wenige Kontraindikation zur Durchführung einer MRT, ältere Herzschrittmacher beispielweise, so dass fast alle GBM-Patienten initial eine diagnostische MRT

erhalten. Neben der reinen Darstellung des Neurokraniums (*anatomical imaging*), besteht ebenfalls die Möglichkeit eines sogenannten *physiological imaging*: hierunter werden Diffusionwichtungen zur Darstellung beispielsweise von frühen Ischämien oder auch Faserbahndarstellungen/Traktographien auf der Grundlage der Diffusions-Tensor-Bildgebung zusammengefasst. Wenngleich die letztgenannten (jüngeren) Modalitäten wichtige Zusatzinformationen bieten, bleibt die anatomische Bildgebung das Fundament der diagnostischen Bildgebung und ist für die OP-Planung unersetzlich. Typischerweise umfasst die Standardbildgebung des GBMs mit Hilfe der MRT native T1- und T2-gewichtete Bilder, eine *fluid attenuated inversion recovery* (FLAIR) - Sequenz und eine post-Kontrastmittel T1-gewichtete Sequenz (T1+KM) [21]. Das *multiforme* Erscheinungsbild des GBMs in der Histologie lässt sich auch in der MRT nachvollziehen: Typischerweise besteht der Tumor in der T1+KM aus einem girlandenförmig und irregulär geformten Kontrastmittelring. Innerhalb dieses Rings liegt die hypodense und nicht Kontrastmittelaufnehmende Tumornekrose. Umgeben wird die Raumforderung von einem peritumoralen Ödem (PTE), dessen Ausdehnung am Besten in der FLAIR-Sequenz sichtbar wird. Die Kontrastmittelaufnahme des Tumors entsteht durch den Verlust der Integrität der Blut-Hirn-Schranke und somit zur Aufnahme des Kontrastmittels in das Tumorgewebe. Diese drei pathognomonischen Tumorkompartimente können in fast allen GBMs nachvollzogen werden, wobei große interindividuelle Unterschiede in der Größe, Form und auch in der Relation der Kompartimente zueinander bestehen. Die frühere Annahme, man könne das Tumorausmaß in der MRT gut anhand der Ausdehnung des Kontrastmittelanteils umreißen, stellte sich leider als trügerisch heraus. Auch stellt das PTE nicht wie früher angenommen eine Begleitreaktion des Tumors dar, ein vasogenes Ödem; vielmehr handelt es sich um eine aktive Invasionszone des Glioblastoms. Zahlreiche Studien konnten zeigen, dass Tumorzellen über den Kontrastmittelaufnehmenden Anteil hinaus bereits das Gehirn infiltriert haben [22–24] und dass eine Resektion über den Kontrastmittelaufnehmenden Tumoranteil hinaus einen Überlebensvorteil bieten kann [25, 26].

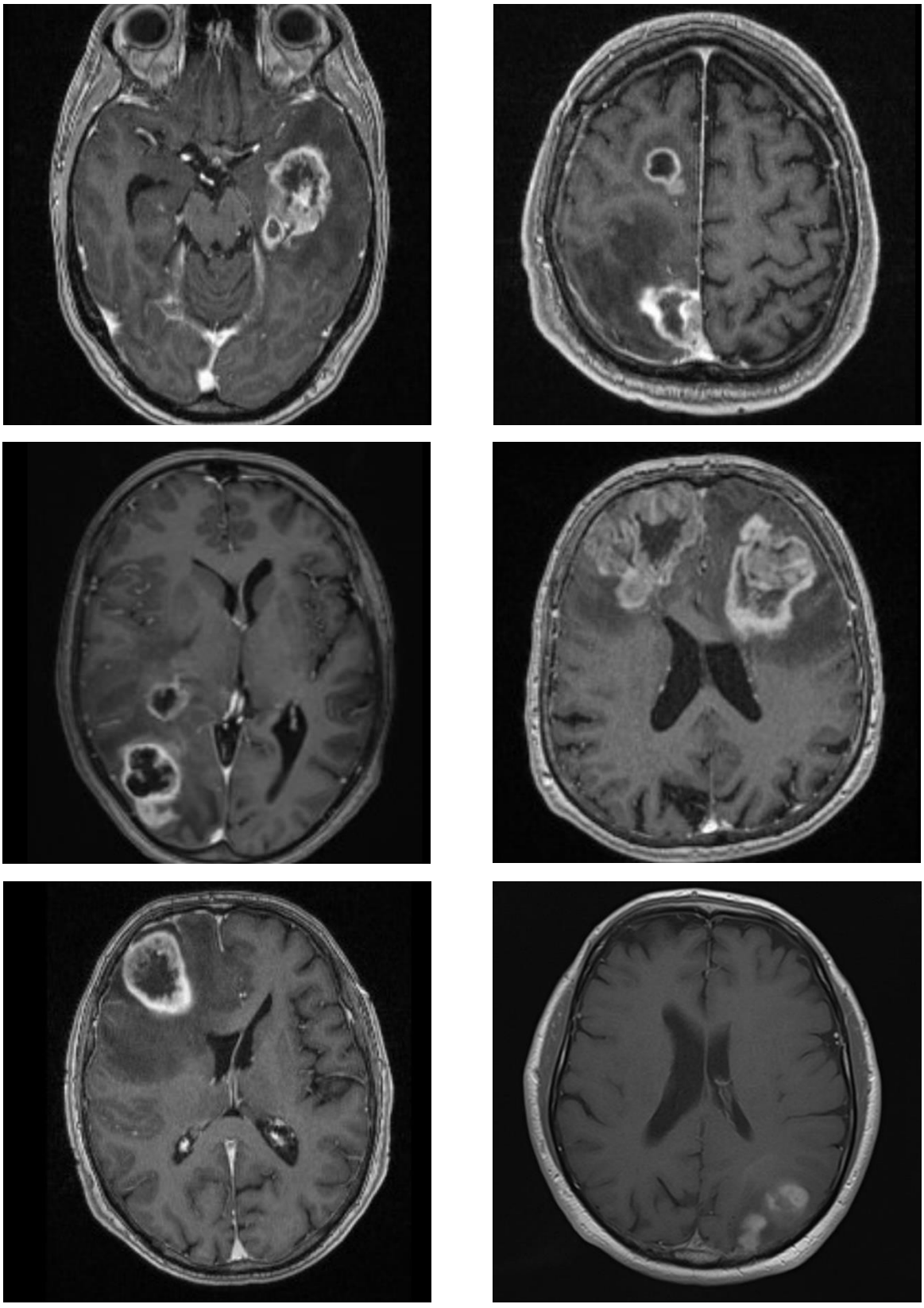

Abbildung 1: Darstellung der Diversität verschiedener Glioblastome in der prätherapeutischen MRT (T1+KM).

Die diffuse und weit ausgedehnte Infiltration des Hirnparenchyms ist eine der Hauptgründe, warum das GBM nicht chirurgisch geheilt werden kann. Dieses Infiltrationsmuster entlang von Faserbahnen, Gefäßen und Neuronen wurde ebenfalls bereits durch Scherer beschrieben (*secondary structure of Scherer*). Des Weiteren bildet der Tumor ein kommunizierendes plastisches Netzwerk innerhalb des infiltrierten Hirns, welches aktiv auf therapeutische Noxen reagieren kann [27, 28]. Diese erstaunliche Fähigkeit erklärt, warum ein Großteil der Tumorrezidive nach einer chirurgischen Resektion im Bereich der Resektionshöhle liegen [29]. Folgerichtig muss das Glioblastom als eine systemische Erkrankung des Gehirns verstanden werden [30]. Des Weiteren besitz das GBM eine Vielzahl an Mechanismen, um der adjuvanten Standardtherapie, bestehend aus Radio- und Chemotherapie mittels Temozolomid, zu widerstehen [31–33]. All diese Fähigkeiten sind jedoch nicht bei jedem GBM in gleichem Maße vorhanden und so multiform der Tumor erscheint, so verschieden sind auch seine klinischen Verläufe und Überlebensraten. Es erscheint entsprechend umso interessanter, einzelne Subgruppen von Glioblastomen bereits prätherapeutisch unterscheiden zu können, um einen tieferen Einblick in das Verhalten des Tumors zu erhalten und nicht zuletzt das Ansprechen auf mögliche Therapieansätze zu prognostizieren. Bereits seit Jahren wird daher beispielsweise versucht, das Glioblastom in molekulare Subgruppen zu unterteilen und die für die jeweilige Gruppe bestmögliche adjuvante Therapie zu finden – die klinische Relevanz dieser Bemühungen bleibt nicht unumstritten, wenngleich die epigenetischen Profile der vier Subgruppen (proneural, neural, klassisch und mesenchymal) klar umrissen sind [34–36]. Erschwerend für diese Klassifikation zeigte sich, dass innerhalb desselben Tumors verschiedene Profile vorliegen können und ein Switch im Behandlungsverlauf zwischen diesen erfolgen kann [37].

Insgesamt existieren nur wenige robuste Biomarker mit prognostischem Wert, klinisch ist das Alter bei Erkrankung und der Karnofsky Performance Score (KPS) als Ausdruck der individuellen Leistungsfähigkeit relevant [38]. Molekularpathologisch ist beim GBM einzig der *MGMT*-Status (O-6-Methylguanine-DNA Methyltransferase) als prädiktiver Marker bezüglich des

Ansprechens auf eine Chemotherapie mit Temozolomid zu nennen [39–41]. Weitere verlässliche Marker zur Einschätzung des individuellen Krankheitsverlaufs und dem möglichen Gesamtüberleben sind daher von großem Interesse, einen entsprechenden radiologischen Marker zur Klassifizierung des GBMs existiert bisher nicht.

In diesem Kontext kommt der prätherapeutischen MRT-Bildgebung ein besonderer Stellenwert zu, da so gut wie alle Patienten eine solche Untersuchung initial erhalten und sie die derzeit exakteste Methode zur Kartierung des Tumors darstellt. Die volumetrische Erfassung des Tumors, seiner einzelnen Kompartimente und die Relation zwischen diesen birgt somit das Potential eines *imaging biomarkers* im Sinne eines eigenständigen prognostischen Faktors und ermöglicht die translationale Verbindung zwischen nicht-invasiver Diagnostik, Klinik und der Integration verschiedenster Grundlagen aus dem Labor.

Fragestellung, Methodik und Ergebnisse der Originalarbeiten

Das Glioblastom hat trotz einer Vielzahl an Bemühungen zur Therapieoptimierung weiterhin eine äußerst schlechte Prognose [4]. Dies liegt zum einen an seiner Wandlungs- und Anpassungsfähigkeit [27, 28]. Andererseits verstehen wir weiterhin viele molekularpathologische Zusammenhänge des Tumors nicht. Ein wissenschaftlich eher vernachlässigter Aspekt im Rahmen der Diagnostik des Glioblastoms birgt hierbei das Potential, ein tieferes Verständnis über die Biologie des Tumors zu erhalten: die volumetrische Auswertung der MRTs der Patienten.

Das Ziel dieser Arbeit ist es daher, anhand der prätherapeutisch durchgeführten MRTs, den Tumor und dessen einzelne Kompartimente besser darzustellen und weitere klinische, pathologische und genetische Daten hiermit zu korrelieren. Grundvoraussetzung hierfür ist allerdings zunächst die Verifizierung einer geeigneten Methode gegenüber anderen Messtechniken (**OA 1**). Insbesondere im Hinblick auf die bisher vorliegenden Forschungsergebnisse anderer Kollegen erfolgte in dieser Arbeit die kritische Auseinandersetzung mit der gewählten Methodik.

In der nachfolgenden Arbeit (**OA 2**) wurde die nun verifizierte Technik der 3D-Volumetrie an einer bizentrischen Patientenkohorte validiert, um den prognostischen Wert der einzelnen prätherapeutisch erhobenen Tumorkompartimente abschätzen zu können. Insbesondere wurde das Augenmerk nicht nur auf die bloßen Werte und damit die Größe der erfassten Tumoranteile gelegt; vielmehr sollte die Relation der Kompartimente zueinander untersucht werden, um weitere Rückschlüsse über das Verhalten des Tumors in Bezug auf die adjuvante Therapie ziehen zu können.

Ein anderer Aspekt dieser Arbeit beschäftigte sich mit der Korrelation der Volumetrie mit einem bereits etablierten histologischen Marker: dem Ki-67 - Index (**OA 3**). Dieser wird routinemäßig bei allen histologischen Untersuchungen von Tumorgeweben erhoben und gibt Auskunft über die Proliferationsrate der

untersuchten Tumorprobe [42]. Ziel dieser Arbeit war es entsprechend, die unterschiedlichen in der histologisch nachgewiesenen Proliferationsraten mit den Daten der Volumetrie zu vergleichen.

Das Glioblastom zeigt in seiner Darstellung in der MRT große interindividuelle Unterschiede. Daher beschäftigten wir uns ebenfalls mit der Frage, ob einzelne *Single Nukleotid Polymorphismen* (SNPs) das Erscheinungsbild des Tumors in der Bildgebung verändern könnten (**OA 4**).

Abschließend untersuchte die letzte Arbeit (**OA 5**) die mögliche Korrelation der volumetrischen mit klinischen Daten, insbesondere im Hinblick auf das Auftreten von Krampfanfällen und deren prognostischen Effekt.

Alle Arbeiten wurden nach Erhalt eines zustimmenden Ethikvotums durchgeführt.

OA 1 - Volumetrische Erfassung des Glioblastoms: Erfahrungen mit verschiedenen Messmethoden und deren Einfluss auf das Überleben.

Henker C, Kriesen T, Glass Ä, Schneider B, Piek J: Volumetric quantification of glioblastoma: experiences with different measurement techniques and impact on survival. *J Neuroonco. 2017;135(2):391-402.*

Fragestellung: Es existiert insgesamt nur wenig Literatur zu einer möglichen Korrelation zwischen den einzelnen Tumorkompartimenten (Tumor, peritumorales Ödem und Nekrose) des GBMs in der MRT und dem Überleben dieser Patienten. Viele Ergebnisse dieser Arbeiten sind widersprüchlich, was vor allem auch an den unterschiedlichen Messmethoden liegen könnte. Daher wollten wir verschiedene Messtechniken miteinander vergleichen und die von uns favorisierte 3D-Volumetrie validieren.

Material und Methoden: In diese Studien wurden 30 Patienten mit einem neu diagnostiziertem GBM prospektiv eingeschlossen. Entsprechend der Einschlusskriterien handelte es sich um primäre GBMs. Alle Patienten wurden initial operiert im Sinne einer *gross-total resection* und erhielten anschließend

einer adjuvante Radiochemotherapie entsprechend des Stupp-Schemas. In der präoperativen MRT mit und ohne Kontrastmittel (T1-, T2- und FLAIR-/TIRM-Wichtung; <7 d vor OP) wurden alle drei Tumorkompartimente mit Hilfe der 3D-Volumetrie erfasst (Tumor, Ödem (PTE), Nekrose) und die hieraus abgeleiteten Ratios errechnet (Nekrose-Tumor Ratio (NTR), Ödem-Tumor Ratio (ETR)). Die Messung erfolgte semi-automatisiert mit Hilfe einer sogenannten *contour expansion* - Technik (SmartBrush, Fa. Brainlab, München, Deutschland). Anschließend erfolgte noch die Vermessung aller Tumorkompartimente entlang ihrer Achsen (X, Y und Z) und eine Abschätzung der Ödemausbildung und Nekroseanteile nach Hammoud [43] zum Vergleich der verschiedenen Messmethoden. Zur Erfassung des residuellen postoperativen Tumoranteils wurden in der postoperative MRT (≤ 48 h nach OP), die verbliebenen Kontrastmittelanteile volumetrisch ermitteln. Die hyperintensen Anteile der Resektionshöhle in der nativen T1-gewichteten MRT wurden hiervon subtrahiert, da sie postoperativen Blutauflagerungen entsprechen und keinem aktiven Tumor. Es wurden nur Patienten eingeschlossen, welche zum Zeitpunkt der initialen MRT keine Steroide einnahmen.

Die statistische Auswertung erfolgte mittels SPSS (IBM, SPSS 22.0, Chicago, USA). Die Überlebensanalyse für kategoriale Prognosefaktoren wurde mittels Cox-Regressionsmodel berechnet, für die volumetrischen Daten per Pearsons-Korrelation und linearer Regression. Zum direkten visuellen Vergleich der verschiedenen Messmethoden wurden Bland-Altman-Plots erstellt, wobei die 3D-Volumetrie als Gold-Standard gesetzt wurde und die Abweichung hiervon aufgetragen wurde. Zum Vergleich der kategorialen Tumorschätzungen und der eindimensionalen Messergebnisse mit der 3D-Volumetrie wurde Cohens κ Koeffizient genutzt. Als Signifikanzniveau wurde $\alpha = 0{,}05$ angenommen.

Ergebnisse: Die demographischen Ergebnisse zeigten das typische Bild einer Patientenpopulation mit Glioblastom, das mediane Alter bei Diagnosestellung betrug 62,5 Jahre, 60% der Patienten waren männlich [38]. Das mediane Überleben betrug 16.2 Monate, ebenfalls passend zu den Ergebnissen anderer Arbeiten [1].

Bezüglich der Volumetrie zeigte sich deutlich, dass die zentrale Nekrose des Tumors und vor allem dessen Relation zur Tumorgröße (NTR) ein valider radiologischer prognostischer Faktor bezüglich des Überlebens der Patienten ist (p = 0,039, bzw. 0,005). Die Tumorgröße und auch die Ausdehnung des peritumoralen Ödems (PTE) zeigten in der linearen Regression keinen Einfluss auf das Überleben.

Der Vergleich unserer Messmethode, der 3D-Volumetrie, mit den artifiziellen Rekonstruktionen geometrischer Figuren anhand von Messungen der Tumorachsen (Würfel, dreiachsiges Ellipsoid, Rotationsellipsoid, Kugel) zeigte eine deutliche Überlegenheit der Volumetrie gegenüber den Rekonstruktionen. Diese Abweichungen, dargestellt anhand von Bland-Altman-Plots, zeigte sich vor allem bei zunehmender Tumorgröße als deutlich ansteigend. Diese zunehmende Divergenz bestätigte sich ebenfalls in der Rekonstruktion der intratumoralen Nekrose (Würfelform). Kategoriale Schätzungen des PTE oder der NTR zeigten nur schwache Übereinstimmungen mit der Volumetrie, gemessen anhand des Cohens κ Koeffizienten (κ = 0,267, bzw. 0,095). Ebenso zeigt die eindimensionale Tumordiametermessung nur eine geringe Übereinstimmung mit den Volumetriewerten (κ = 0,601). Die ausgedehnte Literaturrecherche zeigte sehr divergierende Ergebnisse, sowohl im Bereich von rein rekonstruierten Figuren, als auch semantischer Einschätzung und oder auch volumetrischen Messungen. Hauptursache sind aus unserer Sicht die ungenauen Messmethoden, als auch sehr inhomogene Patientenkollektive mit teilweise fehlender Angabe der adjuvanten Therapien.

Schlussfolgerung: Wir konnten in einer sehr homogenen Patientenkohorte zeigen, dass die 3D-Volumetrie alleinigen Achsmessungen und nachfolgenden Rekonstruktionen in ihrer Genauigkeit deutlich überlegen ist. Des Weiteren zeigt sich die intratumorale Nekrose und insbesondere die NTR als möglicher prognostischer Faktor bezüglich des Überlebens der untersuchten GBM-Patienten.

OA 2 – Die volumetrische Tumorsegmentation des Glioblastoms und ihre Wertigkeit als Prädiktor des Überlebens.

Henker C, Hiepel MC, Kriesen T, Scherer M, Glass Ä, Herold-Mende C, Bendszus M, Langner S, Weber MA, Schneider B, Unterberg A, Piek J: Volumetric assessment of glioblastoma and its predictive value for survival. *Acta Neurochir (Wien). 2019; 161(8):1723-1732.*

Fragestellung: In der existierenden Literatur sind die Ergebnisse zur Wertigkeit von radiologischen prognostischen Faktoren sehr divergierend. Wir untersuchten daher an einer repräsentativen GBM-Kohorte die Daten aus einer Tumorsegmentation auf ihren prognostischen Wert.

Material und Methoden: Im Rahmen einer retrospektiven Datenanalyse wurden 114 Patienten aus zwei neurochirurgischen universitären Abteilungen eingeschlossen, welche an einem primären GBM operiert wurden. Nachfolgend erhielten alle Patienten eine konkomitante Radiochemotherapie entsprechend des Stupp-Schemas. Die Tumorsegmentation erfolgte durch eine semi-automatisierte 3D-Volumertrie, erhoben wurden das Tumorvolumen/Kontrastmittelaufnehmender Anteil (CEV+), die innere Nekrose (CEV-) und das peritumorale Ödem (FLAIR+). Des Weiteren wurden wieder hieraus die beiden Ratios ETR und NTR errechnet (siehe OA1).

Die statistische Auswertung erfolgte mittels SPSS (IBM, SPSS 24.0, Chicago, USA). Der Spearman´s Rangkorrelationskoeffizient (r_s) wurde genutzt, um Korrelationen zwischen den gemessenen Volumina, beziehungsweise den errechneten Ratios, zu ermitteln. Die Überlebensanalyse erfolgte mittels Cox-Regressionsmodel berechnet, sowohl uni-als auch multivariat. Die multivariate Überlebensanalyse wurde für das residuelle Tumorvolumen (RTV) adjustiert, um diesen postoperativen Prognosefaktor zu berücksichtigen. Außerdem wurde eine Einzelanalyse der Daten, welche aus nur einer Abteilung stammten, durchgeführt als Validierungsset. Als Signifikanzniveau wurde $\alpha = 0{,}05$ angenommen.

Ergebnisse: Das mediane Alter der untersuchten Patientenkohorte lag bei 61,9 ± 9,08 Jahren, entspricht also dem typischen Erkrankungsalter dieser Tumorentität.

Des Weiteren wurden mehr männliche als weibliche Patienten eingeschlossen (1,85:1), ebenfalls in Übereinstimmung mit der Tumordominanz bei Männern [1]. Das residuelle Tumorvolumen nach OP (RTV) lag median bei lediglich 0,24 cm^3, das Ausmaß der Resektion (*extent of resection*, EOR) entpsrechend bei median 98,5%. Insgesamt traten die Tumoren in etwa gleich häufig im Bereich der linken als auch der rechten Hemisphäre auf (50% vs. 49,1%), einzig ein Fall betraf beide Hemisphären (0,9%). Häufigster betroffener Hirnlappen war der Temporallappen (41,2%), gefolgt vom Frontallappen (29,8%).

Die Tumorsegmentation spiegelte anhand ihrer volumetrischen Daten das breite Spektrum des GBMs wider mit CEV+-Volumina von 0,604 cm^3 bis hin zu 107 cm^3 (Median CEV+ 20,6 cm^3). Ebenso variierten die gemessenen Nekroseanteile (CEV-) deutlich: von 0 cm^3 bis hin zu 59,5 cm^3 (Median 4,58 cm^3). Ähnliche Ergebnisse zeigte das umgebende Ödem (FLAIR+). Die Ödemratio (ETR) war im Median 2,66, die FLAIR-positive Alteration um den Tumor herum ist somit zumeist fast dreimal so groß wie der Tumor selbst. Die innenliegende Nekrose entsprechend dagegen ungefähr einem Viertel des Tumors (Median NTR 0,259). Die Korrelationsanalyse der Tumorsegmentation zeigte deutlich, dass die größte „Abhängigkeit“ zwischen den einzelnen Volumina zwischen dem CEV+ und dem innen liegenden CEV- bestand (r_s = 0,898, p < 0,001). Diese Korrelation wird eher durch die CEV- als durch den Tumor (CEV+) bestimmt (CEV-/NTR r_s = 0,785 vs. CEV+/NTR r_s = 0,469). Die den Tumor umgebende Invasionszone (FLAIR+) zeigte gegenüber den anderen Volumina eine geringere Korrelation (r_s = 0,691, beziehungsweise r_s = 0,584).

In der univariaten Überlebensanalyse zeigten sich einzig ETR und NTR als signifikante radiologische Prädiktoren für das Überleben (p = 0,016, beziehungsweise p = 0,022). In der nachfolgenden multivariaten Analyse zeigte sich deutlich, dass eine erhöhte NTR (> 0,33) als einziger volumetrischer Faktor einen signifikanten Einfluss auf das Überleben hat (HR 2,63).

Diese Daten konnten im Validierungsset, also der unizentrischen Analyse, nachvollzogen werden.

Schlussfolgerung: Wir konnten anhand unserer bizentrischen Patientenkohorte zeigen, dass der wichtigste präoperative radiologische Prädiktor für das Überleben einzig die NTR ist. Die Nekrose korreliert hierbei deutlich mit der Tumorgröße und in deutlich geringerem Maße mit dem umgebenden FLAIR+-Areal.

OA 3 – Korrelation des Ki-67 Index mit den Ergebnissen der Tumorsegmentation des Glioblastoms und die Wertigkeit als prognostischer Marker.

Henker C, Kriesen T, Schneider B, Glass Ä, Scherer M, Langner S, Erbersdobler A, Piek J: Correlation of Ki-67 Index with Volumetric Segmentation and its Value as a Prognostic Marker in Glioblastoma. *World Neurosurg. 2019; 125: e1093-r1103.*

Fragestellung: Der Ki-67 Index ist ein vielfältig verwendeter histologischer Marker zur Einschätzung der Proliferationsrate eines Tumors. In Bezug auf das Glioblastom gibt es Anhalt für eine Korrelation des Index mit dem Gesamtüberleben. Allerdings gibt es diesbezüglich nur wenige wissenschaftliche Daten, teils divergierend, und ebenso wenige Untersuchungen zur Korrelation des Index mit der Tumorsegmentation. Entsprechend war es das Ziel dieser Untersuchung, den Ki-67 Index mit der Tumorvolumetrie und dem Gesamtüberleben (OS) bei GBM-Patienten zu korrelieren.

Material und Methoden: In diese retrospektive Studie wurden insgesamt 152 Patienten eingeschlossen, welche in unserer Abteilung behandelt wurden. Es handelt sich allseits um primäre GBMs (IDH-Wildtyp). Es folgte die volumetrische Segmentation der Tumoren entsprechend der bereits beschriebenen 3D-Volumetrie (siehe OA 1). Die histologische Erhebung des Ki-67 – Index erfolgte im Rahmen der histologischen Aufarbeitung der Tumorpräparate im Institut für Pathologie der UMR. Hierbei erfolgte nach der immonhistochemischen Färbung des Ki-67 – Proteins die Auszählung von mindestens 1.000 Zellen beziehungsweise drei Hauptgesichtsfeldern (*high power fields*). Für die Überlebensanalyse wurde eine Subpopulation gefiltert, welche alle im Sinne einer

gross-total resection operiert wurden (RTV < 2 cm^3). Adjuvante Therapie wurden ebenfalls erfasst und statistisch ausgewertet.

Die statistische Auswertung erfolgte mittels SPSS (IBM, SPSS 22.0, Chicago, USA). Zur Auswertung der Volumetrie in Bezug auf den Ki-67 – Index wurde Pearson´s chi Quadrat-Test genutzt. Für die uni- und multivariate Überlebensanalyse wurde die Cox Regressionssanalyse verwendet. Des Weiteren wurde die Gesamtkohorte als auch die OS-Subgruppe im Sinne eines Propensity Score Matching (1:1) aufgeteilt, um mögliche Störgrößen und *baseline imbalances* der Kohorten zu reduzieren.

Ergebnisse: Die untersuchte Patientenkohorte entsprach sowohl in Bezug auf die klinischen als auch volumetrischen Angaben einem typischen GBM-Kollektiv [1, 38]. Der durchschnittlich gemessene Ki-67 – Index betrug 22,4%. Dieser zeigte sich unabhängig vom Alter oder Geschlecht der Patienten. Die gemessenen Tumorkompartimente oder hieraus errechneten Ratios zeigten ebenfalls keine signifikante Korrelation mit dem Ki-67 – Index ($p \geq 0{,}399$) oder wurden von diesem beeinflusst ($p \geq 0{,}238$). Diese Werte konnten ebenfalls in der PS-gematchten Kohorte nachvollzogen werden.

Zwischen der Gesamtkohorte und der OS-Subgruppe bestanden lediglich ein Unterschied im präoperativen Karnofsky-Wert, was aufgrund der Tatsache, dass Patienten welche einer *gross-total resection* unterzogen wurden allgemein in einem besseren klinischen Zustand sind, nicht ungewöhnlich erscheint. Alle anderen Patentientencharakteristika und volumetrische Daten zeigten keine signifikanten Unterschiede, die Ergebnisse der beiden Gruppen sind also vergleichbar. Bezüglich des Überlebens zeigte der Ki-67 - Index einen signifikanten Einfluss in Abhängigkeit seines cut-off Werts. In der multivariaten Analyse zeigte sich ein Wert von 20% als signifikant ($p = 0{,}043$).

Schlussfolgerung: Der Ki-67 – Index konnte seinen Wert als unabhängiger prädiktiver Marker bezüglich des Überlebens von GBM-Patienten bestätigen. Einen allgemeinen Zusammenhang mit den gemessenen volumetrischen Daten konnten wir allerdings nicht herstellen. Dies kann vor allem an der intraoperativen

Probenentnahme liegen, welche die intratumoralen Schwankungen des Indexes nicht adäquat widerspiegelt. Hierdurch können die unter Umständen feinen Unterschiede in der Volumetrie der einzelnen Patienten nicht entsprechend korreliert werden.

OA 4 – Einfluss von zehn verschiedenen Polymorphismen auf die präoperative Volumetrie bei Glioblastompatienten.

Henker C, Kriesen T, Fürst K, Goody D, Glass Ä, Pützer BM, Piek J: Effect of 10 different polymorphisms on preoperative volumetric characteristics of glioblastoma multiforme. *J Neurooncol. 2016; 126(3): 585-92.*

Fragestellung: Sogenannte *single nucleotide polymorphismen* (SNPs) kommen ubiquitär in der Bevölkerung vor mit sehr unterschiedlichen Auswirkungen auf die Genexpression der zu codierenden DNA-Sequenzen. Es gibt bisher keine ausreichenden Daten, ob diese SNPs auch auf die Erscheinung eines GBMs in der prätherapeutischen MRT haben. Entsprechend untersuchten wir die Frage, ob zehn verschiedene SNPs innerhalb verschiedener Kandidatengene einen Einfluss auf die Tumorvolumetrie haben.

Material und Methoden: In dieser prospektiven Studie wurden insgesamt 20 Patienten, welche aufgrund eines primären GBMs in unserer Abteilung operiert wurden, eingeschlossen. Die volumetrische Segmentation erfolgte entsprechend der bereits beschriebenen Technik (siehe OA 1). Für die Genanalyse wurden 5 ml Vollblut den in die Studie eingeschlossenen Patienten entnommen und zur Asservierung zunächst eingefroren. Nachfolgend erfolgte die Isolierung der genomischen DNA mit Hilfe des entsprechenden Kits (DNeasy blood & tissue kit, Quiagen). Die Amplifikation der spezifischen DNA-Fragmente wurde mittels PCR durchgeführt (peqGOLD Master Mix, Peqlab). Folgende Zielproteine und ihre entsprechenden SNPs wurden untersucht, dargestellt mit ihren spezifischen ID-Nummern („*rs*“):

Endotheliale Stickstoffmonoxidsynthase (eNOS) rs2070744

	rs1799983
Interleukin-8 (IL-8)	rs4073
Aquaporin-1 (AQP-1)	rs1476597
Aquaporin-4 (AQP4)	rs162007
	rs162008
	rs9951307
	rs3763043
Aquaporin-5 (AQP5)	rs3759129
Apolipoprotein-E (ApoE)	rs429358/rs7412

Die statistische Auswertung erfolgte mittels SPSS (IBM, SPSS 22.0, Chicago, USA). Der Einfluss der einzelnen SNPs auf die volumetrischen Daten wurde unter der Annahme eines entweder dominanten oder rezessiven genetischen Models untersucht. Alle SNPs wurden auf eine Übereinstimmung der harmonischen Allelverteilung entsprechend des Hardy-Weinberg-Equilibriums getestet (Pearson´s chi Quadrat Test). Als Signifikanzniveau wurde $\alpha = 0{,}05$ angenommen.

Ergebnisse: Das gewählte Patientenkollektiv stellte eine typische GBM-Population dar, in diese Studie wurden auch Patienten eingeschlossen, welche beispielsweise nur initial biopsiert wurden; entsprechend erfolgte keine Überlebensanalyse bei stark divergierenden Behandlungsregimen der einzelnen Patienten. Die volumetrischen Daten entsprachen denen, der bereits erwähnten Studien zur Volumetrie von GBM-Patienten (siehe OA 1 & 2) – die selektierten Tumoren entsprachen also dem üblichen Erscheinen dieses Tumors in der präoperativen MRT.

Lediglich ein SNP entsprach nicht dem Hardy-Weinberg-Gleichgewicht (rs2070744, $p = 0{,}040$), alle anderen untersuchten Polymorphismen wiesen eine dem Gleichgewicht entsprechende Allelverteilung auf. Die Analyse der Tumorvolumetrie in Bezug auf das Vorkommen der einzelnen SNPs zeigte, dass ein Polymorphismus im Bereich der Promotorregion des Aquaporin-4 – Gens

(rs162007) mit einer deutlichen Reduktion des peritumoralen Ödems (PTE) im Verhältnis zum Tumor, der ETR, einhergeht. Des Weiteren zeigte ein SNP in der Promotorregion des Interleukin-8 – Gens (rs4073) eine deutliche Assoziation mit einer geringeren Tumormasse, weniger Nekrose und einem reduziertem PTE (p < 0,048).

Schlussfolgerung: Unsere Arbeit konnte erstmalig zeigen, dass es möglicherweise eine Verbindung zwischen einzelnen Polymorphismen und der Größe eines Glioblastoms und dessen Kompartimente in der MRT gibt. Von besonderem Interesse ist hierbei der von uns untersuchte Interleukin-8 Polymorphismus: Andere Arbeiten konnten bereits den Nachweis erbringen, dass dieser funktionelle SNP mit einer deutlichen Reduktion der IL-8 – Konzentration innerhalb einer klinischen Studie an Patienten mit einer idiopathischen pulmonalen Fibrose einhergeht [44]. Die intratumorale IL-8 Konzentration wiederrum korreliert mit dem Tumorwachstum *in vitro* [45, 46]. Die Übereinstimmung dieser Daten mit unseren volumetrischen Untersuchungen, unterstreichen die Möglichkeiten der Volumetrie im Kontext der translationalen Tumorforschung.

OA 5 – Assoziation zwischen volumetrisch erfassten Tumorkompartimenten des Glioblastoms, dem Auftreten von Krampfanfällen und protektive Effekte einer Statinmedikation.

Henker C, Kriesen T, Scherer M, Glass Ä, von Deimling A, Bendszus M, Weber MA, Herold-Mende C, Unterberg A, Piek J: Association between Tumor Compartment Volumes, the Incidence of pretreatment Seizures and Statin-mediated protective Effects in Glioblastoma. *Neurosurgery. 2019; 85(4): E722-E729.*

Fragestellung: Krampfanfälle sind ein häufiges initiales Symptom eines malignen Hirntumors. Warum manche Glioblastome jedoch deutlich epileptogener sind als andere ist noch weitestgehend unbekannt. Daher war es das Ziel dieser Arbeit, mögliche Prädiktoren für das Auftreten von Krampfanfällen zu ermitteln.

Material und Methoden: In dieser bizentrischen retrospektiven Kohortenstudie wurden Patienten eingeschlossen, welche an einem primären GBM (unifokal, supratentoriell) in einem der beiden Studienzentren behandelt wurden. Ähnlich den vorangegangenen Arbeiten erfolgte eine volumetrische Segmentation des Tumors anhand der präoperativen MRT. Des Weiteren wurden alle verfügbaren klinischen Daten im Zeitraum unmittelbar vor der OP erfasst mit besonderem Augenmerk auf die klinische Symptomatik der Patienten. Als Krampfanfall wurden alle Ereignisse entsprechend der Definition der *International League Against Epilepsy* aus dem Jahre 2010 gewertet [47]. Eine Subgruppenanalyse wurde des Weiteren durchgeführt, um den Einfluss von Krampfanfällen auf das Überleben der GBM-Patienten zu untersuchen. Hierfür wurden aus dem Gesamtkollektiv Patienten gefiltert, welche im Sinne einer *gross total resection* operiert wurden (RTV < 2 cm^3) und anschließend entsprechend des Stupp-Schemas nachbehandelt wurden. Die statistische Auswertung erfolgte mittels SPSS (IBM, SPSS 22.0, Chicago, USA). Die Überlebensanalyse erfolgte mittels Cox-Regressionsmodel berechnet. Eine logistische Regressionsanalyse wurde genutzt, um den Einfluss verschiedener Faktoren auf das Auftreten von Krampfanfällen zu untersuchen; diese erfolgte uni- und multivariat. Als Signifikanzniveau wurde $\alpha = 0{,}05$ angenommen.

Ergebnisse: Wir konnten insgesamt 224 Patienten in unsere retrospektive Analyse einschließen. Insgesamt 99 Patienten erfüllten hiervon die Kriterien der Subgruppenanalyse (OS-Analyse). In der Subgruppe traten vergleichbar häufig Krampfanfälle auf (41,4% vs. 33%, $p = 0{,}148$), auch die volumetrischen Daten sind vergleichbar ($p \geq 0{,}102$) mit denen der Gesamtkohorte. Die gemessenen Tumorvolumina waren vergleichbar zu denen aus den vorangegangenen Studien. Das Alter der Patienten bei Diagnose hatte keinen Einfluss auf die jeweiligen Volumina und Ratios ($p = 0{,}252$). Bezüglich der klinischen Symptomatik zeigten sich initial am häufigsten fokale neurologische Ausfälle, alleinig (19%) oder in Kombination mit anderen Symptomen (10% zeigten fokale Defizite und eine Aphasie/Dysphasie). Krampfanfälle wurden insgesamt mit einer Prävalenz von 33% beobachtet, allein 16% der untersuchten GBM-Patienten fielen alleinig durch

einen Krampfanfall auf. Bezüglich des Auftretens von prätherapeutischen Krampfanfällen, zeigte sich in der univariaten Regressionsanalyse ein jüngeres Alter (≤ 60 Jahre), keine Statineinnahme und ein kleiner Tumor mit wenig Nekrose und wenig peritumoralen Ödem als pro-epileptogen ($p \leq 0{,}025$). Der befallene Hirnlappen oder die betroffene Hemisphäre hatten keinen Einfluss auf das prätherapeutische Auftreten von Krampfanfällen (p ≥0,511). In der nachfolgenden multivariablen logistischen Regressionsanalyse zeigten lediglich ein geringes Tumorvolumen (adjustiertes Odd´s Ratio (OR) = 6,42) mit verhältnismäßig wenig Nekrose (NTR ≤ 22%) eine epileptogene Neigung (adj. OR 0,122). Außerdem verbleibt der scheinbar protektive Effekt einer Statineinnahme in der multivariablen Analyse (adj. OR 4,94).

In der Überlebensanalyse der OS-Subgruppe zeigte sich kein Einfluss von Krampfanfällen auf das Überleben der untersuchten Patienten ($p = 0{,}357$); ebenso wenig die Einnahme von Statinen ($p = 0{,}507$). Einzig das Alter bei Diagnosestellung bleibt ein wichtiger klinischer Prognosefaktor ($p = 0{,}012$).

Schlussfolgerung: Unsere Studie konnte zeigen, dass initiale Krampfanfälle vor allem bei jüngeren Patienten auftreten, die an einem relativ kleinen GBM mit wenig innerer Nekrose leiden. Das peritumorale Ödem hatte keinen signifikanten Einfluss auf die Häufigkeit von prätherapeutischen Krampfereignissen, ebenso wenig die Tumorlage (betroffener Lappen oder Hemisphäre). Das Gesamtüberleben wurde durch das initiale Auftreten von Krampfanfällen nicht beeinflusst. Die Einnahme von Statinen schien einen protektiven Effekt zu haben, mit einer deutlichen geringeren Rate von Krampfereignissen.

Diskussion

Die volumetrische Tumorsegmentation existiert seit vielen Jahren, bereits 1979 zeigten Reeves und Marks einen möglichen Zusammenhang zwischen der Größe des GBMs in der präoperativen CT-Bildgebung und dem Überleben [48]. Mit der zunehmenden Verbreitung der MRT-Bildgebung war es anschließend möglich, die einzelnen Kompartimente viel genauer darzustellen und auch zu vermessen. Doch trotz dieser Möglichkeiten der exakten Vermessung etablierte sich in der Literatur zunehmend die eher deskriptive Tumoranalyse mittels graduierter Einschätzungen oder eindimensionaler Messungen. Eine der bekanntesten Arbeiten hierzu stammt aus dem Jahre 1996 von Hammoud [43]: die Größe des perilesionalen Ödems und die innenliegende Nekrose wurden in Bezug auf die Tumorgröße geschätzt und in jeweils drei Grade eingeteilt. Hierbei zeigte sich eine positive Korrelation zwischen der Größe des Ödems, beziehungsweise der Nekrose und dem Überleben. Teile dieser Ergebnisse konnten in einer deutlich größeren Kohorte durch Lacroix et al. im Jahr 2001 nachvollzogen werden (n = 416) – hier zeigte sich in der multivariaten Analyse die Ausdehnung der Nekrose als prognostisch entscheidend [38]. Einschränkend muss allerdings erwähnt werden, dass die Kohorte sehr inhomogen bezüglich der durchgeführten adjuvanten Therapien war, beziehungsweise keinerlei Angaben über die Anzahl der durchgeführten Chemotherapien gemacht wurden. Später wurde ein ganzes Set aus beschreibenden Aspekten des Tumors erarbeitet, um eine standardisierte Charakterisierung jedes Tumors vornehmen zu können, dass sogenannten *VASARI (Visually Accessible Rembrandt Images) MRI feature set* [49]. Neben einer kategorialen Beschreibung wie Multifokalität, betroffener Hemisphäre oder der Infiltration eloquenter Areale, befinden sich auch Schätzungen zum Verhältnis des Ödems beziehungsweise der Nekrose zum soliden Tumoranteil. Diese klare Systematik der Tumorbeschreibung bot erstmals die Möglichkeit einer Standardisierung der radiologischen Betrachtung. Leider flossen hierin keine echten volumetrischen Messungen ein. Die Ergebnisse nachfolgender Studien zur Prognose von GBM-Patienten anhand von VASARI features sind entsprechend

divergierend [49]. Maßgeblich für diese Divergenz im Vergleich zu anderen Arbeiten ist vor allem die verwendete Technik der Segmentation. Diese wird nicht einheitlich verwendet, vielmehr wurde ein Groh der Studien nur mittels eindimensionaler Messungen oder gar Schätzungen durchgeführt. Diese Methoden sind jedoch inadäquat hierfür und können die komplexe Struktur des GBMs in der MRT nicht widergeben. Neben der ungenauen Messmethoden wurden oftmals inhomogene Patientenkollektive ausgewählt, eine Validierung der genutzten Segmentationstechnik ist somit nur eingeschränkt möglich. Die von uns genutzte 3D-Volumetrie mit Hilfe einer semi-automatisierten *contour expansion*-Technik zeigte sich als die valideste und den anderen Techniken überlegen (**OA 1** [50]). Es zeigte sich vor allem eine Überlegenheit gegenüber den Schätzungen einzelner Tumorkompartimente, aber auch die eindimensionalen Messungen und die hieraus abgeleiteten mathematischen Rekonstruktionen können das komplexe und irreguläre Aussehen des Tumors in der MRT nicht widerspiegeln. Des Weiteren konnten wir die Relationen der einzelnen Kompartimente zu- und deren Korrelationen untereinander beschreiben (**OA 1, 2 & 5** [50–52]): In der strukturellen Analyse zeigte sich die deutlichste Korrelation zwischen dem Tumorvolumen und der innenliegenden Nekrose (r_S = 0,898), während zwischen dem PTE und dem Tumor eine geringere Korrelation bestand (r_S = 0,691). Die von uns verwendeten Ratios zur besseren Charakterisierung der Verhältnismäßigkeiten zwischen den Kompartimenten (NTR & ETR) zeigten einen deutlichen Zusammenhang zwischen der Nekrose und dem Tumorkompartiment. In den Überlebensanalysen war vor allem die innenliegende Nekrose prognosebestimmend: liegt beispielsweise das Verhältnis zwischen der Tumormasse und der Nekrose bei mehr als 0,33 (> 33% Nekroseanteil), so beträgt das Sterberisiko (Hazard Ratio) das 2,63-fache gegenüber Patienten mit deutlich weniger Nekrose (NTR ≤ 0,2) [51]. Erklärbar ist diese Beobachtung vor allem durch die Nekrose als Ausdruck einer gesteigerten Resistenz des GBMs gegenüber jedweden Therapien [53]. Somit konnten wir erstmals einen robusten *imaging biomarker* definieren und validieren, die Nekrose-Tumor – Ratio (NTR).

Diese Ergebnisse konnten bereits durch eine andere Arbeitsgruppe mit Hilfe physiologischer MRT-Bildgebung nachvollzogen werden [54]. Die Reliabilität der verwendeten Messmethode wurde bezüglich ihrer Übereinstimmung bei verschiedenen Nutzern der Volumetrie (*intraobserver* und *interobserver agreement*) bereits durch andere Arbeitsgruppen bestätigt [55, 56].

Neben dem Nutzen der Volumetrie als eigenständigen Prädiktor für das Überleben von GBM-Patienten, lassen sich auch andere Biomarker hiermit vergleichen und in Relation setzen. Unabhängig von der Tumorentität, ist der Ki-67 – Index einer der am weitesten verbreiteten histologischen Marker zur Einschätzung der Wachstumsgeschwindigkeit eines Tumors. Entsprechend ist der Index deutlich höher bei malignen Tumoren als bei langsam wachsenden Entitäten. Eine Korrelationsanalyse mit der präoperativen Tumorvolumetrie erbrachte jedoch keine signifikante Übereinstimmung der beiden Marker (**OA 3**). In der multivariaten Überlebensanalyse, gruppiert nach verschiedenen Ki-67 – Grenzwerten, zeigte sich ein Einfluss auf das Überleben nur bei einem Grenzwert von 20% des Index [57]. Die mangelnde Korrelation zwischen dem histologischen Index und der Tumorvolumetrie lässt sich vor allem dadurch erklären, dass der Index zum einen keinen Rückschluss auf die tatsächliche Progression des Tumors zulässt [58]. Andererseits ist der Index stark davon abhängig vom Ort der chirurgischen Probenahme, welcher unter Umständen nicht repräsentativ für den gesamten Tumor ist. Dies ist ein entscheidender Vorteil der Volumetrie, da sie die Gesamtheit des untersuchten Tumors erfassen kann. Des Weiteren erlaubt sie eine nicht-invasive Untersuchung im zeitlichen Verlauf und kann somit auch Veränderungen in der Tumorkomposition erfassen, welche eventuell nicht durch einzelne Tumorproben erfasst werden können. Eine weitere Einschränkung des Ki-67 – Index ist seine oftmals nicht automatisierte Erhebung und es existieren diverse Techniken zur Färbung und Messung der markierten Zellen ohne bis heute definierten, einheitlichen Standard.

Einen weiteren Vorteil bietet die Volumetrie durch ihre nicht-invasive Möglichkeit der Phänotypanalyse und nachfolgendem Vergleich mit dem individuellen Genotyp. Im Rahmen einer *Proof-of-Principle* – Studie untersuchten wir 10 häufig

vorkommende Einzelnukleotidpolymorphismen (SNPs) auf ihren Einfluss auf die Tumorvolumetrie (**OA 4**). Die Auswahl der Kandidaten-SNPs erfolgte hierbei nach ihrem möglichen Einfluss auf die einzelnen Kompartimente. Beispielsweise steuern die intrazellulären Wasserproteine (Aquaporine) die intra- und extrazelluläre Wasserhomöostase und eine genetische Aberration könnte entsprechend einen Einfluss auf das Ausmaß des peritumoralen Ödems haben. Weitere SNPs könnten die Endothelintegrität, die Zytokinproduktion oder die Lipoproteine beeinflussen und somit auch die Ausprägung der Tumorsegmente beeinträchtigen. Die Korrelation zwischen Phäno- und Genotyp erbrachte für einen Aquaporin-Polymorphismus einen Zusammenhang mit der Ausprägung des peritumoralen Ödems, der ETR [59]. Interessanterweise zeigte ein SNP im Interleukin-8 – Gen einen signifikanten Einfluss auf alle Tumorkompartimente. Homozygote Allelträger zeigten eine deutliche Reduktion aller Volumina, vermutlich aufgrund einer verminderten Zytokinproduktion wie *in vivo* - Studien zeigen konnten [44, 60].

Neben der Integration genetischer Informationen, bietet die Volumetrie auch die Möglichkeit klinische Daten hierauf zu beziehen. Lange Zeit galt ein initialer Krampfanfall als erstes Symptom des Glioblastoms als prognostisch günstig [61]. Dieser gedachte Zusammenhang zeigte sich in unserer Studie nicht. Vielmehr konnten wir zeigen, dass die klinische Erscheinung des Krampfanfalls ein Surrogat für eine spezifische Subpopulation von GBM-Patienten darstellt (**OA 5**): Patienten mit einem kleinen Tumor und vor allem einer nur sehr geringen Nekrose (NTR ≤ 0,2) erlitten deutlich häufiger einen Krampfanfall [52]. So hatten Patienten mit einem Tumorvolumen von ≤ 16cm^3 (dies entspricht einer Kugel mit einem Durchmesser von 3,13 cm) eine fast 7fach höhere Wahrscheinlichkeit einen prätherapeutischen Krampfanfall zu erleiden, als ein Patient mit einem Tumorvolumen von größer 40cm^3, also einem Volumen, welches etwa dem eines Golfballs entspricht (40,7cm^3). Diese Patienten waren auch jünger, wenngleich dieser Effekt in der multivariaten Analyse nicht mehr nachvollziehbar war (p = 0,495). Der mögliche positive Effekt auf das Überleben durch einen Krampfanfall lässt sich aus unserer Sicht durch das klinisch sehr frühe in Erscheinung treten

dieser Tumoren erklären. Somit kann eine ausgedehnte chirurgische Resektion viel häufiger erfolgen. Andere Arbeitsgruppen konnten nachweisen, dass die Glutamathomöostase bei epileptogeneren Tumoren verändert ist [62]. Ob diese Glutamatüberversorgung auch die Progression des Tumors beeinflusst und somit Einfluss auf das Überleben nimmt ist bisher unklar. Des Weiteren zeigte die Einnahme von Statinen eine signifikante Reduktion von Krampfanfällen und somit einen neuroprotektiven Effekt in unserer Studie.

Die volumetrische 3D-Tumorsegmentation bietet die Möglichkeit, nicht-invasiv eine Vielzahl an klinischen und experimentellen Daten im Hinblick auf ihren Einfluss auf das Erscheinungsbild in der MRT zu überprüfen. Wenngleich sie zeitintensiver ist als beispielsweise Schätzungen oder eindimensionale Messungen, ist ihre große Stärke ihre Genauigkeit, welche zwingend notwendig für ihre Verwendung ist. Es gibt einige Ansätze zur vollständigen Automatisierung der Volumetrie [63, 64], wenngleich die Ergebnisse aus unserer Sicht in Bezug auf ihre Präzision dies noch nicht zulassen.

Zusammenfassung und Ausblick

Die vorliegende Arbeit beschäftigte sich mit den Möglichkeiten der prätherapeutischen Vermessung des Glioblastoms in der MRT. Hierbei sollten neben der hierfür geeigneten Technik auch die Möglichkeiten der Korrelation verschiedenster Daten, mit denen der Volumetrie untersucht werden. Im Rahmen der Verifizierung verschiedener Messtechniken, zeigte sich die 3D-Volumetrie als die präziseste. Diese Ergebnisse konnten nachfolgend verifiziert werden und ein tieferer Einblick in die Relationen zwischen den einzelnen Tumorkompartimenten gelang. So zeigte sich das Verhältnis zwischen der im Tumor gelegenen Nekrose und dem Tumor selbst (NTR) als prognostisch unabhängiger *imaging biomarker*.

Die Ergebnisse der Volumetrie zeigten keine Korrelation mit dem Ki-67 – Index, welcher zwar einen Anhalt für die Wachtumstendenz eines Tumors zeigt, jedoch großen intratumoralen Schwankungen unterliegt und nicht zwingend mit der Progression des Tumors zusammenhängt. Die Volumetrie kann hingegen ein umfassenderes Bild des Tumors zum Zeitpunkt der MRT abbilden.

So gelang es auch die irreführende Annahme, ein initialer Krampfanfall als erstes klinisches Zeichen des GBMs sei prognostisch günstig, zu revidieren. Wir konnten nachweisen, dass epileptogene Tumoren deutlich kleiner in der MRT sind und weniger Nekrose enthalten, der Krampfanfall also eher ein Surrogatparameter für eine spezifische Subgruppe von Patienten darstellt.

Im Rahmen einer weiteren Studie konnten einzelne genetische Polymorphismen mit der Volumetrie korreliert werden und somit der Phäno- dem Genotyp zugeordnet werden. Die Volumetrie kann hierdurch klinisch relevante genetische Informationen von solchen mit geringem oder keinerlei Effekt filtern. So folgte aufgrund der in dieser Arbeit genannten Studie zum Einfluss verschiedener Polymorphismen auf die Volumetrie eine multizentrische Studie zur detaillierteren Analyse, deren Daten in naher Zukunft veröffentlich werden. Außerdem stellte die Studie die Bedeutung des Interleukin-8 für die Tumorprogression des

Glioblastoms heraus; diese Ergebnisse führten bereits zu Etablierung einer neuen 3D-Zellkultur zur tieferen Analyse der Zytokineeffekte auf GBM-Zellen.

Die Volumetrie bietet eine Fülle an Möglichkeiten, nicht nur zur reinen Tumoranalyse, sondern vielmehr gewährt sie uns tiefere Einblicke in die Biologie des Glioblastoms. Sie erweitert unsere Palette an bisher bekannten Markern zur Abschätzung des Überlebens von Tumorpatienten um einen validen *imaging biomarker*.

Danksagung

Ohne die Unterstützung meiner Familie, vieler Kollegen, sowie interner und externer Kooperationspartner wäre die vorliegende Arbeit nicht möglich gewesen.

Besonderem Dank gilt hierbei:

Herrn Prof Dr. med. em. Dr. med. h.c. Jürgen Piek, der mich seit meinem Wechsel an die Universitätsmedizin Rostock in seiner Abteilung stets unterstützt hat. Durch sein Vertrauen in meine Arbeit und Fähigkeiten, gab er mir die Möglichkeit, mich wissenschaftlich, aber auch persönlich zu entfalten.

Herrn Dr. med. Thomas Kriesen für die tatkräftige Datenakquise und -auswertung, die gemeinsamen wissenschaftlichen Ausflüge, Diskussionen und die uns verbindende Freundschaft.

Herrn Prof. Dr. med. Sönke Langner möchte ich danken für die exzellente wissenschaftliche, aber auch klinische und private Zusammenarbeit. Seine Ideen, Korrekturen und Eingebungen waren stets ein wichtiger Aspekt meiner Arbeit.

Des Weiteren möchten ich mich bei den Kollegen der Klinik für Neurochirurgie des Universitätsklinikums in Heidelberg für die ausgesprochen gute wissenschaftliche Kooperation bedanken.

Dr. phil. nat. Björn Schneider danke ich für die fruchtbare wissenschaftliche Zusammenarbeit, die Hilfestellung während der Planung meiner Experimente und nicht zuletzt der Umsetzung einer prospektiven Biobank in unserer Abteilung.

Frau Prof. Dr. med. Brigitte Vollmar danke ich für die Unterstützung zur Umsetzung meiner klinischen Forschungsergebnisse in eine experimentelle Zellkultur.

Meiner Ehefrau Dr. med. Verena Henker, sowie unseren Kindern Carla Helena Sophie, Tristan Julius und Ella Aurelia danke ich für das entgegengebrachte Vertrauen, die Geduld und vor allem für die meinige Entlastung während den vielen Jahren der wissenschaftlichen Arbeit und des Verfassens dieser Arbeit. All diese Mühen wären ohne dieses Verständnis nicht möglich gewesen.

Curriculum vitae

Dr. med. Christian Henker

Geburtsdatum	05.10.1980
Geburtsort	Dresden
Wohnhaft	Primelweg 9
	18057 Rostock
Familienstand	verheiratet, 3 Kinder

Ausbildung

Schulausbildung

07/2000	Erwerb der allgemeinen Hochschulreife am Adolf-Reichwein-Gymnasium, Heusenstamm

Zivildienst

2000-2001	Zivildienst innerhalb der Johanniter-Unfallhilfe, Rodgau

Studium

2002	Immatrikulation an der Georg-August-Universität Göttingen
2009	Approbation als Arzt

Berufliche Laufbahn

10/2009	Assistenzarzt innerhalb der Klinik für Neurochirurgie der
- 12/2012	Universitätsmedizin Kiel (Prof. Dr. med. H. M. Mehdorn)

seit 01/2013 Assistenzarzt innerhalb der Abteilung für Neurochirurgie, Universitätsmedizin Rostock (Prof. Dr. med. Dr. h.c. J. Piek)

07/2016 Facharzt für Neurochirurgie

12/2016 Funktionsoberarzt

08/2018 Oberarzt der Abteilung für Neurochirurgie, Universitätsmedizin Rostock

Dissertation

03.01.2012 Innerhalb der Abteilung Thorax-, Herz- und Gefäßchirurgie der Universität Göttingen. Thema: "Klinischer Einfluss des eNOS T-786C - Polymorphismus auf Mortalität und Morbidität kardiochirurgischer Patienten".

Mitgliedschaften

Ordentliche Mitgliedschaft der Deutschen Gesellschaft für Neurochirurgie (DGNC)

Mitglied der Deutschen Gesellschaft für Neurointensiv- und Notfallmedizin (DGNI)

Mitglied der Deutschen interdisziplinären Vereinigung für Intensiv- und Notfallmedizin (DIVI)

Publikationsliste

Popov AF, **Henker C**, Schmitto JD, Stojanovic T, Wiese CH, Seipelt R, Schoendube FA, Quintel M, Hinz J. The eNOS T-786C polymorphism for hospital mortality and morbidity in cardiac surgical patients. *J Cardiovasc Surg (Torino). 2010 Apr;51(2):265-72.*

Jensen-Kondering U, **Henker C**, Dörner L, Hugo HH, Jansen O. Differentiation of primary central nervous system lymphomas from high grade astrocytomas by qualitative analysis of the signal intensity curves derived from dynamic susceptibility-contrast magnetic resonance imaging. *Neurol Res. 2012 Dec;34(10):984-8.*

Giese H, Sauvigny T, Sakowitz OW, Bierschneider M, Güresir E, **Henker C**, Höhne J, Lindner D, Mielke D, Pannewitz R, Rohde V, Scholz M, Schuss P, Regelsberger J. German Cranial Reconstruction Registry (GCRR): protocol for a prospective, multicentre, open registry. *BMJ open, 2015, vol. 5, no. 9, pp. E009273.*

Henker C, Kriesen T, Fürst K, Goody D, Glass Ä, Pützer BM, Piek J. Effect of 10 different polymorphisms on preoperative volumetric characteristics of glioblastoma multiforme. *Journal of Neuro-oncology. 2016;126(3):585-592.*

Henker C, Schmelter C, Piek J. Komplikationen und Überwachungsstandards in Deutschland nach elektiven Kraniotomien. *Der Anästhesis, 2017, 66: 412.*

Henker C, Kriesen T, Glass Ä, Schneider B, Piek J. Volumetric quantification of glioblastoma: experiences with different measurement techniques and impact on survival. *Journal of Neuro-oncology. 2017; 135: 391.*

Henker C, Hoppmann MC, Sherman MUS, Glass Ä, Piek J. Validation of a Novel Clinical Score: The Rostock Functional and Cosmetic Cranioplasty Score. *J Neurotrauma. 2018;35(8):1030-1036.*

Henker C, Kriesen T, Schneider B, Glass Ä, Scherer M, Langner S, Erbersdobler A, Piek J. Correlation of Ki-67 Index with Volumetric Segmentation and its Value as a Prognostic Marker in Glioblastoma. *World Neurosurgery. 2019; 125:e1093-e1103.*

Henker C, Kriesen T, Scherer M, Glass Ä, von Deimling A, Bendszus M, Weber, MA, Herold-Mende C, Unterberg A, Piek J. Association Between Tumor Compartment Volumes, the Incidence of Pre-treatment Seizures and Statin-mediated Protective Effects in Glioblastoma. *Neurosurgery. 2019; 85(4):E722-E729.*

Henker C, Hiepel MC, Kriesen T, Scherer M, Glass Ä, Herold-Mende C, Bendszus M, Langner S, Weber MA, Schneider B, Unterberg A, Piek J. Volumetric assessment of glioblastoma and its predictive value for survival. *Acta Neurochir (Wien). 2019;161(8):1723-1732.*

Literaturverzeichnis

1. Ostrom QT, Gittleman H, Truitt G et al. (2018) CBTRUS Statistical Report: Primary Brain and Other Central Nervous System Tumors Diagnosed in the United States in 2011–2015. Neuro Oncol 20(Suppl 4): iv1-iv86. doi: 10.1093/neuonc/noy131

2. European Commission (2008) Communication from the Commission tot he European Parliament, the Council, the European Economic and Social Committee and the Committee oft he regions on Rare Diseases: Europe's challenges. https://ec.europa.eu/health/rare_diseases/experts_committee_en. Accessed 22 Mar 2019

3. Ostrom QT, Gittleman H, Liao P et al. (017) CBTRUS Statistical Report: Primary brain and other central nervous system tumors diagnosed in the United States in 2010-2014. Neuro Oncol 19(suppl_5): v1-v88. doi: 10.1093/neuonc/nox158

4. Stupp R, Hegi ME, Mason WP et al. (2009) Effects of radiotherapy with concomitant and adjuvant temozolomide versus radiotherapy alone on survival in glioblastoma in a randomised phase III study: 5-year analysis of the EORTC-NCIC trial. The Lancet Oncology 10(5): 459–466. doi: 10.1016/S1470-2045(09)70025-7

5. Ostrom QT, Cioffi G, Gittleman H et al. (2019) CBTRUS Statistical Report: Primary Brain and Other Central Nervous System Tumors Diagnosed in the United States in 2012-2016. Neuro Oncol 21(Supplement_5): v1-v100. doi: 10.1093/neuonc/noz150

6. Alcantara Llaguno S, Sun D, Pedraza AM et al. (2019) Cell-of-origin susceptibility to glioblastoma formation declines with neural lineage restriction. Nat Neurosci 22(4): 545–555. doi: 10.1038/s41593-018-0333-8

7. DeAngelis LM, Mellinghoff IK (2011) Virchow 2011 or how to ID(H) human glioblastoma. J Clin Oncol 29(34): 4473–4474. doi: 10.1200/JCO.2011.37.5873

8. Stoyanov GS, Dzhenkov DL (2018) On the Concepts and History of Glioblastoma Multiforme - Morphology, Genetics and Epigenetics. Folia Med (Plovdiv) 60(1): 48–66. doi: 10.1515/folmed-2017-0069

9. Ferguson S, Lesniak MS (2005) Percival Bailey and the classification of brain tumors. Neurosurg Focus 18(4): e7. doi: 10.3171/foc.2005.18.4.8

10. Peiffer J, Kleihues P (1999) Hans-Joachim Scherer (1906-1945), pioneer in glioma research. Brain Pathol 9(2): 241–245. doi: 10.1111/j.1750-3639.1999.tb00222.x

11. Aldape K, Zadeh G, Mansouri S et al. (2015) Glioblastoma: pathology, molecular mechanisms and markers. Acta Neuropathol 129(6): 829–848. doi: 10.1007/s00401-015-1432-1

12. James CD, Olson JJ (1996) Molecular genetics and molecular biology advances in brain tumors. Curr Opin Oncol 8(3): 188–195. doi: 10.1097/00001622-199605000-00004

13. Ishii N, Tada M, Hamou MF et al. (1999) Cells with TP53 mutations in low grade astrocytic tumors evolve clonally to malignancy and are an unfavorable prognostic factor. Oncogene 18(43): 5870–5878. doi: 10.1038/sj.onc.1203241

14. Lai A, Kharbanda S, Pope WB et al. (2011) Evidence for sequenced molecular evolution of IDH1 mutant glioblastoma from a distinct cell of origin. J Clin Oncol 29(34): 4482–4490. doi: 10.1200/JCO.2010.33.8715

15. Parsons DW, Jones S, Zhang X et al. (2008) An integrated genomic analysis of human glioblastoma multiforme. Science 321(5897): 1807–1812. doi: 10.1126/science.1164382

16. Sanson M, Marie Y, Paris S et al. (2009) Isocitrate dehydrogenase 1 codon 132 mutation is an important prognostic biomarker in gliomas. J Clin Oncol 27(25): 4150–4154. doi: 10.1200/JCO.2009.21.9832

17. Yan H, Parsons DW, Jin G et al. (2009) IDH1 and IDH2 mutations in gliomas. N Engl J Med 360(8): 765–773. doi: 10.1056/NEJMoa0808710

18. Dang L, White DW, Gross S et al. (2009) Cancer-associated IDH1 mutations produce 2-hydroxyglutarate. Nature 462(7274): 739–744. doi: 10.1038/nature08617

19. Vigneswaran K, Neill S, Hadjipanayis CG (2015) Beyond the World Health Organization grading of infiltrating gliomas: advances in the molecular genetics of glioma classification. Ann Transl Med 3(7): 95. doi: 10.3978/j.issn.2305-5839.2015.03.57

20. Louis DN, Perry A, Reifenberger G et al. (2016) The 2016 World Health Organization Classification of Tumors of the Central Nervous System: a summary. Acta Neuropathol 131(6): 803–820. doi: 10.1007/s00401-016-1545-1

21. Pope WB, Brandal G (2018) Conventional and advanced magnetic resonance imaging in patients with high-grade glioma. Q J Nucl Med Mol Imaging 62(3): 239–253. doi: 10.23736/S1824-4785.18.03086-8

22. Eidel O, Burth S, Neumann J-O et al. (2017) Tumor Infiltration in Enhancing and Non-Enhancing Parts of Glioblastoma: A Correlation with Histopathology. PLoS ONE 12(1): e0169292. doi: 10.1371/journal.pone.0169292

23. Lasocki A, Gaillard F, Tacey MA et al. (2016) The incidence and significance of multicentric noncontrast-enhancing lesions distant from a histologically-proven glioblastoma. J Neurooncol 129(3): 471–478. doi: 10.1007/s11060-016-2193-y

24. Kelly PJ, Daumas-Duport C, Kispert DB et al. (1987) Imaging-based stereotaxic serial biopsies in untreated intracranial glial neoplasms. J Neurosurg 66(6): 865–874. doi: 10.3171/jns.1987.66.6.0865

25. Lasocki A, Gaillard F (2019) Non-Contrast-Enhancing Tumor: A New Frontier in Glioblastoma Research. AJNR Am J Neuroradiol 40(5): 758–765. doi: 10.3174/ajnr.A6025

26. Grabowski MM, Recinos PF, Nowacki AS et al. (2014) Residual tumor volume versus extent of resection: predictors of survival after surgery for glioblastoma. J Neurosurg 121(5): 1115–1123. doi: 10.3171/2014.7.JNS132449

27. Osswald M, Jung E, Sahm F et al. (2015) Brain tumour cells interconnect to a functional and resistant network. Nature 528(7580): 93–98. doi: 10.1038/nature16071

28. Osswald M, Solecki G, Wick W et al. (2016) A malignant cellular network in gliomas: potential clinical implications. Neuro Oncol 18(4): 479–485. doi: 10.1093/neuonc/now014

29. Rapp M, Baernreuther J, Turowski B et al. (2017) Recurrence Pattern Analysis of Primary Glioblastoma. World Neurosurg 103: 733–740. doi: 10.1016/j.wneu.2017.04.053

30. Sahm F, Capper D, Jeibmann A et al. (2012) Addressing diffuse glioma as a systemic brain disease with single-cell analysis. Arch Neurol 69(4): 523–526. doi: 10.1001/archneurol.2011.2910

31. Caragher SP, Sachdev S, Ahmed A (2017) Radiotherapy and Glioma Stem Cells: Searching for Chinks in Cellular Armor. Curr Stem Cell Rep 3(4): 348–357. doi: 10.1007/s40778-017-0102-8

32. Miranda-Gonçalves V, Cardoso-Carneiro D, Valbom I et al. (2017) Metabolic alterations underlying Bevacizumab therapy in glioblastoma cells. Oncotarget 8(61): 103657–103670. doi: 10.18632/oncotarget.21761

33. Jiapaer S, Furuta T, Tanaka S et al. (2018) Potential Strategies Overcoming the Temozolomide Resistance for Glioblastoma. Neurol Med Chir (Tokyo) 58(10): 405–421. doi: 10.2176/nmc.ra.2018-0141

34. Verhaak RGW, Hoadley KA, Purdom E et al. (2010) Integrated genomic analysis identifies clinically relevant subtypes of glioblastoma characterized by abnormalities in PDGFRA, IDH1, EGFR, and NF1. Cancer Cell 17(1): 98–110. doi: 10.1016/j.ccr.2009.12.020

35. Abedalthagafi M, Barakeh D, Foshay KM (2018) Immunogenetics of glioblastoma: the future of personalized patient management. NPJ Precis Oncol 2: 27. doi: 10.1038/s41698-018-0070-1

36. Wang Q, Hu B, Hu X et al. (2018) Tumor Evolution of Glioma-Intrinsic Gene Expression Subtypes Associates with Immunological Changes in the Microenvironment. Cancer Cell 33(1): 152. doi: 10.1016/j.ccell.2017.12.012

37. Fedele M, Cerchia L, Pegoraro S et al. (2019) Proneural-Mesenchymal Transition: Phenotypic Plasticity to Acquire Multitherapy Resistance in Glioblastoma. International journal of molecular sciences 20(11): 2746

38. Lacroix M, Abi-Said D, Fourney DR et al. (2001) A multivariate analysis of 416 patients with glioblastoma multiforme: prognosis, extent of resection, and survival. J Neurosurg 95(2): 190–198. doi: 10.3171/jns.2001.95.2.0190

39. Gerson SL (2004) MGMT: its role in cancer aetiology and cancer therapeutics. Nat Rev Cancer 4(4): 296–307. doi: 10.1038/nrc1319

40. Esteller M, Garcia-Foncillas J, Andion E et al. (2000) Inactivation of the DNA-repair gene MGMT and the clinical response of gliomas to alkylating agents. N Engl J Med 343(19): 1350–1354. doi: 10.1056/NEJM200011093431901

41. Hegi ME, Diserens A-C, Gorlia T et al. (2005) MGMT gene silencing and benefit from temozolomide in glioblastoma. N Engl J Med 352(10): 997–1003. doi: 10.1056/NEJMoa043331

42. Chen W-J, He D-S, Tang R-X et al. (2015) Ki-67 is a valuable prognostic factor in gliomas: evidence from a systematic review and meta-analysis. Asian Pac J Cancer Prev 16(2): 411–420. doi: 10.7314/apjcp.2015.16.2.411

43. Hammoud MA, Sawaya R, Shi W et al. (1996) Prognostic significance of preoperative MRI scans in glioblastoma multiforme. J Neurooncol 27(1): 65–73. doi: 10.1007/bf00146086

44. Ahn M-H, Park B-L, Lee S-H et al. (2011) A promoter SNP rs4073TA in the common allele of the interleukin 8 gene is associated with the development of idiopathic pulmonary fibrosis via the IL-8 protein enhancing mode. Respir Res 12: 73. doi: 10.1186/1465-9921-12-73

45. Sun S, Wang Q, an Giang et al. (2011) Knockdown of CypA inhibits interleukin-8 (IL-8) and IL-8-mediated proliferation and tumor growth of glioblastoma cells through down-regulated NF-κB. J Neurooncol 101(1): 1–14. doi: 10.1007/s11060-010-0220-y

46. Ahn S-H, Park H, Ahn Y-H et al. (2016) Necrotic cells influence migration and invasion of glioblastoma via NF-κB/AP-1-mediated IL-8 regulation. Sci Rep 6: 24552. doi: 10.1038/srep24552

47. Berg AT, Berkovic SF, Brodie MJ et al. (2010) Revised terminology and concepts for organization of seizures and epilepsies: report of the ILAE Commission on Classification and Terminology, 2005-2009. Epilepsia 51(4): 676–685. doi: 10.1111/j.1528-1167.2010.02522.x

48. Reeves GI, Marks JE (1979) Prognostic significance of lesion size for glioblastoma multiforme. Radiology 132(2): 469–471. doi: 10.1148/132.2.469

49. Wangaryattawanich P, Hatami M, Wang J et al. (2015) Multicenter imaging outcomes study of The Cancer Genome Atlas glioblastoma patient cohort: imaging predictors of overall and progression-free survival. Neuro Oncol 17(11): 1525–1537. doi: 10.1093/neuonc/nov117

50. Henker C, Kriesen T, Glass Ä et al. (2017) Volumetric quantification of glioblastoma: experiences with different measurement techniques and impact on survival. J Neurooncol 135(2): 391–402. doi: 10.1007/s11060-017-2587-5

51. Henker C, Hiepel MC, Kriesen T et al. (2019) Volumetric assessment of glioblastoma and its predictive value for survival. Acta Neurochir (Wien) 161(8): 1723–1732. doi: 10.1007/s00701-019-03966-6

52. Henker C, Kriesen T, Scherer M et al. (2019) Association Between Tumor Compartment Volumes, the Incidence of Pretreatment Seizures, and Statin-Mediated Protective Effects in Glioblastoma. Neurosurgery 85(4): E722-E729. doi: 10.1093/neuros/nyz079

53. Raza SM, Lang FF, Aggarwal BB et al. (2002) Necrosis and glioblastoma: a friend or a foe? A review and a hypothesis. Neurosurgery 51(1): 2-12; discussion 12-3. doi: 10.1097/00006123-200207000-00002

54. Stadlbauer A, Zimmermann M, Doerfler A et al. (2018) Intratumoral heterogeneity of oxygen metabolism and neovascularization uncovers 2 survival-relevant subgroups of IDH1 wild-type glioblastoma. Neuro Oncol 20(11): 1536–1546. doi: 10.1093/neuonc/noy066.

55. Kubben PL, Postma AA, Kessels AGH et al. (2010) Intraobserver and interobserver agreement in volumetric assessment of glioblastoma multiforme resection. Neurosurgery 67(5): 1329–1334. doi: 10.1227/NEU.0b013e3181efbb08

56. Visser M, Müller DMJ, van Duijn RJM et al. (2019) Inter-rater agreement in glioma segmentations on longitudinal MRI. Neuroimage Clin 22: 101727. doi: 10.1016/j.nicl.2019.101727

57. Henker C, Kriesen T, Schneider B et al. (2019) Correlation of Ki-67 Index with Volumetric Segmentation and its Value as a Prognostic Marker in Glioblastoma. World Neurosurg 125: e1093-e1103. doi: 10.1016/j.wneu.2019.02.006

58. Chung WJ, Lyons SA, Nelson GM et al. (2005) Inhibition of Cystine Uptake Disrupts the Growth of Primary Brain Tumors. J Neurosci 25(31): 7101–7110. doi: 10.1523/JNEUROSCI.5258-04.2005

59. Henker C, Kriesen T, Fürst K et al. (2016) Effect of 10 different polymorphisms on preoperative volumetric characteristics of glioblastoma multiforme. J Neurooncol 126(3): 585–592. doi: 10.1007/s11060-015-2005-9

60. Lee W-P, Tai D-I, Lan K-H et al. (2005) The -251T allele of the interleukin-8 promoter is associated with increased risk of gastric carcinoma featuring diffuse-type histopathology in Chinese population. Clin Cancer Res 11(18): 6431–6441. doi: 10.1158/1078-0432.CCR-05-0942

61. Toledo M, Sarria-Estrada S, Quintana M et al. (2015) Prognostic implications of epilepsy in glioblastomas. Clin Neurol Neurosurg 139: 166–171. doi: 10.1016/j.clineuro.2015.10.002

62. Dührsen L, Sauvigny T, Ricklefs FL et al. (2019) Seizures as presenting symptom in patients with glioblastoma. Epilepsia 60(1): 149–154. doi: 10.1111/epi.14615

63. Porz N, Bauer S, Pica A et al. (2014) Multi-modal glioblastoma segmentation: man versus machine. PLoS ONE 9(5): e96873. doi: 10.1371/journal.pone.0096873

64. Steed TC, Treiber JM, Patel KS et al. (2015) Iterative probabilistic voxel labeling: automated segmentation for analysis of The Cancer Imaging Archive glioblastoma images. AJNR Am J Neuroradiol 36(4): 678–685. doi: 10.3174/ajnr.A4171

Selbständigkeitserklärung

Hiermit erkläre ich, Dr. med. Christian Henker, dass ich die vorliegende Arbeit selbständig angefertigt habe. Alle hier verwendeten Ergebnisse und Daten anderer sind vollständig aufgeführt und korrekt zitiert.

Ich versichere weiterhin, dass die vorliegende Arbeit nicht zuvor bei der hiesigen oder einer anderen Fakultät zur Eröffnung eines Habilitationsverfahrens eingereicht wurde.

Des Weiteren erkläre ich, dass ich die deutsche Staatsbürgerschaft besitze und mir die Habilitationsordnung, sowie alle zugehörigen Bestimmungen bekannt sind.

Rostock, den 15.01.2020 Dr. med. Christian Henker

Originalarbeiten

OA 1: Volumetric quantification of glioblastoma: experiences with different measurement techniques and impact on survival.
Henker C, Kriesen T, Glass Ä, Schneider B, Piek J.
Journal of Neurooncology - 2017.

OA 2: Volumetric assessment of glioblastoma and its predictive value for survival.
Henker C, Hiepel MC, Kriesen T, Scherer M, Glass Ä, Herold-Mende C, Bendszus M, Langner S, Weber MA, Schneider B, Unterberg A, Piek J.
Acta Neurochirurgica – 2019.

OA 3: Correlation of Ki-67 Index with Volumetric Segmentation and its Value as a Prognostic Marker in Glioblastoma.
Henker C, Kriesen T, Schneider B, Glass Ä, Scherer M, Langner S, Erbersdobler A, Piek J.
World Neurosurgery - 2019.

OA4: Effect of 10 different polymorphisms on preoperative volumetric characteristics of glioblastoma multiforme.
Henker C, Kriesen T, Fürst K, Goody D, Glass Ä, Pützer BM, Piek J.
Journal of Neurooncology – 2016.

OA 5: Association between Tumor Compartment Volumes, the Incidence of pretreatment Seizures and Statin-mediated protective Effects in Glioblastoma.
Henker C, Kriesen T, Scherer M, Glass Ä, von Deimling A, Bendszus M, Weber MA, Herold-Mende C, Unterberg A, Piek J.
Neurosurgery - 2019.

J Neurooncol (2017) 135:391–402
DOI 10.1007/s11060-017-2587-5

CLINICAL STUDY

Volumetric quantification of glioblastoma: experiences with different measurement techniques and impact on survival

Christian Henker[1] · Thomas Kriesen[1] · Änne Glass[2] · Björn Schneider[3] · Jürgen Piek[1]

Received: 24 April 2017 / Accepted: 25 July 2017 / Published online: 28 July 2017
© Springer Science+Business Media, LLC 2017

Abstract The potential impact of different radiological features of glioblastoma multiforme (GBM) on overall survival (OS) like tumor volume, peritumoral edema (PTE), necrosis volume, necrosis-tumor ratio (NTR) and edema-tumor ratio (ETR) is still very controversial. To determine the influence of volumetric data on OS und to compare different measuring techniques described in literature. We prospectively evaluated preoperative MR images from 30 patients harboring a primary supratentorial GBM. All patients received gross-total tumor resection followed by standard radiation and chemotherapy (temozolomide). By 3D semi-automated segmentation, we measured tumor volume, necrosis volume, PTE, postoperative residual tumor volume and calculated ETR, NTR and the extent of resection. After critical review of the existing literature we compared alternative measuring techniques with the gold standard of 3D segmentation. Statistical analysis showed a significant impact of the preoperative tumor and necrosis volumes on OS ($p = 0.041$, respectively $p = 0.039$). Furthermore, NTR also showed a significant association with OS ($p = 0.005$). Comparison of previously described measuring techniques and scorings with our results showed that no other technique is reliable and accurate enough as a predictive tool. The critical review of previously published studies revealed mainly inaccurate measurement techniques and patient selection as potential reasons for inconsistent results. Preoperatively measured necrosis volume and NTR are the most important radiological features of GBM with a strong influence on OS. No other measuring techniques are specific enough and comparable with 3D segmentation.

Keywords Glioblastoma · Imaging · Prognostic factors · Survival · Volumetric quantification

Introduction

Glioblastoma multiforme (GBM) is the most prevalent malignant glioma in adults with still the worst prognosis [1]. Despite of ongoing efforts in combination of multimodal treatment with surgical resection followed by radiotherapy, the prognosis and overall survival (OS) is still poor, with a median survival of ~14.6 months [2, 3]. For better assessment of patients harboring GBM several variables predicting the prognosis of these patients have been studied. As clinical variables, the age and the Karnofsky performance status (KPS) of the patients are significant predictors of survival [4, 5]. The extent of resection (EOR) of enhancing tumor during surgery is presumed to be one of the most important and partially controllable factors influencing OS [4, 6–8]. During the last decades, a lot of effort has been made to find an imaging predictor to make the already existing predictors more robust and reliable.

The widespread use of magnetic resonance imaging (MRI) for the diagnosis of GBM can also help assess its pattern; the hallmarks of GBM on MRI are the

Electronic supplementary material The online version of this article (doi:10.1007/s11060-017-2587-5) contains supplementary material, which is available to authorized users.

✉ Christian Henker
Christian.Henker@med.uni-rostock.de

[1] Department of Neurosurgery, University Medicine of Rostock, Schillingallee 35, 18057 Rostock, Germany

[2] Institute for Biostatistics and Informatics in Medicine, University Medicine of Rostock, Ernst-Heydemann-Str. 8, 18057 Rostock, Germany

[3] Institute for Pathology, University Medicine of Rostock, Strempelstraße 14, 18057 Rostock, Germany

contrast-enhancing tumor with its central necrosis and surrounding peritumoral edema (PTE) Each of these tumor segments and size can potentially help us infer into the tumor biology and hopefully its response to different treatments, as well as a potential imaging marker to predict the patients' OS.

One of the first approaches of measuring the tumor volume as a prognostic factor was made by Reeves and Marks in 1979, showing that larger GBMs are associated with decreased in survival time after treatment [9]. Later on volume itself, it has been estimated using formulas to reconstruct the tumor as a spheroid or ellipsoid [10–12]. Pierallini and colleagues showed that a significant correlation between the amount of necrosis within the tumor and OS exists in 1995 [13]. With the help of more subtle and easier available software programs, the volumetric assessment has become readily and quickly available. However, later studies indeed supported these findings, but also found opposing results despite more accurate measurement techniques [4–6, 12, 14–17]. Beside the appealing issue of finding a robust prognostic factor from a non-invasive imaging modality which is already the gold standard, it is very important to be able to accurately quantify the surgical resection of a tumor as it is still the most important prognostic factor for the OS of these patients [4, 6].

To overcome these problems the aim of our study was to test the hypothesis of a possible influence of imaging predictors on the OS, and to reevaluate different measurement techniques against the gold standard of semi-automatic segmentation.

Materials and methods

This study was approved by the local ethics committee according to the Declaration of Helsinki. All subjects gave informed consent.

Patient selection

In this single-institution prospective study, 30 patients older than 18 years with newly diagnosed histologically proven primary GBM were enrolled. Definition of primary GBM was based on *IDH1* mutation status or according to the guideline by Ohgaki and Kleihues [18]. All patients had been treated in our department between January 2012 and December 2014. At the time of the initial MRI scan all patients were steroid-naïve, the lesions were non-cystic, not multifocal and intended surgery was a maximum feasible resection of the tumor. Post-operative MRI was performed within 48 h after surgery. All patients received adjuvant radiotherapy and concomitant chemotherapy with temozolomide according to the EORTC 26981/22981; NCIC CE3 trial [19]. The primary endpoint of our study was the OS, calculated by the difference between time point of surgery and date of tumor-related death of all patients enrolled. All clinical data were taken from the hospitals own records.

The *MGMT* promoter methylation status was determined from formalin-fixed paraffin embedded specimens taken during surgery using MethyLight real-time PCR method as described [20].

MRI acquisition and volumetric analysis

All MRI scans were done in-house (obtained on 1,5- or 3-Tesla scanners) following an exact protocol to avoid bias from diverging imaging procedures. Preoperative scans were done at earliest 1 week before surgery, postoperative scans within 48 h after surgery. Evaluated imaging sequences included 3D postcontrast T1/MPR (Multiplanar Reformation) and 2D precontrast T2/FLAIR (Fluid Attenuated Inversion Recovery). Measured volumes on preoperative MRIs were:

- "tumor": enhancing area on postcontrast T1/MPR reflecting viable tumor with disrupted blood–brain barrier including any region of central necrosis,
- "necrosis": non-enhancing region within the tumor on postcontrast T1/MPR, patients with cystic lesions defined as bright T2/FLAIR signal and low T1/MPR signal were excluded, and
- "PTE": area of hyperintensity on T2/FLAIR sequence reflecting a zone of partly infiltrative tumor as well as vasogenic edema excluding the tumor volume.

Residual tumor volume (RTV) was measured on postoperative 3D pre- and postcontrast T1/MPR sequences, subtracting the precontrast T1/MPR signals within the resection cavity reflecting blood from the postcontrast T1/MPR enhancement which represented the residual tumor. The extent of resection (EOR) was calculated using the following formula: [("tumor"−RTV)/"tumor"]×100%.

Afterwards, ratios were calculated reflecting the relationships between the different tumor proportions towards each other: edema-tumor ratio (ETR, PTE volume divided by the tumor volume) and necrosis-tumor ratio (NTR, Necrosis volume divided by the tumor volume). Qualitative assessment of GBMs included the side and the location of the tumor and functional grading according to Sawaya et al. [21]. Quantitative volumetric measurement was performed in a semi-automated fashion by manually marking the region of interest (ROI) using SmartBrush® (Brainlab, Feldkirchen, Germany).

We searched through the Pubmed database to find representative works of pretreatment volumetric measurements of GBMs. The list of selected papers is not exhaustive and

should give an overview of the recently published results. The selected papers were reviewed and the used measurement techniques were noted for comparison. Descriptive volumetric assessments included PTE and necrosis grading according to Hammoud et al. [10]. To compare calculated values gained from axis measurements of GBM segments we tested four different volume formulas (see supplementary data). For necrosis volume, only cuboid formula was used for calculation. All measurements were performed by the same neurosurgeon (CH) to rule out inter-observer variability.

Statistical analysis

All data were stored and analyzed using SPSS 22.0 software (SPSS, Chicago, IL, USA). Descriptive statistics were computed for continuous and categorical variables. The statistics computed included mean, median, standard deviation (SD), minimum and maximum of continuous variables (outlined as mean ± SD), frequencies and percentages of categorical factors. The Cox proportional hazards regression model was used to assess the independence of OS from categorical prognostic factors. Linear regression analysis was applied to appraise the independence of OS from continuous prognostic factors (volumetric data), because we had no censored OS data. All p values resulted from two-sided statistical tests and values of $p < 0.05$ were considered to be statistically significant. The linear relationship between two variables was evaluated by the most familiar measure of dependence between two quantities, the Pearson correlation coefficient.

Direct comparison of measured volumes was done by a modified Bland-Altman-plot [22]. Originally two different results were plotted as a difference against their arithmetic mean. Because we defined 3D volumetric measurement as the gold standard of measurement the difference against our results were plotted in true values of volume (cm^3). Limits of agreement were calculated with the formula mean value ± 1.96 × SD.

For categorical volume values and the maximum tumor diameter as a one-dimensional value we split our 3D measured volumes into fitting categories and tested the difference in our values by using Cohen's ƙ coefficient [23].

Results

Demographic, clinical, and volumetric characteristics

A total of 30 patients met the inclusion criteria, with an age 61.6 ± 7.92 (range 47–78 years) and a male to female ratio of 1.5:1 representing a typical population harboring a primary GBM (Table 1). Median OS was 16.2 ± 9.45 months, ranged from 3.3 to 49.8 months. KPS was 79.3 ± 17.0 and at median 90%, distribution of the tumor was equal on both sides, 14/30 (46.7%) were situated in the temporal lobe. 63.3% of tumors were located near-eloquent areas according to the definition from Sawaya et al. [21]. Most patients had a low comorbidity index according to Charlson (20/30, 66.7% with 0 points) [24]. A consistent distribution was also observed concerning the RPA classification of patients and the *MGMT* status (10/29 (34.5%) methylated vs 19/29 (65.5%) non-methylated). *MGMT* status could only been validated in 29 of 30 patients due to technical problems. All patients received adjuvant radio- and chemotherapy according to EORTC 26981/22981; NCIC CE3 trial, as required by the inclusion and exclusion criteria [19].

Table 1 Patient characteristics

		n (%)			n (%)
Age, median (range), years		62.5 (47–78)	Tumor location	Temporal	14 (46.7)
Sex	Male	18 (60.0)		Frontal	4 (13.3)
	Female	12 (40.0)		Parietal	9 (30.0)
Charlson index[a]	0	20 (66.7)		Occipital	3 (10.0)
	1	5 (16.7)	Tumor side	Left	15 (50.0)
	2	5 (16.7)		Right	15 (50.0)
KPS, median (range), %		90 (40–100)	Functional grading[b]	I	7 (23.3)
RPA	3	3 (10.0)		II	19 (63.3)
	4	17 (56.7)		III	4 (13.3)
	5	10 (33.3)	*MGMT* status	Meth	10 (34.5)
OS, median (range), days		16.2 (3.3–49.8)		Non-meth	19 (65.5)

KPS Karnofsky performance status, *MGMT* O6-methylguanin-DNA-methyltransferase status (methylated vs. non-methylated), *OS* overall survival, *RPA* recursive partitioning analysis

[a] According to Charlson et al. [24]

[b] According to Sawaya et al. [21]

The volumetric data gained by manual semi-automated measurement is displayed in the supplementary Table 2. The mean tumor volume was 36.7 ± 32.0 cm^3 with a large range of up to 132.5 cm^3. The PTE is mostly double the size than that of the tumor itself (mean ETR 2.45 ± 2.98, respectively median ETR 1.78) and the inner necrosis represented more than a quarter of the tumor (mean NTR 0.22 ± 0.12, respectively median NTR 0.23). Median resection rate was 98.5% as the intended operation was planned as a gross total resection. One patient had an EOR of 67% due to a RTV of 0.871 cm^3 with an initial tumor volume of 2.813 cm^3. The correlation analysis of the volumetric data (Supplementary Table 1) reveals strong coherency between the tumor volume, its adjacent PTE and inner necrosis volume ($r = 0.550$; $p = 0.002$, respectively $r = 0.878$; $p < 0.001$). Otherwise, the ETR was not related to the tumor volume ($r = -0.224$; $p = 0.234$), illustrating the fact that some GBMs involve distinctly larger PTE as compared to others, as it has been shown in a previous work from our institute [25]. The amount of necrosis in relation to the tumor is not dependent on or correlated with the ETR ($r = -0.160$; $p = 0.399$).

Impact on survival

The demographic data of all included patients showed no significant impact on the OS (see Table 2). The Cox regression analysis found no significant difference between the

Table 2 Impact of demographic data, grade of resection and measured volumes on survival

		n (%)	*p* value[a]	HR	Mean OS (m)
Age, years	≤55	7 (23.3)	0.503		20.8 ± 13.8
	>55 to ≤ 65	13 (43.3)	0.687	1.22 (vs. ≤ 55)	16.7 ± 8.41
	>65	10 (33.3)	0.271	1.79 (vs. ≤ 55)	14.2 ± 6.78
Sex	Male	18 (60.0)			16.8 ± 7.65
	Female	12 (40.0)	0.808	1.10 (vs. male)	16.8 ± 12.0
KPS, %	≤70	10 (33.3)	0.376	2.26 (vs. > 90)	17.5 ± 12.6
	>70 to ≤ 90	17 (56.7)	0.234	2.55 (vs. > 90)	15.2 ± 6.88
	>90	3 (10.0)	0.164		23.7 ± 10.2
RPA	Class 3	3 (10.0)	0.415	2.44 (vs. class 5)	13.3 ± 3.61
	Class 4	17 (56.7)	0.203	1.06 (vs. class 5)	16.5 ± 8.12
	Class 5	10 (33.3)	0.885		18.4 ± 12.7
Charlson[b]	0	20 (66.7)	0.285	2.10 (vs. 2)	15.2 ± 10.1
	1	5 (16.7)	0.151	1.28 (vs. 2)	19.8 ± 5.85
	2	5 (16.7)	0.697		20.0 ± 9.56
Functional grading[c]	I	7 (23.3)	0.381		14.3 ± 6.64
	II	19 (63.3)	0.263	0.595 (vs. I)	18.3 ± 10.8
	III	4 (13.3)	0.857	1.12 (vs. I)	14.0 ± 6.12
MGMT	Meth	10 (34.5)			18.9 ± 13.3
	Non-meth	29 (65.5)	0.542	1.28 (vs. meth.)	15.8 ± 7.19
RTV, cm^3	≤2	25 (83.3)			17.7 ± 9.54
	>2	5 (16.7)	0.332	1.63 (vs. ≤ 2)	12.2 ± 8.36
EOR, %	≤95	9 (30.0)	0.512	1.34 (vs. > 98)	15.0 ± 7.44
	>95 to ≤ 98	6 (20.0)	0.351	1.62 (vs. > 98)	15.1 ± 6.54
	>98	15 (50.0)	0.610		18.6 ± 11.5
	Tumor	PTE	Necrosis	ETR	NTR
Pearson´s correlation	0.243	0.774	0.223	0.125	**0.023**
Linear regression[d]	**0.041**	–[a]	**0.039**	–[a]	**0.005**

Statistical significant values are presented in boldtype (significant ≤ 0.05)

EOR extent of resection, *ETR* edema-tumor ratio, *HR* hazard ratios, *KPS* Karnofsky performance status, *m* months, *MGMT* O6-methylguanin-DNA-methyltransferase status (methylated vs. non-methylated), *NTR* necrosis-tumor ratio, *OS* overall survival, *PTE* peritumoral edema, *RPA* recursive partitioning analysis, *RTV* residual tumor volume

[a] *p*-values gained from Cox Regression Analysis for Hazard Ratios (HR)

[b] According to Charlson et al. [24]

[c] According to Sawaya et al. [21]

[d] Both PTE and ETR dropped out during linear regression analysis due to not being significant

different groups stratified for sex, age classes, KPS and RPA classification. Subsequently, a trend was seen in decreased survival for older patients (OS 20.8 ± 13.8 months for age ≤55 years vs. OS 14.2 ± 6.78 months for age >65 years) with a reduced KPS (OS 17.5 ± 12.6 months for KPS ≤70% vs OS 23.7 ± 10.2 months for KPS >90%), the OS distribution in Charlson comorbidity and RPA classes was homogeneous. The functional grading according to Sawaya et al. and *MGMT* promoter status had no impact on the OS [21]. The EOR showed a trend of increased OS correlating to a resection rate of ≥98% of tumor volume, highlighted by the distinct difference of OS from volume of residual tumor (OS 17.4 ± 9.8 months for RTV ≤ 2 cm^3 vs OS 12.0 ± 8.87 months for RTV > 2 cm^3, $p = 0.332$).

For volumetric data (tumor, necrosis, PTE, ETR and NTR) there is only a significant coherency between NTR and the OS in univariate regression analysis ($p = 0.023$) (Table 2). The multiple linear regression analysis (backward elimination) also stated a significant influence of the tumor volume ($p = 0.041$), necrosis volume ($p = 0.039$) and NTR ($p = 0.005$) on OS, while PTE and ETR were dropped from the analysis due to not being significant.

Review of the literature

We found a total number of 15 articles in compliance with our criteria of volumetric analysis of GBMs and their potential impact on the OS (Table 3), and one review regarding the influence of PTE on OS [26]. We divided the matching 15 publications into two categories according to the applied measurement technique; "quantitative analysis" for data gained by a 3D measurement and "descriptive analysis" for volume ratings and the formulas used with axis measurements to reconstruct a 3D model. One focus of reviewing the mentioned papers beside the applied volumetric techniques was patient selection and treatment regimens. Only one paper excluded patients harboring cystic lesions [10], patients with known glucocorticoid medication on initial MRI with potential bias on PTE were excluded in only four publications [10, 16, 27, 28]. We found limitations regarding the measurements techniques used and the treatment regimens in most of the reviewed publications. The obtained results were inconsistent, in six papers the volume of necrosis was not associated with a decrease in OS, while in four papers it showed a significant impact. The other measured tumor compartments were similarly contradictory [4, 29–31].

Comparison of measurement techniques

To compare the different previously published measurement techniques providing 3D reconstruction models we used a modified Bland–Altman plot. The advantage of this method is the visualization of disagreements in the gained data. To reconstruct 3D volume models from major axis measurements of the tumor we used four different formulas as described in the particular papers [10–12, 30] The plots in Fig. 1 show an increasing deviation from the baseline "real" 3D data with rising tumor volume. The limits of agreement are drawn in thin lines within the plots clarifying that there are outliers in every reconstruction model we tested in comparison to our volumetric assessment.

Comparing categorical data like ratings of edema and NTR or the maximum tumor diameter we used Cohen's ƙ coefficient (Table 4) [23]. None of these descriptive values reached a good agreement with our 3D volumes, only the maximum tumor diameter was in moderate accordance.

Discussion

We could clearly demonstrate the importance of pretreatment necrosis and its ratio to the tumor volume (NTR) correlating with decreasing OS in our prospective study of patients undergoing surgical resection of a primary GBM, followed by radio- and chemotherapy.

The presence of necrosis is a histological hallmark of GBM, warranting the malignant tumor grade [32]. A potential hypothesis, why increased necrosis potentially is associated with a decreased OS, was given by Raza et al. [33]. The intratumoral hypoxia selects for a subpopulation of cells with diminished apoptotic potential. These cells that survive hypoxia are likely to proliferate even under apoptosis-inducing therapies causing an increased resistance. Other studies showed that the hypoxic perinecrotic areas within GBMs harbor quiescent stem-like tumor cells, potentially being responsible for the drug- and radioresistance of these tumors, inevitable leading to recurrence [34, 35].

The patient survival was not influenced by KPS, age, Charlson comorbidity index, *MGMT* promoter status or functional grading in our series. These factors are usually considered to affect the OS. Our cohort is highly selected and is evenly distributed regarding pretreatment characteristics of patients and the adjuvant therapies. The selection of patients with omitted influence of these factors on the OS, does not present a bias in our study and thus can serve as a sign of quality regarding the presented subset of GBM patients.

The RTV and EOR also had no significant influence on the OS, although there was a distinct trend. Our stratification into three subgroups of EOR with limits of 95% and 98% of resection possibly also divided the effect of EOR into too small groups loosing statistical strength. Again our highly selected patient cohort leads to an loss of significance of these factors caused by a greater number

Table 3 Review of the literature

Quantitative analyses	Year	n	Exclusion criteria	Therapy	ROI	Measurement technique	Results	Limitations
Lacroix et al. [4]	2001	416	Not mentioned	100% surgery (47% gross-total resection, 53% reductive surgery or biopsy) 100% radiotherapy unknown % of chemotherapy	EOR	Quantitative volumetric measurement	Resection of more than 98% of tumor volume is associated with an increased OAS	Mixed treatment regimens
Zinn et al. [5]	2011	52	Not mentioned	No data available	Edema Enhancing tumor Necrosis	Quantitative volumetric measurement	High edema volume is associated with decreased OAS	No treatment regimens mentioned; analysis after stratification of edema volumes, omitting medium volumes
Iliadis et al. [16]	2012	65	Glucocorticoids at initial MRI	100% surgery (29% biopsy, 51% subtotal res., 20% total res.) 100% radiotherapy 100% chemotherapy	Edema (+tumor) Tumor (+necrosis) Necrosis Net-enhancing tumor	Quantitative volumetric measurement	Edema without significant impact on OAS or PFS; necrosis decreased PFS not OAS, net-enhancing tumor decreased OAS	Mixed treatment regimens; type of surgery did not influence OAS, but high residual tumor volume decreased OAS
Grabowski et al. [6]	2014	128	Not mentioned	100% surgery (resection range: 56.9–100%) 100% radiotherapy 100% chemotherapy	Tumor Net-Enhancing tumor Postop. edema	Quantitative volumetric measurement	Tumor volume, EOR, net-enhancing tumor volume and postop. edema decreased OAS ($2\ cm^3$ and 98% cutoff for residual tumor volume and EOR)	Necrosis not separately analyzed
Wangaryatta -wanich et al. [15]	2015	94	Not mentioned	No data available	Edema Tumor Necrosis ETR NTR	Quantitative volumetric measurement VASARI features	Edema ($\geq 85\ cm^3$) and enhancing tumor volume with decreased OAS; but no significance after age & KPS adjustment; necrosis without impact on OAS	No treatment regimens mentioned; analysis after stratification and formation of subgroups
Descriptive analyses	**Year**	**n**	**Exclusion criteria**	**Therapy**	**ROI**	**Measurement technique**	**Results**	**Limitations**
Pierallini et al. [13]	1996	18	Not mentioned	100% surgery (10% total resection, 90% subtotal resection or biopsy) 100% radiotherapy	Edema	Severe or mild edema (no clear definition)	Extent of edema had no effect on OAS	No clear edema definition, heterogenous patient selection
					Tumor	Maximum diameter (cm)	Maximum diameter of tumor had no effect on OAS	
					Necrosis	Ratio of presumed necrosis and tumor area	Necrosis/tumor-ratio ≥ 0.5 decreased OAS	

Table 3 (continued)

Descriptive analyses	Year	n	Exclusion criteria	Therapy	ROI	Measurement technique	Results	Limitations
Hammoud et al. [10]	1996	48	Cystic lesion, multifocal disease, glucocorticoids at initial MRI	100% surgery (100% Gross-total resection) 100% radiotherapy 100% chemotherapy	Edema	I = amount of edema is less than tumor volume II = amount of tumor and edema are equal III = edema is greater than tumor volume	Extent of edema correlated with decreased OAS	
					Tumor	$V = \pi(a \cdot b \cdot c)/6$	Tumor volume had no effect on OAS	
					Necrosis	0 = no necrosis I = necrosis is less than 25% of tumor volume II = necrosis is 25–50% of tumor volume III = amount of necrosis is >50% of tumor	Amount of necrosis correlated with decreased OAS	
Xue and Albright [12]	1999	99	Not mentioned	100% surgery (41% "maximum feasible resection", 59% biopsy) 87% radiotherapy 59% chemotherapy	Tumor	$1 = 4/3\ \pi\ r^3$ (r = radius of maximum cross sectional diameter) $2 = 4/3\ \pi\ a \cdot b \cdot c$ (a = max. cross sectional diameter, b = max. perpendicular diameter to a, c = number of CT-scan slices)	Tumor volume had no effect on OAS; strong correlation between both measurement techniques	Only CT-scans; 20% anaplastic astrocytoma/80% GBM (with separate statistical analysis); unknown EOR; stratification of tumor volume (cut-off 34 cm^3)
Lacroix et al. [4]	2001	416	Not mentioned	100% surgery (47% gross-total resection, 53% cytoreductive surgery or biopsy) 100% radiotherapy Unknown % of chemotherapy	Edema	0 = no edema I = amount of edema is less than tumor volume II = amount of tumor and edema are equal III = edema is greater than tumor volume	In univariate analysis extent of edema decreased OAS, which disappeared when adjusted to other significant predictors in multivariate analysis	Comparison only between edema grade 0 + I and II + III subgroups, necrosis between 0 and I-III; unknown number of chemotherapy treatments
					Necrosis	Adapted from Hammoud et al. (see above)	Amount of necrosis correlated with decreased OAS	

Table 3 (continued)

Descriptive analyses	Year	n	Exclusion criteria	Therapy	ROI	Measurement technique	Results	Limitations
Pope et al. [29]	2005	110	Not mentioned	100% surgery (approximately 25% biopsy) "Mostly" radiotherapy "Mostly" chemotherapy	Edema	0 = no edema I = edema extends < 1 cm perilesional II = edema extends > 1 cm perilesional	Extent of edema correlated with decreased OAS	Tumor volume not analyzed; unknown chemo- and radiotherapy numbers; 40.9% of patients alive at the time of analysis
					Necrosis	0 = no necrosis I = necrosis	Presence of necrosis does not affect OAS	
					EOR	Estimation (<20%, 20–89%, 90–99%, 100%)	EOR without impact on OAS	
Ramnarayan et al. [30]	2007	121	Multifocal disease Mixed or variant histology	100% surgery (23.1% "surgical excision", 76.9% biopsy) 75.2% radiotherapy 20.7% chemotherapy	Edema	0 = no edema I = edema extents < 5 cm perilesional II = edema extents > 5 cm perilesional	Extent of edema (>5 cm) correlated with decreased OAS	19% WHO Grade III tumors, 81% Grade IV Gliomas; no difference between Grade III & IV tumors in OAS; no difference between biopsy and resection on OAS; 74,4% CT-Scans, 25,6% MRI
					Tumor	Product of largest perpendicular diameters (cm^2)	Tumor size correlated with decreased OAS	
Schoenegger et al. [27]	2009	109	Glucocorticoids on initial MRI	100% surgery (33% total resection, 53.2% subtotal resection, 13.6% biopsy) 85.3% radiotherapy 78% chemotherapy	Edema	I = edema extends ≤ 1 cm perilesional II = edema extends > 1 cm perilesional	Extent of edema (>1 cm) correlated with decreased OAS	Tumor size only measured in 56 cases; stratification of tumor size (cut-off 4 cm)
					Tumor	Largest diameter in cm on T2-weighted images	Tumor size had no effect on OAS	
Li et al. [31]	2012	30	Not mentioned	100% surgery (no definition what kind of operation), 100% radiotherapy 100% chemotherapy	Edema	I = no edema II = edema	Detection of edema is correlated with decreased OAS (univariate analysis)	Surgical treatment not defined or mentioned

Table 3 (continued)

Descriptive analyses	Year	n	Exclusion criteria	Therapy	ROI	Measurement technique	Results	Limitations
Gutman et al. [14]	2013	75	Not mentioned	no data available	Edema VASARI features	Estimated proportion of edema: 0%, <5%, 6–33%, 34–67%, 68–95%, >95%, 100%	Proportion of edema is not correlated with decreased OAS	No measurement, only estimation of edema volume; no survival data nor treatment plans published; tumor volume includes total FLAIR abnormality
					Tumor	Major axis length (mm) on T2-weighted FLAIR imaging + edema	Major axis length of total lesion correlates with decreased OAS	
					Necrosis	Estimated proportion of necrosis: 0%, <5%, 6–33%, 34–67%, 68–95%, >95%, 100%	Proportion of necrosis is not correlated with decreased OAS	
Nestler et al. [11]	2015	83	Not mentioned	100% surgery (100% total resection) 100% radiotherapy 100% chemotherapy	Edema	Circular = yes/no if surrounding the whole tumor	Circular edema had no effect on OAS	Very specific edema definition; little information about patient and survival data
					Tumor	$V = 4/3\ \pi\ a \cdot b \cdot c$ Cysts were noted and the largest one was measured (ml)	Tumor volume had no effect on OAS, detection of cysts had no influence OAS	
					Necrosis NTR	$V = 4/3\ \pi\ a \cdot b \cdot c$	Necrosis volume is not correlated with decreased OAS, neither NTR	
Wu et al. [28]	2015	87	Biopsy glucocorticoids on initial MRI	100% surgery (100% Gross-total resection) 82.8% radiotherapy 62% chemotherapy	Edema	Adapted from Schoenegger et al. (see above)	Extent of edema (≥1 cm) correlated with decreased OAS	Stratification of tumor diameter (cut-off 5 cm)
					Tumor	Largest diameter in cm on T2-weighted images	Tumor diameter had no effect on OAS	
					Necrosis	I = no necrosis II = necrosis	Presence of necrosis is correlated with decreased OAS	

ETR edema-tumor ratio, *NTR* necrosis-tumor ratio, *OAS* overall survival, *PTE* peritumoral edema, *ROI* region of interest

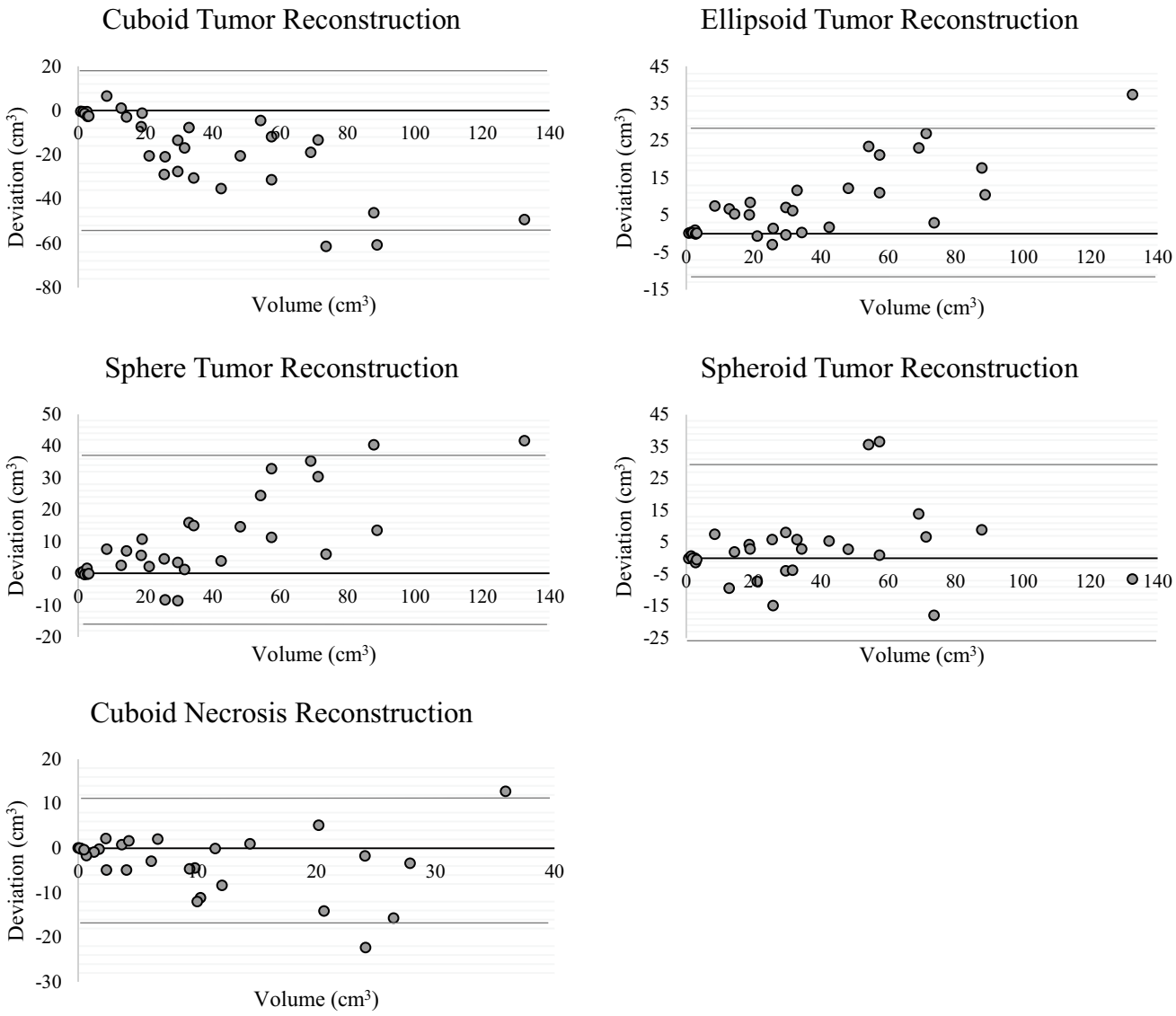

Fig. 1 Comparison of different volume reconstruction models with "true" volumetric data via Bland–Altman plots. Horizontal data represents "true"/3D volumetric data gained from semi-automated segmentation, vertical values displaying the deviation from "true" data; limits of agreement are indicated by thin lines encompassing the values

Table 4 Agreement of categorical data and "true" values

	ƙ[a]	Annotation
Maximum diameter of tumor	0.601	= Moderate agreement
Hammoud rating of edema[b]	0.267	= Light agreemente
Hammoud rating of necrosis-tumor ratio[b]	0.095	= Very weak agreement

[a] According to Cohen's ƙ coefficient [23]

[b] According to Hammoud et al. [10]

of patients with lesser EOR and greater RTV. The cut-off value of 2 cm^3 for RTV was chosen according to the work of Grabowski et al. and Chaichana et al. [6, 36]. It is contestable if it can be used as a general cut-off point for residual tumor volumes. According to the work of Grabowski and colleagues, our experience also supports the importance of RTV rather than EOR, not reflecting the remaining tumor burden. Therefore, the functional grading, according to Sawaya et al., is also not advantageous as a predictive marker [21]. A tumor located in an eloquent area may not be accessible for gross total resection. In this case, regardless of tumor site, RTV is more important than location/functional grading alone as confirmed by our data. Again, showing that EOR had no impact on OS in our cohort is not a general statement, but shows the uniform surgical treatment of all enrolled patients.

Furthermore, our data showed no impact of the PTE on OS. PTE harbors an infiltration zone of the tumor containing stem-like GBM cells and not only a reactive edema, giving an explanation why recurrence of GBM mostly occurs at the margin of resection [37, 38]. Thus, it seems as a logical conclusion that a large PTE or ETR leads to a decrease in the OS. Zinn and colleagues stated that peritumoral FLAIR signal abnormality "captures a distinct aspect of tumor biology largely independent of tumor size and volumes of necrosis" [5]. They found a positive correlation between contrast enhancement volumes ("active tumor") and FLAIR abnormality, but not between FLAIR and necrosis volumes. In our cohort, we found a significant correlation between PTE and both volumes, tumor ($p = 0.002$) and necrosis ($p = 0.002$). Vice versa the ETR is not correlated with any of the other tumor compartments and without significant impact on OS in general.

Tumor volume showed no influence on the OS in our cohort which is in accordance with most of the reviewed publications. Similarly, the problem of PTE influenced by glucocorticoids, including cystic GBMs can largely affect tumor and necrosis volume. Only one of the 15 analyzed studies excluded cystic lesions [10].

A "conditio sine qua non" for all these analyses is an exact measurement technique. The visual comparison we utilized by frequently used 3D reconstruction models, calculated from 2D axis measurements, showed a constant deviation from "real" values from our 3D measurements. The difference of measured volumes is enlarged with rising tumor or necrosis volumes, revealing the inability of each reconstruction model to display the complex and always asymmetrical morphology of the tumor. We used a quantitative, semi-automated segmentation available within a standard neuronavigation software. The advantage of this method is a manual selection of the ROI supported by the software via contour expansion. One aspect of every user-dependent tumor segmentation, regardless of the method used, is inter-observer variability [6, 39]. The diverging assessments of every tumor segment can only be solved by a fully automated segmentation. In our opinion up to now, no such program is available, beside promising data for enhancing tumor segments from other colleagues [40].

Besides the measurement techniques itself, the key is the quality of source data. To gain maximum accuracy, all analyzed MRI scans should be obtained following the same protocol and the slice thickness as well as the gap between each slice especially must be as thin as possible. For tumor and necrosis segmentation we used a slice thickness of 0.9 mm, but most of the published data lack this information or use a much larger slice thickness (3–6 mm). A lot of recent studies use data from The Cancer Imaging Archive (TCIA) from a patient cohort of The Cancer Genome Atlas (TCGA) [5, 14, 15, 41]. Being easily available with a large number of data and imaging series from a lot of different centers makes it very appealing. As TCIA states on their own homepage, "image data sets are also extremely heterogeneous in terms of scanner modalities, manufacturers and acquisition protocols". If not precisely matched, the value of the MRI source data is limited.

One limitation of our study is the small sample size. To overcome this drawback, a multi-center follow-up study has already been conducted, giving us a deeper insight into the potential and applicability of 3D volumetric assessments of GBMs.

Conclusion

Our comprehensive analysis of pretreatment imaging variables highlighted the significance of necrosis of GBM for the OS in a very uniform patient cohort. Additionally, we could demonstrate that a semi-automated 3D volumetric assessment of all tumor compartments is the only reliable and accurate measurement technique compared to others recently described. Volumetric assessment is inalienable for pretreatment analysis and resection control and should therefore be included not only in the field of research but also in routine clinical practice.

Compliane with ethical standards

Conflict of interest The authors have nothing to disclose and no conflicts of interest.

References

1. Ostrom QT, Bauchet L, Davis FG et al (2014) The epidemiology of glioma in adults: a "state of the science" review. Neuro Oncol 16(7):896–913. doi:10.1093/neuonc/nou087
2. Stupp R, Hegi ME, Mason WP et al (2009) Effects of radiotherapy with concomitant and adjuvant temozolomide versus radiotherapy alone on survival in glioblastoma in a randomised phase III study: 5-year analysis of the EORTC-NCIC trial. Lancet Oncol 10(5):459–466. doi:10.1016/S1470-2045(09)70025-7
3. Weller M, van den Bent M, Hopkins K et al (2014) EANO guideline for the diagnosis and treatment of anaplastic gliomas and glioblastoma. Lancet Oncol 15(9):e395–e403. doi:10.1016/S1470-2045(14)70011-7
4. Lacroix M, Abi-Said D, Fourney DR et al (2001) A multivariate analysis of 416 patients with glioblastoma multiforme: prognosis, extent of resection, and survival. J Neurosurg 95(2):190–198. doi:10.3171/jns.2001.95.2.0190
5. Zinn PO, Mahajan B, Sathyan P et al (2011) Radiogenomic mapping of edema/cellular invasion MRI-phenotypes in glioblastoma multiforme. PLoS ONE 6(10):e25451. doi:10.1371/journal.pone.0025451
6. Grabowski MM, Recinos PF, Nowacki AS et al (2014) Residual tumor volume versus extent of resection: predictors of survival after surgery for glioblastoma. J Neurosurg 121(5):1115–1123. doi:10.3171/2014.7.JNS132449

7. Stummer W, Pichlmeier U, Meinel T et al (2006) Fluorescence-guided surgery with 5-aminolevulinic acid for resection of malignant glioma: a randomised controlled multicentre phase III trial. Lancet Oncol 7(5):392–401. doi:10.1016/S1470-2045(06)70665-9
8. Li YM, Suki D, Hess K et al (2016) The influence of maximum safe resection of glioblastoma on survival in 1229 patients: can we do better than gross-total resection? J Neurosurg 124(4):977–988. doi:10.3171/2015.5.JNS142087
9. Reeves GI, Marks JE (1979) Prognostic significance of lesion size for glioblastoma multiforme. Radiology 132(2):469–471. doi:10.1148/132.2.469
10. Hammoud MA, Sawaya R, Shi W et al (1996) Prognostic significance of preoperative MRI scans in glioblastoma multiforme. J Neurooncol 27(1):65–73
11. Nestler U, Lutz K, Pichlmeier U et al (2015) Anatomic features of glioblastoma and their potential impact on survival. Acta Neurochir 157(2):179–186. doi:10.1007/s00701-014-2271-x
12. Xue D, Albright RE Jr (1999) Preoperative anaplastic glioma tumor volume effects on patient survival. J Surg Oncol 72(4):199–205
13. Pierallini A, Bonamini M, Osti MF et al (1996) Supratentorial glioblastoma: neuroradiological findings and survival after surgery and radiotherapy. Neuroradiology 38(Suppl 1):30
14. Gutman DA, Cooper LAD, Hwang SN et al (2013) MR imaging predictors of molecular profile and survival: multi-institutional study of the TCGA glioblastoma data set. Radiology 267(2):560–569. doi:10.1148/radiol.13120118
15. Wangaryattawanich P, Hatami M, Wang J et al (2015) Multicenter imaging outcomes study of the cancer genome atlas glioblastoma patient cohort: imaging predictors of overall and progression-free survival. Neuro Oncol 17(11):1525–1537. doi:10.1093/neuonc/nov117
16. Iliadis G, Kotoula V, Chatzisotiriou A et al (2012) Volumetric and MGMT parameters in glioblastoma patients: survival analysis. BMC Cancer 12:3. doi:10.1186/1471-2407-12-3
17. Crawford FW, Khayal IS, McGue C et al (2009) Relationship of pre-surgery metabolic and physiological MR imaging parameters to survival for patients with untreated GBM. J Neurooncol 91(3):337–351. doi:10.1007/s11060-008-9719-x
18. Ohgaki H, Kleihues P (2013) The definition of primary and secondary glioblastoma. Clin Cancer Res 19(4):764–772. doi:10.1158/1078-0432.CCR-12-3002
19. Mirimanoff R-O, Gorlia T, Mason W et al (2006) Radiotherapy and temozolomide for newly diagnosed glioblastoma: recursive partitioning analysis of the EORTC 26981/22981-NCIC CE3 phase III randomized trial. J Clin Oncol 24(16):2563–2569. doi:10.1200/JCO.2005.04.5963
20. Eads CA, Danenberg KD, Kawakami K et al (2000) MethyLight: a high-throughput assay to measure DNA methylation. Nucleic Acids Res 28(8):E32
21. Sawaya R, Hammoud M, Schoppa D et al (1998) Neurosurgical outcomes in a modern series of 400 craniotomies for treatment of parenchymal tumors. Neurosurgery 42(5):1044–1055 (discussion 1055-6)
22. Bland JM, Altman DG (1999) Measuring agreement in method comparison studies. Stat Methods Med Res 8(2):135–160
23. Cohen J (1968) Weighted kappa: nominal scale agreement with provision for scaled disagreement or partial credit. Psychol Bull 70(4):213–220
24. Charlson ME, Pompei P, Ales KL et al (1987) A new method of classifying prognostic comorbidity in longitudinal studies: development and validation. J Chronic Dis 40(5):373–383
25. Henker C, Kriesen T, Furst K et al (2016) Effect of 10 different polymorphisms on preoperative volumetric characteristics of glioblastoma multiforme. J Neurooncol 126(3):585–592. doi:10.1007/s11060-015-2005-9
26. Liu S-Y, Mei W-Z, Lin Z-X (2013) Pre-operative peritumoral edema and survival rate in glioblastoma multiforme. Onkologie 36(11):679–684. doi:10.1159/000355651
27. Schoenegger K, Oberndorfer S, Wuschitz B et al (2009) Peritumoral edema on MRI at initial diagnosis: an independent prognostic factor for glioblastoma? Eur J Neurol 16(7):874–878. doi:10.1111/j.1468-1331.2009.02613.x
28. Wu C-X, Lin G-S, Lin Z-X et al. (2015) Peritumoral edema on magnetic resonance imaging predicts a poor clinical outcome in malignant glioma. Oncol Lett 10(5):2769–2776. doi:10.3892/ol.2015.3639
29. Pope WB, Sayre J, Perlina A et al (2005) MR imaging correlates of survival in patients with high-grade gliomas. AJNR Am J Neuroradiol 26(10):2466–2474
30. Ramnarayan R, Dodd S, Das K et al (2007) Overall survival in patients with malignant glioma may be significantly longer with tumors located in deep grey matter. J Neurol Sci 260(1–2):49–56. doi:10.1016/j.jns.2007.04.003
31. Li W-B, Tang K, Chen Q et al. (2012) MRI manifestions correlate with survival of glioblastoma multiforme patients. Cancer Biol Med 9(2):120–123. doi:10.3969/j.issn.2095-3941.2012.02.007
32. Louis DN, Perry A, Reifenberger G et al (2016) The 2016 World Health Organization Classification of Tumors of the central nervous system: a summary. Acta Neuropathol 131(6):803–820. doi:10.1007/s00401-016-1545-1
33. Raza SM, Lang FF, Aggarwal BB et al (2002) Necrosis and glioblastoma: a friend or a foe? A review and a hypothesis. Neurosurgery 51(1):2–12 (discussion 12–3)
34. Ishii A, Kimura T, Sadahiro H et al (2016) Histological characterization of the tumorigenic "Peri-Necrotic Niche" harboring quiescent stem-like tumor cells in glioblastoma. PLoS ONE 11(1):e0147366. doi:10.1371/journal.pone.0147366
35. Fidoamore A, Cristiano L, Antonosante A et al. (2016) Glioblastoma stem cells microenvironment: the paracrine roles of the niche in drug and radioresistance. Stem Cells Int. doi:10.1155/2016/6809105
36. Chaichana KL, Cabrera-Aldana EE, Jusue-Torres I et al. (2014) When gross total resection of a glioblastoma is possible, how much resection should be achieved? World Neurosurg 82(1–2):e257–65. doi:10.1016/j.wneu.2014.01.019
37. Chen J, Li Y, Yu T-S et al (2012) A restricted cell population propagates glioblastoma growth after chemotherapy. Nature 488(7412):522–526. doi:10.1038/nature11287
38. Eidel O, Burth S, Neumann J-O et al (2017) Tumor infiltration in enhancing and non-enhancing parts of glioblastoma: a correlation with histopathology. PLoS ONE 12(1):e0169292. doi:10.1371/journal.pone.0169292
39. Odland A, Server A, Saxhaug C et al (2015) Volumetric glioma quantification: comparison of manual and semi-automatic tumor segmentation for the quantification of tumor growth. Acta Radiol 56(11):1396–1403. doi:10.1177/0284185114554822
40. Porz N, Habegger S, Meier R et al (2016) Fully automated enhanced tumor compartmentalization: man vs. machine reloaded. PLoS ONE 11(11):e0165302. doi:10.1371/journal.pone.0165302
41. Mazurowski MA, Desjardins A, Malof JM (2013) Imaging descriptors improve the predictive power of survival models for glioblastoma patients. Neuro Oncol 15(10):1389–1394. doi:10.1093/neuonc/nos335

Acta Neurochirurgica (2019) 161:1723–1732
https://doi.org/10.1007/s00701-019-03966-6

ORIGINAL ARTICLE - BRAIN TUMORS

Volumetric assessment of glioblastoma and its predictive value for survival

Christian Henker[1] · Marie Cristin Hiepel[1] · Thomas Kriesen[1] · Moritz Scherer[2] · Änne Glass[3] · Christel Herold-Mende[2] · Martin Bendszus[4] · Sönke Langner[5] · Marc-André Weber[5] · Björn Schneider[6] · Andreas Unterberg[2] · Jürgen Piek[1]

Received: 21 April 2019 / Accepted: 29 May 2019 / Published online: 28 June 2019
© Springer-Verlag GmbH Austria, part of Springer Nature 2019

Abstract

Background The objective of this study was to evaluate the morphology of glioblastoma on structural pretreatment magnetic resonance imaging (MRI), defining imaging prognostic factors.

Method We conducted a retrospective analysis of MR images from 114 patients harboring a primary glioblastoma, derived from two neurosurgical departments. Tumor segmentation was carried out in a semi-automated fashion. Tumor compartments comprised contrast-enhancing volume (CEV+), perifocal hyperintensity on fluid-attenuated inversion recovery (FLAIR) images (FLAIR+) excluding CEV+, and a non-enhancing area within the CEV+ lesion (CEV−). Additionally, two ratios were calculated from these volumes, the edema-tumor ratio (ETR) and necrosis-tumor ratio (NTR). All patients received surgical resection, followed by concomitant radiation and chemotherapy.

Results Tumor segmentation revealed the strongest correlation between the CEV+ volume and the CEV−, presenting intratumoral necrosis ($p < 0.001$). The relation between the tumor surrounding the FLAIR+ area and the CEV+ volume and the ETR is inversely correlated ($p = 0.001$). The most important prognostic factor in multivariable analysis was NTR (HR 2.63, $p = 0.016$). The cut-off value in our cohort for NTR was 0.33, equivalent to a decrease in survival if the necrotic core of the tumor (CEV−) accounts for more than 33% of the tumor mass itself (CEV+).

Conclusions Our data emphasizes the importance of the necrosis-tumor ratio as a biomarker in glioblastoma imaging, rather than single tumor compartment volumes. NTR can help to identify a subset of tumors with a higher resistance to therapy and a dismal prognosis.

This article is part of the Topical Collection on *Brain Tumors*

Electronic supplementary material The online version of this article (https://doi.org/10.1007/s00701-019-03966-6) contains supplementary material, which is available to authorized users.

✉ Christian Henker
Christian.Henker@med.uni-rostock.de

[1] Department of Neurosurgery, University Medicine of Rostock, Schillingallee 35, 18055 Rostock, Germany

[2] Department of Neurosurgery, Heidelberg University Hospital, Heidelberg, Germany

[3] Institute for Biostatistics and Informatics in Medicine, University Medicine of Rostock, Rostock, Germany

[4] Department of Neuroradiology, Heidelberg University Hospital, Heidelberg, Germany

[5] Institute of Diagnostic and Interventional Radiology, Pediatric Radiology and Neuroradiology, University Medicine of Rostock, Rostock, Germany

[6] Institute for Pathology, University Medicine of Rostock, Rostock, Germany

Keywords Glioblastoma · Magnetic resonance imaging · Necrosis · Neuroimaging · Prognosis · Survival

Introduction

Glioblastoma is the most aggressive yet most common intrinsic adult brain tumor [24]. In recent decades, the prognosis of patients with glioblastoma has improved. Despite increased knowledge regarding the genetic and epigenetic characteristics of this tumor, we do not yet fully understand or control this pathology.

Magnetic resonance imaging (MRI) is the gold standard for detection and assessment of every tumor within the brain. The main advantages of MRI are its superior and non-invasive presentation of all soft tissue tumor compartments in a spatial manner, which is essential during neurosurgical treatment planning [36]. Furthermore, pathophysiological patterns can be visualized, such as the intratumoral blood flow, cellular density, and central necrosis [2, 21]. By repeated assessment,

the response of the tumor to treatment regimens can also be visualized, as well as the extent of resection (EOR) or the residual tumor volume (RTV) after surgical resection. The typical imaging sequences gathered during anatomical MR imaging are pre-gadolinium T1, post-gadolinium T1, T2-weighted imaging, and spin echo T2 fluid-attenuated inversion recovery (FLAIR), ideally obtained with 3D sequences [8]. The contrast enhancement typically appears as an irregularly shaped ring–enhancing mass, representing a breakdown of the blood-brain barrier (BBB) from the tumor-induced angiogenesis [5, 16]. The inner part usually shows no contrast enhancement, representing the decayed or necrotic core of the tumor. In most cases, the area of contrast enhancement is surrounded by a mixture of vasogenic edema and tumor cell infiltration [7, 27]. Because nearly all patients with glioblastoma will receive an MRI initially and during treatment, qualitative imaging characteristics have already been evaluated as prognostic factors for overall survival (OS), distinguishing between more or less invasive tumors, or to predict the response to therapy [10, 17, 26]. With an ongoing refinement of the resolving capacities and increasing availability of MRI scans, additional quantitative markers were introduced, such as tumor compartment volumes [17]. However, the results have often been inconsistent because of the use of different measurement techniques or patient cohorts [13].

As every glioblastoma appears to be unique in its imaging morphology and its histological components and response to treatment, here we aimed to define robust imaging prognostic factors for OS within the scope of the existing literature. To overcome limitations from previous studies, we wanted to define a very consistent patient cohort regarding the applied treatment regimes. Glioblastoma segmentation is challenging due to the heterogeneous morphology on pretreatment MRI. The used measurement technique was already evaluated as being superior to others [13]. Additionally, we wanted to report a more precise view of the relationship between the different tumor compartments.

Methods and materials

Study design

The study was conducted at two neurosurgical university departments. The protocol was approved by both the Institutional Review Boards and Ethics Committees according to the Declaration of Helsinki in its present form. Informed consent was obtained from all participants. The STROBE statement checklist for cohort studies was used as a reporting guideline.

For inclusion into our retrospective study, patients had to be older than 18 years and harboring a supratentorial and histological proven *IDH-1* wild-type glioblastoma, based on IDH-1 R132 mutation status [4]. Only patients after surgical resection were included; the residual tumor burden had to be < 3 cm^3 (following Sales et al. [29]), as proven by postoperative volumetric analysis. All patients received adjuvant radiation therapy and concomitant chemotherapy with temozolomide, according to the Stupp protocol [30]. The primary endpoint of the study was the OS, calculated as the difference between the time point of surgery and the date of tumor-related death of the patient or the end of the study (January 2018). If patients died before completion of the Stupp protocol, they were not excluded according to the initial study [31]. All clinical data were taken from the hospital records, including demographic data, reoperation during the study, implantation of carmustine (BCNU) wafer during surgery, and chemotherapies in addition to the Stupp protocol. Furthermore, the Karnofsky performance status (KPS) at admission and the age-adjusted Charlson comorbidity index score were measured [3, 15]. For statistical analysis, data were partly grouped as follows: age (< 60 years, ≥ 60 years), Charlson comorbidity index (≤ 2, 3–4, ≥ 5), and KPS ($\geq 80\%$, $< 80\%$). The *MGMT* promoter methylation status was determined from formalin-fixed paraffin-embedded specimens obtained during surgery and by using the MethyLight real-time PCR method, as previously described [6]. The STROBE statement checklist for cohort studies was used as a reporting guideline.

MRI analyses

Preoperative MRI scans were obtained at least 1 week before surgery, and postoperative scans were obtained within 48 h after surgery (1 T and 5 T or 3 T). At the time of the initial MRI scan, all patients were steroid-naive, excluding the potential bias of glucocorticoids on edema volume. The minimum MRI protocol consisted of unenhanced and contrast-enhanced 3D T1-weighted (T1w) MPRage datasets with 1-mm isotropic voxel size and secondary multiplanar reformation (MPR) in all three planes, with 1-mm slice thickness, and 2D pre-contrast T2-weighted (t2w) and FLAIR images. In addition to qualitative data (affected lobe and hemisphere), semi-automated volumetric measurement techniques were used, as previously described [13]. In brief, the region of interest (ROI) was manually marked with the aid of a contour expansion algorithm (SmartBrush®, Brainlab AG, Feldkirchen, Germany). Derived volumes were (i) contrast-enhancing volume (CEV+) on post-contrast T1w images, including the central non-enhancing area (appropriate to the former designation "tumor"), (ii) hyperintensity on FLAIR images surrounding the lesion (FLAIR+) excluding the CEV ("edema"), and (iii) the non-enhancing area within the CEV+ lesion (CEV−) on post-contrast T1w images ("necrosis"). The volume of tumor cysts (typically appearing with a bright signal on T2w within the tumor, well-circumscribed, and corresponding to a low signal on T1w) was also measured and finally subtracted from

the initial tumor volume. Finally, for a better representation of the relationship between the different tumor compartments, two ratios were calculated: the edema-tumor ratio (ETR; edema volume divided by tumor volume) and the necrosis-tumor ratio (NTR; necrosis divided by tumor volume). To assess the RTV on postoperative MR datasets, plain T1w images were semi-automatically subtracted from the post-contrast T1w dataset using the vendor's software (Syngo VB 17, Siemens, Erlangen, Germany) to differentiate postoperative hemorrhage within the resection cavity from contrast enhancement reflecting residual CEV+. Figure 1 illustrates parts of the preoperative planning with an integrated volumetric assessment of a typical glioblastoma patient. All measurements were performed by an experienced physician, blinded to the outcome data.

Statistical analyses

Descriptive statistics computed for continuous variables include mean ± standard deviation (SD) or, if skewed, median with the interquartile range (IQR; Q1, Q3). The distributions of the independent groups are shown as boxplots with additionally indicated sample means (by "x"). For categorical variables, frequencies and proportions (%) are given. The *U*-test was performed to compare independent groups, and Spearman's correlation coefficient was computed and tested to be zero to assess associations between volumes and respective ratios. The Cox proportional hazards model was used to assess the independence of OS from prognostic factors by estimating hazard ratios (HR) and their 95% confidence intervals (95% CI) and testing HRs to be 1. First, univariate analyses were performed for several candidate factors. Variables with small p values were selected for a multiple approach to calculating adjusted HRs, 95% CIs, and p values reflecting associations between OS and influencing factors. This analysis was adjusted for RTV as a covariate. A single-institute analysis was added to the analysis of the whole bi-centric study as an internal validation (Supplementary Table 1). The significance level was set to $\alpha = 0.05$.

All data were processed using IBM Corp (version 24.0, IBM SPSS Advanced Statistics for Windows, Armonk, NY).

Results

A total of 114 patients were included in our bi-centric cohort study. The mean age was 61.9 ± 9.08 years with a male-to-female ratio of 1.85:1 (Table 1), which is comparable to

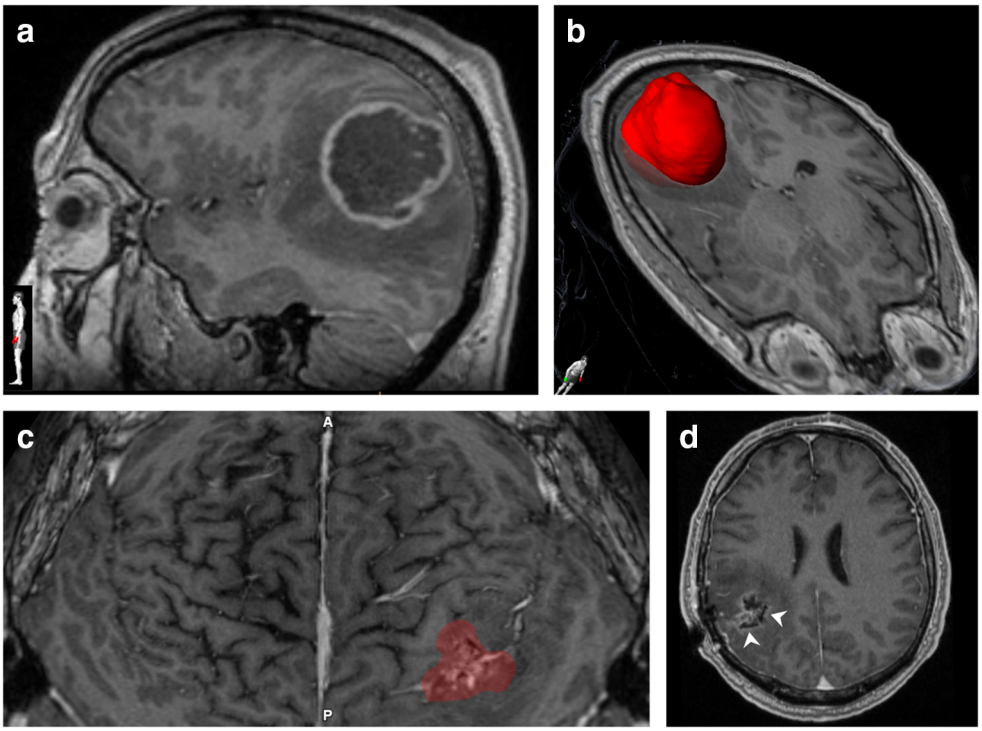

Fig. 1 Example of a volumetric assessment during surgical planning of a glioblastoma patient. **a** Post-contrast T1w MRI in the sagittal plane of a 53-year-old male patient. The tumor was situated within the right parietal lobe. **b** After volumetric measurement, the surface of the CEV+ part of the tumor can be fully visualized within all MRI slices and planes (CEV+ = 51.28 cm^3, FLAIR+ = 159.1 cm^3, CEV− = 30.70 cm^3, ETR = 3.103, NTR = 0.599). **c** Mercator projection of the brain surface viewed from above for the neurosurgical planning. The CEV+ is translucent visible and is situated behind the central sulcus. **d** Postoperative MRI (post-contrast T1W) confirming a gross total resection; four carmustine wafers were implanted during surgery (two of them are marked with white arrows). The OS of the patient was 25.53 months, and a concomitant radio- and chemotherapy according to the Stupp scheme followed the resection

Table 1 Patient characteristics

		n (%)
Age	Mean ± SD (range) (years)	61.9 ± 9.08 (31–81)
Sex	Male	74 (64.9)
	Female	40 (35.1)
Charlson index	1	71 (62.3)
	2	35 (30.7)
	3	8 (7)
KPS	Median (Q1; Q3) (%)	85 (70; 90)
MGMT status	Meth.	28 (43.1)
	Non-meth.	37 (56.9)
Reoperation		25 (21.9)
Carmustin wafer		35 (30.7)
Add. chemotherapy		42 (36.8)
OS	Median (Q1; Q3) (months)	14.72 (11.3; 21.3)

KPS = Karnofsky performance status; OS = overall survival; Q1 = 25% quantile/lower quartile; Q3 = 75% quantile/upper quartile; SD = standard deviation

previous patient cohorts. [1]. The age-adjusted Charlson comorbidity index was low in 62.3% (≤ 2), appropriate to the age of our study population. The KPS ranged between 40 and 100%, with a median value of 85%.

The most common affected lobe by the glioblastoma was the temporal lobe (41.2%; 47/114), followed by the frontal (29.8%; 34/114) and parietal (20.2%; 23/114) lobe (Table 2). The hemispheric distribution was nearly equal, with 50% left-sided (57/114) and 49.1% right-sided (56/114) tumors; one tumor was bilaterally located (0.9%). Cystic components within the CEV+ mass were detected in 15 cases (13.2%). The *MGMT* promoter methylation status was available in 65 patients, with 56.9% being non-methylated (37/65). During initial surgical tumor resection, in 30.7% of all cases, carmustine wafers were implanted (only in one of the two participating departments, wafers were implanted). The mean number of implanted wafers was 6.91, with a range of 4–10 wafers. Reoperation was performed in 21.9% (25/114) of all cases during treatment. Forty-two patients (36.8%) received additional chemotherapy after the completion of the Stupp protocol, mostly a combination of various drugs (27.2%; 31/114) including teniposide (17.5%; 20/114), BCNU (16.7%; 19/114), and bevacizumab (13.2%; 15/114).

Volumetric tumor assessment

The included patients do reflect the broad spectrum of different sizes and shapes of glioblastoma, ranging from very small CEV+ volumes (0.604 cm^3) up to very large lesions with more than 100 cm^3 of volume (Table 2). The quality of the source data for our study was high, with a mean slice thickness of only 1 mm for the CEV+, CEV−, and residual volume assessments. The surrounding FLAIR+ area was, in most cases, nearly threefold larger than the CEV+ (median ETR 2.66); the maximum measured FLAIR+ volume was 221.6 cm^3. The inner necrotic core of the tumor (CEV−) was smaller than 7.5 cm^3 in 59.6% of cases (68/114); the median volume was

Table 2 Tumor characteristics

		n (%)
Tumor location	Left	57 (50)
	Right	56 (49.1)
	Bilateral	1 (0.9)
	Temporal	47 (41.2)
	Frontal	34 (29.8)
	Others	33 (28.9)
Tumor cysts		15 (13.2)
CEV+ volume	Median (Q1; Q3) (cm^3)	20.6 (9.88; 42.2)
	Range (cm^3)	0.604–107
FLAIR+ volume	Median (Q1; Q3) (cm^3)	65.0 (21.3; 129)
	Range (cm^3)	0–222
CEV− volume	Median (Q1; Q3) (cm^3)	4.58 (1.65; 12.7)
	Range (cm^3)	0–59.5
Cyst volume	Median (Q1; Q3) (cm^3)	10.9 (5.58; 17.1)
	Range (cm^3)	1.04–42.4
ETR	Median (Q1; Q3)	2.66 (1.54; 4.69)
	Range	0–31.8
NTR	Mean (± SD)	0.259 (0.140)
	Range	0–0.625
EOR	Median (Q1; Q3) (%)	98.5 (96.5; 100)
	Range (%)	57–100
RTV	Median (Q1; Q3) (cm^3)	0.24 (0.0; 0.79)
	Range (cm^3)	0–2.86

EOR = extent of resection; ETR = edema-tumor ratio; NTR = necrosis-tumor ratio; Q1 = 25% quantile/lower quartile; Q3 = 75% quantile/upper quartile; RTV = residual tumor volume

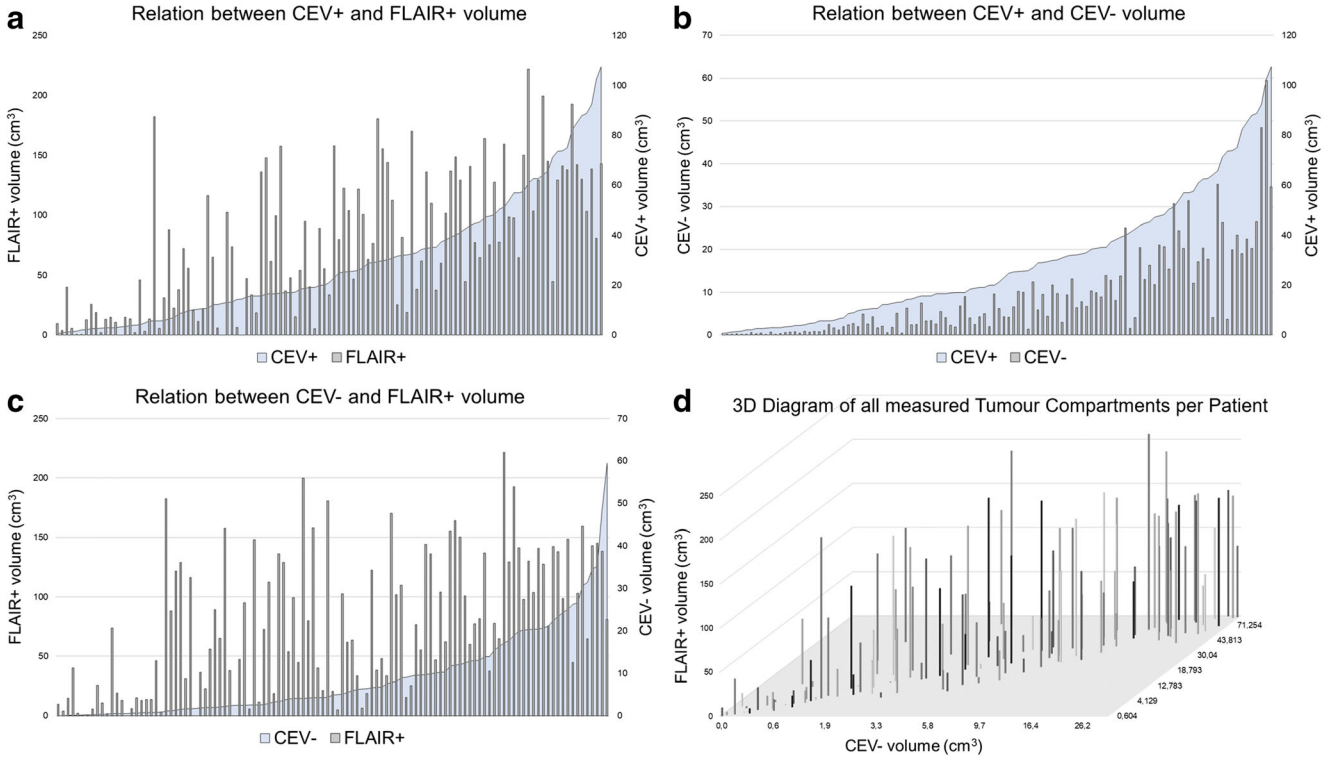

Fig. 2 Correlation scatter plot matrix of the measured tumor compartment volumes and derived ratios. The data is displayed as scatter plots for every possible pair of values; a polynomial trend line is integrated. Spearman's rank correlation coefficient (r_S) accompanied by the corresponding p value is displayed on the mirrored side of the matrix. The strongest correlation was observed between the CEV+ and CEV− volumes, delineated in bold type

4.58 cm^3, ranging from 0 to 59.47 cm^3. Thus, the CEV− represents mostly one-quarter of the whole CEV+ volume (mean NTR 0.259 ± 0.140 cm^3). The correlation analysis of the different tumor compartments showed the strongest relationship between the CEV+ and its inner CEV− ($r_S = 0.898$, $p < 0.001$) with an almost linear relationship (Figs. 2 and 3). The association of the NTR with the CEV+ was not as strong as the CEV− and the CEV+ ($r_S = 0.469$, $p < 0.001$), reflecting the diversity of the proportions of each tumor compartment towards each other. The surrounding FLAIR+ also showed a moderate correlation with the CEV+ volume ($r_S = 0.691$, $p < 0.001$) with the CEV+. By contrast, the ETR was negatively associated with the tumor volume ($r_S = -0.361$, $p = 0.001$); a rise in CEV+ was accompanied by a non-proportional increase in the FLAIR+ volume.

Survival analysis

Four patients completed the trial, resulting in censored data. The median OS was 14.8 months, ranging from 1.02 to 80.2 months. The sex of patients did not affect OS, whereas age at initial diagnosis of ≥ 65 years compared with that (< 65 years) of younger patients decreased the OS in multivariable analyses (HR 1.57) (Tables 3 and 4). An additional administration of chemotherapies after the Stupp protocol showed no influence on OS ($p = 0.939$), similar to a reoperation during the disease ($p = 0.251$). If carmustine wafers were implanted during the first operation, they positively influenced and prolonged the lifespan of these patients: the median OS was 14.94 months for those without carmustine wafers being implanted with an HR of 1.91 versus 22.86 months for patients with implanted wafers ($p = 0.004$). These results could also be comprehended within the multivariable analysis ($p = 0.021$, HR 1.76). Regarding the different tumor volumes, only the two ratios (ETR and NTR) showed effects on the OS in univariate analysis ($p = 0.016$ and 0.022, respectively). In multivariable analysis, NTR still showed a significant decrease in OS for patients with a higher amount of CEV− within the CEV+ volume (HR = 2.63, $p = 0.016$). This strong influence on the OS is particularly emphasized because a difference of only 13% of CEV− in relation to the whole tumor volume (CEV+) separated the analyzed groups (> 0.33 vs. ≤ 0.2). The lack of influence of the CEV+ is in line with the results shown in Fig. 4b: after splitting the patient cohort at a CEV+ of 20 cm^3, the times to event did not diverge between groups. RTV had no impact on survival ($p = 0.215$), mainly because the residual volume was < 1 cm^3 in 81% of included patients. The intergroup analysis of the ETR showed no

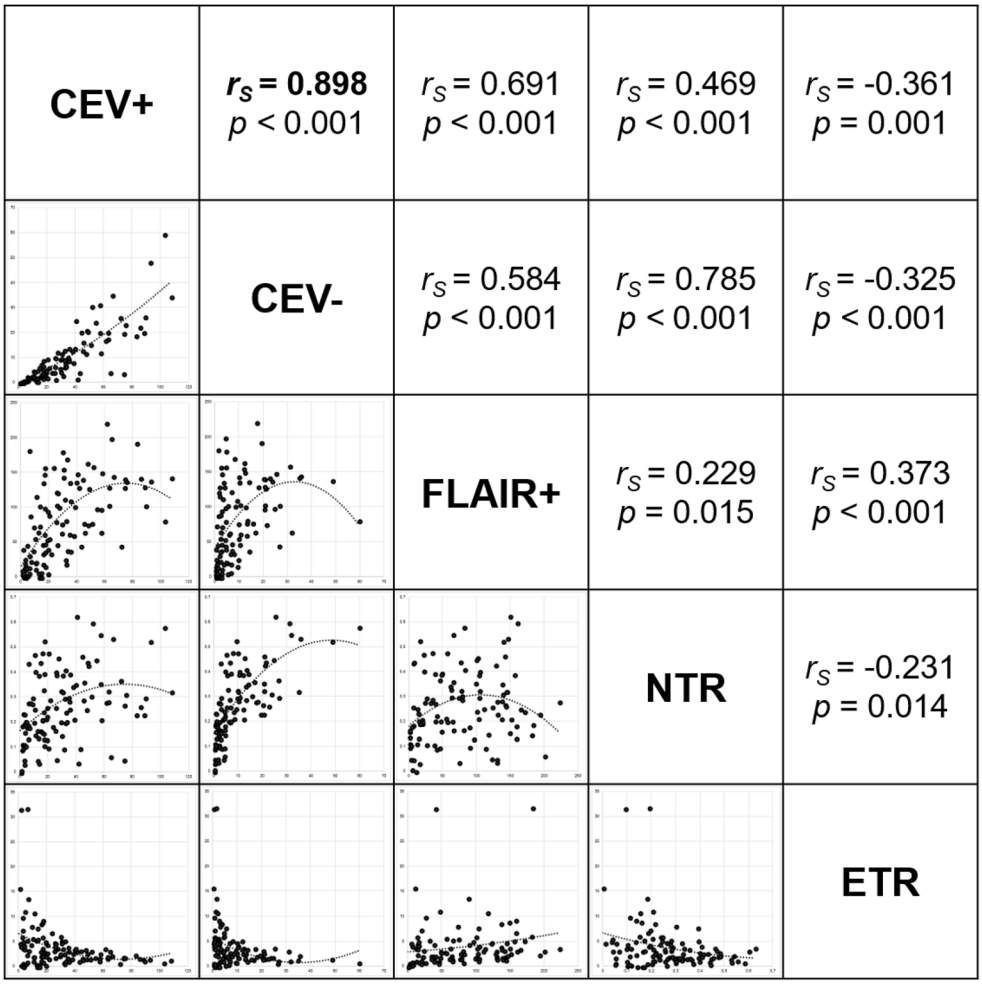

Fig. 3 Diagrams of each glioblastoma volume and their relationships with each other. **a** The increasing area in the background represents the CEV+ volume in ascending order for all patients within our cohort. The single bars show the associated FLAIR+ volumes for each patient. The diagram displays the diverging expansion of the peritumoral FLAIR+ volume with an only fair correlation with the CEV+ volumes. **b** Similar to the first diagram, the CEV+ volume is shown as the background area, accompanied by single bars for the corresponding CEV− volumes. In contrast to **a**, a strong correlation between both volumes is clearly visible. **c** The background area in this diagram shows the CEV− volume, and the bars are standing for the respective FLAIR+ volume. A strong fluctuation is visible between both volumes. **d** The 3D diagram illustrates the diverging composition of every GBM regarding its three compartments. Similar to the scatter plot matrix, with an increased tumor volume, the necrosis volume is strongly correlated and rising. In contrast, the FLAIR+ volume (*z*-axis) shows stronger fluctuations in its characteristics

significant impact on OS in multivariable analysis ($p = 0.293$). The results were confirmed within a single-institute analysis as an internal validation of our data (Supplementary Table 1).

Discussion

In the present study, we analyzed the structure and architecture of glioblastoma on pretreatment MRI. One of the major difficulties of tumor segmentation is defining its borders: the contrast-enhancing area of the tumor marks the truly vital tumor compartment, but its limit does not define the end of the actual tumor extent, as the imaging might suggest. Already in 1987, Kelly and colleagues showed that an "isolated tumor cell infiltration extended at least as far as T2 prolongation on magnetic resonance images" [16]. These findings were later confirmed by others [7], showing that the surrounding "edema" harbors a vital infiltration zone of the tumor, as it builds a widely ramified functional network [23]. Therefore, some neurosurgeons propagate even resection of the FLAIR+ area, if functionally justifiable [20]. Furthermore, not only is this peritumoral brain zone (PBZ) already infiltrated by tumor cells but these cells also show different phenotypes from those from the tumor mass [19].

With a rising CEV+ volume, the scattering of the corresponding FLAIR+ volumes increased; in the case of a rising CEV+ volume, the FLAIR+ volume (in relation to the increasing CEV+) becomes smaller. This phenomenon can partly be explained by the shear space within the brain that is occupied by the tumor and its mass effect on the

Table 3 Influence of clinical and radiological data on OS

	Variable	Univariable analysis†			Median OS (months)
		HR	95% CI	*p* value	
Sex	Male vs. female*	1.01	0.68–1.45	0.973	17.53 vs. 17.43
Age	All groups	–	–	0.045	
	≥ 65 years vs. < 65 years*	1.30	0.871–1.92	0.203	12.70 vs. 15.85
Charlson index	All groups	–	–	0.227	
	≥ 5 vs. ≤ 2*	1.92	0.91–4.03	0.085	12.86 vs. 18.46
KPS	< 80% vs. ≥ 80%	1.17	0.778–1.76	0.452	13.39 vs. 14.81
MGMT	Unmeth. vs. meth.*	1.32	0.78–2.25	0.304	17.82 vs. 20.81
Reoperation	No vs. yes*	1.31	0.83–2.06	0.251	16.38 vs. 20.19
Carmustin wafer	No vs. yes*	1.91	1.22–2.96	0.004	14.94 vs. 22.86
Add. chemotherapy	Yes vs. no*	1.01	0.68–1.51	0.939	17.19 vs. 17.64
Cystic tumor	No vs. yes*	104	0.60–1.8	0.887	17.45 vs. 17.60
CEV+ volume	All groups	–	–	0.659	
	> 40 cm^3 vs. ≤ 16 cm^3*	1.06	0.66–1.7	0.819	16.16 vs. 17.22
FLAIR+ volume	All groups	–	–	0.573	
	> 100 cm^3 vs. ≤ 50 cm^3*	1.11	0.66–1.86	0.698	18.25 vs. 16.37
CEV− volume	All groups	–	–	0.121	
	> 10 cm^3 vs. ≤ 3 cm^3*	1.29	0.83–2.02	0.265	14.52 vs. 17.35
ETR	All groups	–	–	0.016	
	≤ 2 vs. > 4*	1.43	0.91–1.17	0.121	13.59 vs. 17.21
NTR	All groups	–	–	0.022	
	> 0.33 vs. ≤ 0.2*	1.69	1.04–2.73	0.033	13.08 vs. 18.08

ETR = edema-tumor ratio; KPS = Karnofsky performance status; NTR = necrosis-tumor ratio

† Cox regression analysis

surrounding parenchyma. Otherwise, the FLAIR+ tumor component has the highest fluctuation in its volume, independent of the CEV+ volume (Fig. 3d). Thus, it is worth discussing whether the pretreatment FLAIR+ volume can serve as a quantitative surrogate parameter of a tumor infiltration on MRI. Within a small series of glioblastoma patients, Tamura et al. observed an increased proliferation index (Ki-67) within broad FLAIR+ lesions compared with smaller FLAIR+ volumes [33]. In our series, the pretreatment FLAIR+ volume does not affect the OS after resection of the CEV+ volume, thus being an unreliable prognostic marker.

Table 4 Multivariable survival analysis

	Variable	Multiple model†		
		Adj. HR	95% CI	*p* value
Age	≥ 65 years vs. < 65 years	1.57	1.02–2.42	0.043
KPS	< 80% vs. ≥ 80%	1.18	0.740–1.89	0.482
Necrosis volume	All groups	–	–	0.108
	> 10 cm^3 vs. ≤ 3 cm^3*	0.650	0.302–1.40	0.271
ETR	All groups	–	–	0.293
	≤ 2 vs. > 4*	1.134	0.681–1.89	0.630
NTR	All groups	–	–	0.018
	> 0.33 vs. ≤ 0.2*	2.63	1.20–5.76	0.016
Carmustin wafer	No vs. yes	1.76	1.09–2.83	0.021

Adj. = adjusted; CI = confidence interval; ETR = edema-tumor ratio; HR = hazard ratio; KPS = Karnofsky performance status; NTR = necrosis-tumor ratio

† Cox regression analysis

Our data do not support the hypothesis that the additional surgical resection of the FLAIR+ volume (supramarginal resection) is associated with prolonged survival; we found that a larger FLAIR+ volume does not inevitably lead to a larger residual tumor burden after resection and a reduced OS. Tumor recurrence almost always occurs at the resection margin [22, 25]. This phenomenon cannot be totally accounted for by a larger amount of residual tumor cells at the resection margin or beyond this limit; rather, it seems that the PBZ responds to the surgical tissue damage by formation of a "recurrence-prone microenvironment" [28], promoting the tumor recurrence at the resection margin. In our opinion, a supramarginal resection will always reduce the residual tumor mass, whether it respects the FLAIR+ borders or not.

Regarding the OS, the NTR is an independent prognostic factor in our patient cohort. The single tumor compartments did not affect the OS in multivariable analyses, neither did the ETR. Figure 4 illustrates the missing link between the "tumor volume" (CEV+) and the OS with nearly identical survival times after splitting the cohort at a tumor volume of 20 cm^3. Our data highlight the importance of ratios rather than volumes of single tumor compartment because the size of one compartment cannot always be linked to the size of other tumor segments.

As our results indicate, a higher NTR can serve as an imaging parameter for a more invasive and resistant type of glioblastoma. This thesis is supported by a study of Taylor et al., in which the amount of necrosis likewise correlated with OS [34]. Furthermore, these authors correlated a higher percentage of necrosis with the mesenchymal subtype of glioblastoma. The mesenchymal subtype at initial diagnosis and the recurrence of glioblastoma are associated with a poor outcome [35]. Others used the CEV− as a surrogate parameter predicting the *MGMT* methylation status, which was methylated in patients with a larger amount of necrosis [11]. Unfortunately, the mentioned study did not raise quantitative volumes rather than using a three-level classification for necrosis estimation. In our cohort, neither the volume of the necrosis (CEV−) nor the NTR correlated with the *MGMT* methylation status ($p = 0.257$ and 0.475, respectively). Furthermore, in 53% of cases at the mentioned study, the amount of necrosis in relation to the whole tumor volume was rated larger than 50%—in our cohort, only 6% of the measured glioblastoma (7/114) had an NTR of > 0.5. This divergence illustrates a common problem associated with semantic imaging definitions: a visual estimation cannot reliably rate a 3-dimensional and irregularly shaped tumor, as we already demonstrated [13]. Also, in our study, the CEV− correlates strongly with the CEV+, which was not recorded at all in the above-cited study and might have biased the mentioned results. Qualitative and quantitative analyses by Kanas et al. demonstrated the supremacy of quantitative data over qualitative ratings but came to the same results regarding the *MGMT* methylation status [14]. A valid conclusion from both studies might, therefore, be that

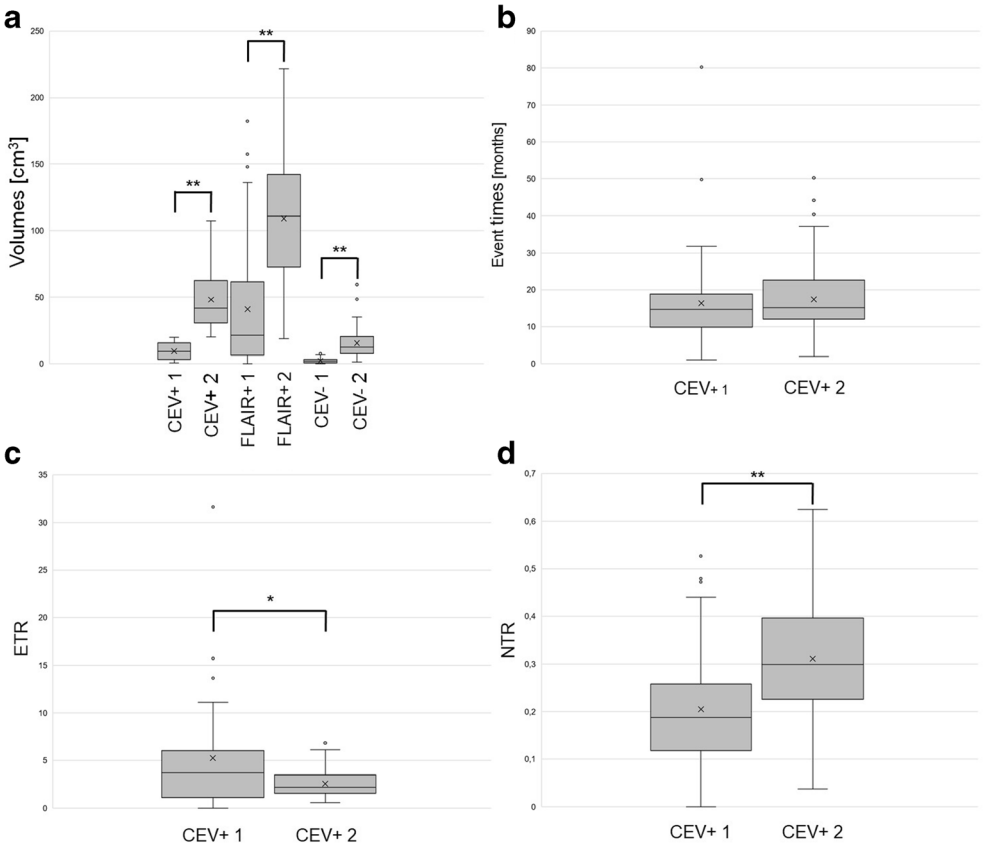

Fig. 4 Box plot diagram after splitting the patient cohort at a CEV+ volume of 20 cm^3, which nearly bisected the cohort (CEV+ 1 = ≤ 20 cm^3 volume, $n = 56$; CEV+ 2 = > 20 cm^3 volume, $n = 58$). The distribution of corresponding volumes, event times, and ratios is shown. **a** All measured tumor volumes showed an equally significant increase from compartments CEV+ 1 to CEV+ 2. **b** There is no statistically significant difference for the OS when comparing the two groups ($p = 0.338$). **c** The ETR of both groups showed a significant reduction for increasing volume, reflecting the negative correlation shown in Fig. 3. **d** The NTR, in contrast to the ETR, strongly correlates positively with an increasing tumor volume. *U*-test; **p* value < 0.05; ***p* value < 0.001; x within boxplot = mean values

glioblastomas with a larger necrotic core are more often methylated, which seems contradictive to the widespread assumption that a methylated *MGMT* promoter is correlated with an increased OS, while a larger amount of necrosis is unfavorable regarding the OS and might promote resistance to radiation therapy and chemotherapy [2, 12, 17, 32]. As our data shows, only the NTR could be used as a prognostic imaging factor for the stratification of glioblastoma patients in terms of their OS.

Limitations

One limitation of our study is its retrospective nature. The preselected patient cohort is both a strength and a limitation. All patients underwent surgical resection with only a small residual tumor volume, followed by a concomitant therapy. Therefore, study conclusions cannot be transferred without restriction to all patients harboring a glioblastoma. Another bias is concealed within the semi-automatic assessment of tumor compartments, with a potential interobserver variability, although these issues seem to be neglectable in other studies [9, 18]. Furthermore, we did not include machine learning algorithms in our analyses, since we aimed at an approach that is adapted to the clinical setting and comparable to the existing literature.

Conclusion

Our structural imaging analysis demonstrates the broad divergence of every glioblastoma on pretreatment MRI. Only the CEV− volume is strongly correlated with the size of the lesion itself (CEV+); the surrounding FLAIR+ volume showed no distinct correlation with the tumor mass. For the first time, our comprehensive imaging analysis was able to demonstrate that only the ratio between the necrotic core and its bearing CEV+, the NTR, is a robust prognostic imaging marker. Therefore, the NTR can identify patients with a subtype of glioblastoma, apparently being more resistant to an adjuvant therapy after surgical resection.

Acknowledgments The authors would like to thank Prof. Günther Kundt for his valuable statistical suggestions and the patients who participated in this study.

Compliance with ethical standards Informed consent was obtained from all individual participants included in the study.

Conflict of interest The authors declare that they have no conflict of interest.

Ethical approval All procedures performed in studies involving human participants were in accordance with the ethical standards of both institutional research committees and with the 1964 Helsinki declaration and its later amendments or comparable ethical standards (registration number 005/2003, respectively).

References

1. Bauchet L, Mathieu-Daudé H, Fabbro-Peray P, Rigau V, Fabbro M, Chinot O, Pallusseau L, Carnin C, Lainé K, Schlama A, Thiebaut A, Patru MC, Bauchet F, Lionnet M, Wager M, Faillot T, Taillandier L, Figarella-Branger D, Capelle L, Loiseau H, Frappaz D, Campello C, Kerr C, Duffau H, Reme-Saumon M, Trétarre B, Daures J-P, Henin D, Labrousse F, Menei P, Honnorat J (2010) Oncological patterns of care and outcome for 952 patients with newly diagnosed glioblastoma in 2004. Neuro-Oncology 12(7): 725–735
2. Belden CJ, Valdes PA, Ran C, Pastel DA, Harris BT, Fadul CE, Israel MA, Paulsen K, Roberts DW (2011) Genetics of glioblastoma: a window into its imaging and histopathologic variability. Radiographics 31(6):1717–1740
3. Charlson ME, Pompei P, Ales KL, MacKenzie CR (1987) A new method of classifying prognostic comorbidity in longitudinal studies: development and validation. J Chronic Dis 40(5):373–383
4. Chen L, Voronovich Z, Clark K, Hands I, Mannas J, Walsh M, Nikiforova MN, Durbin EB, Weiss H, Horbinski C (2014) Predicting the likelihood of an isocitrate dehydrogenase 1 or 2 mutation in diagnoses of infiltrative glioma. Neuro-Oncology 16(11):1478–1483
5. Davies DC (2002) Blood-brain barrier breakdown in septic encephalopathy and brain tumours. J Anat 200(6):639–646
6. Eads CA, Danenberg KD, Kawakami K, Saltz LB, Blake C, Shibata D, Danenberg PV, Laird PW (2000) MethyLight: a high-throughput assay to measure DNA methylation. Nucleic Acids Res 28(8):E32
7. Eidel O, Burth S, Neumann J-O, Kieslich PJ, Sahm F, Jungk C, Kickingereder P, Bickelhaupt S, Mundiyanapurath S, Baumer P, Wick W, Schlemmer H-P, Kiening K, Unterberg A, Bendszus M, Radbruch A (2017) Tumor infiltration in enhancing and non-enhancing parts of glioblastoma: a correlation with histopathology. PLoS One 12(1):e0169292
8. Ellingson BM, Bendszus M, Boxerman J, Barboriak D, Erickson BJ, Smits M, Nelson SJ, Gerstner E, Alexander B, Goldmacher G, Wick W, Vogelbaum M, Weller M, Galanis E, Kalpathy-Cramer J, Shankar L, Jacobs P, Pope WB, Yang D, Chung C, Knopp MV, Cha S, van den Bent MJ, Chang S, Yung WKA, Cloughesy TF, Wen PY, Gilbert MR (2015) Consensus recommendations for a standardized brain tumor imaging protocol in clinical trials. Neuro-Oncology 17(9):1188–1198
9. Fyllingen EH, Stensjøen AL, Berntsen EM, Solheim O, Reinertsen I (2016) Glioblastoma segmentation: comparison of three different software packages. PLoS One 11(10):e0164891
10. Hammoud MA, Sawaya R, Shi W, Thall PF, Leeds NE (1996) Prognostic significance of preoperative MRI scans in glioblastoma multiforme. J Neuro-Oncol 27(1):65–73
11. Han Y, Yan L-F, Wang X-B, Sun Y-Z, Zhang X, Liu Z-C, Nan H-Y, Hu Y-C, Yang Y, Zhang J, Yu Y, Sun Q, Tian Q, Hu B, Xiao G, Wang W, Cui G-B (2018) Structural and advanced imaging in predicting MGMT promoter methylation of primary glioblastoma: a region of interest based analysis. BMC Cancer 18(1):215
12. Hegi ME, Diserens A-C, Gorlia T, Hamou M-F, de Tribolet N, Weller M, Kros JM, Hainfellner JA, Mason W, Mariani L, Bromberg JEC, Hau P, Mirimanoff RO, Cairncross JG, Janzer RC, Stupp R (2005) MGMT gene silencing and benefit from temozolomide in glioblastoma. N Engl J Med 352(10):997–1003
13. Henker C, Kriesen T, Glass Ä, Schneider B, Piek J (2017) Volumetric quantification of glioblastoma. Experiences with different measurement techniques and impact on survival. J Neuro-Oncol 135(2):391–402
14. Kanas VG, Zacharaki EI, Thomas GA, Zinn PO, Megalooikonomou V, Colen RR (2017) Learning MRI-based

classification models for MGMT methylation status prediction in glioblastoma. Comput Methods Prog Biomed 140:249–257
15. Karnofsky DA, Abelmann WH, Craver LF, Burchenal JH (1948) The use of the nitrogen mustards in the palliative treatment of carcinoma. With particular reference to bronchogenic carcinoma. Cancer 1(4):634–656
16. Kelly PJ, Daumas-Duport C, Kispert DB, Kall BA, Scheithauer BW, Illig JJ (1987) Imaging-based stereotaxic serial biopsies in untreated intracranial glial neoplasms. J Neurosurg 66(6):865–874
17. Lacroix M, Abi-Said D, Fourney DR, Gokaslan ZL, Shi W, DeMonte F, Lang FF, McCutcheon IE, Hassenbusch SJ, Holland E, Hess K, Michael C, Miller D, Sawaya R (2001) A multivariate analysis of 416 patients with glioblastoma multiforme: prognosis, extent of resection, and survival. J Neurosurg 95(2):190–198
18. Lee M, Woo B, Kuo MD, Jamshidi N, Kim JH (2017) Quality of radiomic features in glioblastoma multiforme: impact of semi-automated tumor segmentation software. Korean J Radiol 18(3): 498–509
19. Lemée J-M, Clavreul A, Menei P (2015) Intratumoral heterogeneity in glioblastoma: don't forget the peritumoral brain zone. Neuro-Oncology 17(10):1322–1332
20. Li YM, Suki D, Hess K, Sawaya R (2016) The influence of maximum safe resection of glioblastoma on survival in 1229 patients: can we do better than gross-total resection? J Neurosurg 124(4): 977–988
21. Mabray MC, Barajas RF, Cha S (2015) Modern brain tumor imaging. Brain Tumor Res Treat 3(1): 8–23
22. Norden AD, Young GS, Setayesh K, Muzikansky A, Klufas R, Ross GL, Ciampa AS, Ebbeling LG, Levy B, Drappatz J, Kesari S, Wen PY (2008) Bevacizumab for recurrent malignant gliomas: efficacy, toxicity, and patterns of recurrence. Neurology 70(10): 779–787
23. Osswald M, Jung E, Sahm F, Solecki G, Venkataramani V, Blaes J, Weil S, Horstmann H, Wiestler B, Syed M, Huang L, Ratliff M, Karimian Jazi K, Kurz FT, Schmenger T, Lemke D, Gömmel M, Pauli M, Liao Y, Häring P, Pusch S, Herl V, Steinhäuser C, Krunic D, Jarahian M, Miletic H, Berghoff AS, Griesbeck O, Kalamakis G, Garaschuk O, Preusser M, Weiss S, Liu H, Heiland S, Platten M, Huber PE, Kuner T, von Deimling A, Wick W, Winkler F (2015) Brain tumour cells interconnect to a functional and resistant network. Nature 528(7580):93–98
24. Ostrom QT, Gittleman H, Stetson L, Virk S, Barnholtz-Sloan JS (2018) Epidemiology of intracranial gliomas. Prog Neurol Surg 30: 1–11
25. Petrecca K, Guiot M-C, Panet-Raymond V, Souhami L (2013) Failure pattern following complete resection plus radiotherapy and temozolomide is at the resection margin in patients with glioblastoma. J Neuro-Oncol 111(1): 19–23
26. Pope WB, Sayre J, Perlina A, Villablanca JP, Mischel PS, Cloughesy TF (2005) MR imaging correlates of survival in patients with high-grade gliomas. AJNR Am J Neuroradiol 26(10):2466–2474
27. Price SJ, Jena R, Burnet NG, Hutchinson PJ, Dean AF, Peña A, Pickard JD, Carpenter TA, Gillard JH (2006) Improved delineation of glioma margins and regions of infiltration with the use of diffusion tensor imaging: an image-guided biopsy study. AJNR Am J Neuroradiol 27(9):1969–1974
28. Ratel D, van der Sanden B, Wion D (2016) Glioma resection and tumor recurrence: back to Semmelweis. Neuro-Oncology 18(12): 1688–1689
29. Sales AHA, Bette S, Barz M, Huber T, Wiestler B, Ryang Y-M, Schmidt-Graf F, Liesche F, Combs SE, Meyer B, Gempt J (2019) Role of postoperative tumor volume in patients with MGMT-unmethylated glioblastoma. J Neuro-Oncol
30. Stupp R, Hegi ME, Mason WP, van den Bent, Martin J, Taphoorn MJB, Janzer RC, Ludwin SK, Allgeier A, Fisher B, Belanger K, Hau P, Brandes AA, Gijtenbeek J, Marosi C, Vecht CJ, Mokhtari K, Wesseling P, Villa S, Eisenhauer E, Gorlia T, Weller M, Lacombe D, Cairncross JG, Mirimanoff R-O (2009) Effects of radiotherapy with concomitant and adjuvant temozolomide versus radiotherapy alone on survival in glioblastoma in a randomised phase III study: 5-year analysis of the EORTC-NCIC trial. Lancet Oncol 10(5):459–466
31. Stupp R, Mason WP, van den Bent MJ, Weller M, Fisher B, Taphoorn MJB, Belanger K, Brandes AA, Marosi C, Bogdahn U, Curschmann J, Janzer RC, Ludwin SK, Gorlia T, Allgeier A, Lacombe D, Cairncross JG, Eisenhauer E, Mirimanoff RO (2005) Radiotherapy plus concomitant and adjuvant temozolomide for glioblastoma. N Engl J Med 352(10):987–996
32. Tabatabai G, Hegi M, Stupp R, Weller M (2012) Clinical implications of molecular neuropathology and biomarkers for malignant glioma. Curr Neurol Neurosci Rep 12(3):302–307
33. Tamura R, Ohara K, Sasaki H, Morimoto Y, Yoshida K, Toda M (2018) Histopathological vascular investigation of the peritumoral brain zone of glioblastomas. J Neuro-Oncol 136(2):233–241
34. Taylor EN, Ding Y, Zhu S, Cheah E, Alexander P, Lin L, Aninwene GE, Hoffman MP, Mahajan A, Mohamed ASR, McDannold N, Fuller CD, Chen CC, Gilbert RJ (2017) Association between tumor architecture derived from generalized Q-space MRI and survival in glioblastoma. Oncotarget 8(26):41815–41826
35. Wang Q, Hu B, Hu X, Kim H, Squatrito M, Scarpace L, deCarvalho AC, Lyu S, Li P, Li Y, Barthel F, Cho HJ, Lin Y-H, Satani N, Martinez-Ledesma E, Zheng S, Chang E, Sauvé C-EG, Olar A, Lan ZD, Finocchiaro G, Phillips JJ, Berger MS, Gabrusiewicz KR, Wang G, Eskilsson E, Hu J, Mikkelsen T, DePinho RA, Muller F, Heimberger AB, Sulman EP, Nam D-H, Verhaak RGW (2017) Tumor evolution of glioma-intrinsic gene expression subtypes associates with immunological changes in the microenvironment. Cancer Cell 32(1):42–56 e6
36. Zhou M, Scott J, Chaudhury B, Hall L, Goldgof D, Yeom KW, Iv M, Ou Y, Kalpathy-Cramer J, Napel S, Gillies R, Gevaert O, Gatenby R (2018) Radiomics in brain tumor. Image assessment, quantitative feature descriptors, and machine-learning approaches. AJNR Am J Neuroradiol 39(2):208–216

Publisher's note Springer Nature remains neutral with regard to jurisdictional claims in published maps and institutional affiliations.

Correlation of Ki-67 Index with Volumetric Segmentation and its Value as a Prognostic Marker in Glioblastoma

Christian Henker[1], Thomas Kriesen[1], Björn Schneider[2], Änne Glass[3], Moritz Scherer[4], Sönke Langner[5], Andreas Erbersdobler[2], Jürgen Piek[1]

OBJECTIVE: **Previous research has shown a strong correlation between the Ki-67 proliferation index and grade of malignancy in astrocytoma. Ki-67 has also shown encouraging results as a prognostic marker for patients' overall survival (OS). We focus on whether the index is linked to the appearance of glioblastoma on pretreatment magnetic resonance imaging (MRI) or to OS.**

METHODS: **In our retrospective study, only isocitrate dehydrogenase *IDH* wild-type glioblastoma was included ($n = 152$). Ki-67 index was quantified via immunohistochemistry. On all pretreatment MRI, tumor compartments (tumor, necrosis, and edema) were volumetrically assessed. An OS subpopulation was filtered from the total cohort (residual tumor volume ≤2 cm^3). In addition, a propensity score matching was executed.**

RESULTS: **All volumetric assessed tumor volumes correlated with each other ($P \leq 0.011$), although the Ki-67 index showed no correlation with any of the measured volumes. Concerning the OS, a cutoff value of 20% for the Ki-67 index showed a significant influence on patients' OS in multivariate analysis ($P = 0.043$).**

CONCLUSIONS: **The unique appearance of every glioblastoma on MRI seems to be independent of the Ki-67 index. Furthermore, the Ki-67 index did show a distinct prognostic value for OS within our cohort at a cutoff value of 20% for Ki-67.**

INTRODUCTION

Glioblastoma is the most aggressive and also the most common glioma in adults.[1] Despite decades of ongoing efforts within both clinical diagnostics and conducted therapy, the overall survival (OS) of glioblastoma remains dismal. Even after gross total resection, followed by concomitant radiation and chemotherapy, the median OS of these patients reaches only 18.8 months.[2] As the term multiforme already implies, the appearance of the tumor is heterogenous. Areas of necrotic tissue are surrounded by pseudopalisading cells, both being histologic hallmarks of the tumor. In addition, the tumor shows a high neovascularization rate, microvascular hyperplasia, hemorrhages, and intratumoral thrombosis.[3-5] Some of these distinguishing features can be recognized within cranial magnetic resonance imaging (MRI), the gold standard for the initial visualization of the tumor and for surgical planning. The appearance of the different tumor compartments and their relationship between each other can serve as a predictive marker.[6] Other established predictive markers are the age of the patient, the Karnofsky Performance Status (KPS) and *MGMT* methylation status.[7,8]

Key words
- Glioblastoma
- Ki-67
- Magnetic resonance imaging
- Neuroimaging
- Prognosis
- Prognostic marker
- Segmentation

Abbreviations and Acronyms
3D: Three-dimensional
HR: Hazard ratio
KPS: Karnofsky Performance Status
MRI: Magnetic resonance imaging
OS: Overall survival
PS: Propensity score
RTV: Residual tumor volume
T1w: T1-weighted

From the [1]Department of Neurosurgery and Institutes for [2]Pathology, [3]Biostatistics and Informatics in Medicine, and [5]Diagnostic and Interventional Radiology, University Medicine of Rostock, Rostock, Germany; and [4]Department of Neurosurgery, Heidelberg University Hospital, Heidelberg, Germany

To whom correspondence should be addressed: Christian Henker, M.D. [E-mail: christian.henker@med.uni-rostock.de]

Citation: World Neurosurg. (2019). https://doi.org/10.1016/j.wneu.2019.02.006

Journal homepage: www.journals.elsevier.com/world-neurosurgery

Available online: www.sciencedirect.com

1878-8750/$ - see front matter © 2019 Elsevier Inc. All rights reserved.

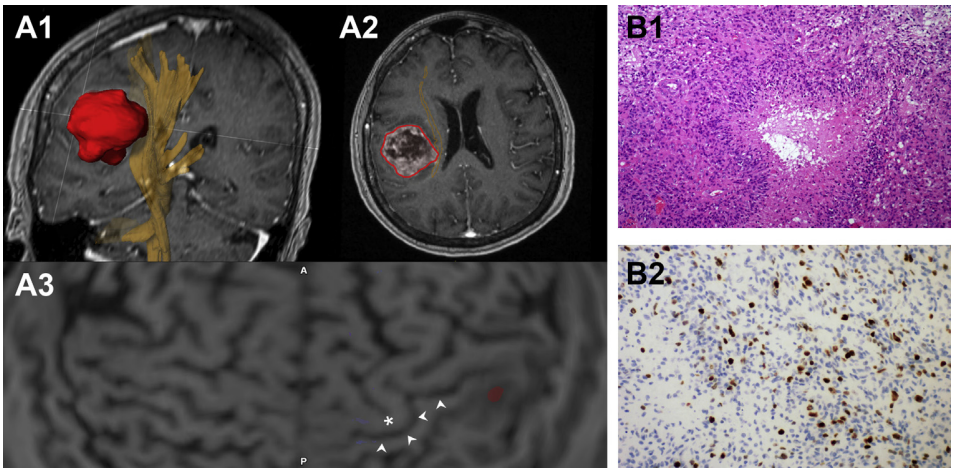

Figure 1. A three-dimensional volumetric assessment of a glioblastoma and the corresponding histologic images. (**A**) The screenshots were taken during the surgical planning with the neuronavigation software (Elements [Brainlab AG]). The pretreatment magnetic resonance imaging is showing a right-sided glioblastoma, situated within the parietal lobe. (**A1**) Three-dimensional reconstruction of the tumor (*masked red*) in relation to the corticospinal tract (*masked yellow*) in a coronary view from anterior. (**A2**) Axial section of the magnetic resonance imaging, used for marking the region of interest before adjusting at the other planes (sagittal and coronary planes). (**A3**) Mercator projection of the brain surface from above, the hand knob is marked with an asterisk (representing the motor area of the hand). The white arrows show the central sulcus. The measured tumor volume was 16.6 cm^3. (**B**) Hematoxylin-eosin stain (**B1**, 100×) and an immunohistologic image (**B2**, 200×), stained for Ki-67, of the same glioblastoma shown in (**A**). The hematoxylin-eosin stain shows the typical histologic appearance of a glioblastoma with a centrally located necrosis, surrounded by pseudopalisading cells. The Ki-67 nuclear stain shows the highly proliferating character of the tumor; the proliferation index was specified with 20%.

The Ki-67 antibody is an IgG1 class monoclonal antibody, first described by Gerdes et al. in 1983.[9] During all active phases of the cell cycle, the Ki-67 protein is expressed and is detectable.[10] Because the protein is absent in quiescent cells (G_0 phase), Ki-67 is useful to distinguish between growing and nonproliferating cells. Furthermore, the percentage of proliferating cells (Ki-67 labeling index) can be used to discriminate more aggressive phenotypes of tumors. An increase in Ki-67 index correlates with an increasing grade of malignancy in astrocytoma.[11,12] Within a meta-analysis of the existing studies, regarding Ki-67 index as prognostic factor, the value of the index seems to be important for progression and survival estimation.[13] Little is known about the correlation between the proliferation marker Ki-67 and its potential impact on the appearance on pretreatment MRI, because the proportions of the different tumor compartments can also serve as a predictor for OS.

To fill this gap, the aim of our study was to determine whether the Ki-67 index can be correlated to the different volumetric compartments of a glioblastoma on MRI and if the proliferation index can reflect the diverse appearance of every glioblastoma on imaging studies. Furthermore, we wanted to evaluate the potential of the index as a prognostic marker for these patients.

METHODS

Study Design

The protocol was approved by the appropriate institutional review board/ethic committee according to the Declaration of Helsinki. In our retrospective study, 152 patients harboring a primary glioblastoma were included. Only adults (>18 years) with newly diagnosed and histologically proven *IDH* wild-type glioblastoma were included and all of them were treated between February 2007 and November 2015. Definition of *IDH* wild-type glioblastoma was based on isocitrate dehydrogenase 1 R132 mutation status.[14] At the time of the initial MRI scan, all patients were steroid naive, excluding the potential bias of steroids on the peritumoral edema. All clinical data were taken from the hospital's own records. Besides demographic data, the pretreatment KPS and the age-adjusted Charlson Comorbidity Index were collected at admission, primary developed to predict the 1-year mortality.[15,16] For statistical survival analysis, data were partly grouped in classes as followed: age (≤60 years, >60–70 years, and >70 years), Charlson Comorbidity Index (≤2, 3–4, and ≥5) and KPS (≥70% and <70%). A second analyses was executed with dichotomized groups (age ≤60 years vs. >60 years; KPS <90% vs. ≥90%).

For OS analysis, a subpopulation was filtered from the initial patient cohort. All patients within this subgroup were treated with a surgical resection and the remaining tumor burden was <2 cm^3, proved by postoperative volumetric analysis (see next paragraph). The primary end point for this subgroup was the OS, calculated by the difference between the time point of surgery and date of tumor-related death of the patient or the end of the study (January 2018).

Volumetric Assessment

Preoperative MRI scans were performed at the earliest 1 week before surgery; postoperative scans within 48 hours after surgery

Table 1. Clinicopathologic and Imaging Characteristics

Variable	Total Sample (n = 152)	Overall Survival Total (n = 76)	*P* Value*
Sex, n (%)			
Male	81 (53.3)	43 (56.6)	0.468
Female	71 (46.7)	33 (43.4)	
Age, n (%)			
≤60 years	43 (28.3)	26 (34.2)	
>60–≤70 years	37 (24.3)	23 (30.3)	0.211
>70 years	72 (47.4)	27 (35.5)	
Charlson Comorbidity Index, n (%)			
1	68 (44.7)	44 (57.9)	
2	50 (32.6)	22 (28.9)	0.115
3	34 (22.4)	10 (13.2)	
Karnofsky Performance Status, n (%)			
≥70%	94 (61.8)	57 (75)	**0.006**
<70%	56 (36.8)	17 (22.4)	
Ki-67 index (%), mean ± SD	22.4 ± 10.5	22.6 ± 10.7	0.877
Tumor volume (cm^3), mean ± SD	34.9 ± 27.1	34.6 ± 29.6	0.936
Edema volume (cm^3), mean ± SD	89.4 ± 62.5	82.3 ± 61.5	0.417
Necrosis volume (cm^3), mean ± SD	9.85 ± 10.8	10.8 ± 12.8	0.573
Edema tumor ratio, mean ± SD	4.37 ± 7.71	3.29 ± 3.12	0.245
Necrosis tumor ratio, mean ± SD	0.25 ± 0.13	0.26 ± 0.14	0.572

SD, standard deviation.
*Student *t* test. Statistical significant values are presented in bold type (significant ≤0.05).

(1.5 T or 3 T). The qualitative assessment included the tumor side (left vs. right) and the affected lobe(s). Minimum MRI protocol consisted of axial plain and contrast-enhanced three-dimensional (3D) T1-weighted (T1w) magnetization-prepared rapid acquisition with gradient echo data sets with 1 mm isotropic voxel size and secondary multiplanar reformation in coronal and sagittal plane and two-dimensional precontrast T2-weighted and fluid-attenuated inversion recovery images. Quantitative volumetric measurement was performed in a semi-automated fashion by manually marking the region of interest using a contour-expansion algorithm (SmartBrush [Brainlab AG, Feldkirchen, Germany]) as previously described.[6] Measured volumes on preoperative MRIs were defined as:

- Tumor: enhancing area on postcontrast T1w images including the central necrosis
- Necrosis: nonenhancing region within the tumor on post-contrast T1w images
- Edema: area of hyperintensity on fluid-attenuated inversion recovery images surrounding the lesion, excluding the tumor volume
- Cystic lesions: bright signal on T2-weighted imaging within the tumor, well circumscribed, and corresponding to a low signal on T1w. The cystic volumes were measured and subtracted from the total tumor volume, not confounding the vital tumor volume by secreted fluids.

Figure 1 shows a typical surgical planning procedure before resection of a glioblastoma. The volumetric assessment via a 3D volumetric measurement can be integrated into the 3 planes of the MRI. Also, reconstructions in 3D can be made, providing a better spatial visualization of the tumor and its surrounding structures.

- Residual tumor volume (RTV) was measured on postoperative magnetic resonance data sets. To assess RTV, the plain T1w images were semi-automatically subtracted from the post-contrast T1w data set using the Vendors software (Syngo VB 17 [Siemens, Erlangen, Germany]) to differentiate postoperative hemorrhage within the resection cavity from contrast enhancement reflecting vital tumor.

From the derived volumes, 2 ratios were calculated: the edema/tumor ratio (edema volume divided by the tumor volume) and necrosis/tumor ratio (necrosis volume divided by the tumor volume). This measurement technique has already been validated, being superior to other tumor assessments.[6] All measurements were performed by experienced neurosurgeons (C.H. and T.K.), blinded to the clinical data of the patients at time of measurement.

Immunohistochemistry

Ki-67 immunohistochemistry was performed using a mouse-derived anti-Ki-67 primary IgG1 antibody (clone MIB-1, dilution 1:500 [Dako, Hamburg, Germany]). Slides were processed on an automatic immunohistochemistry system (AutostainerLink48 [Dako]), according to routine protocols. Quantification of Ki-67 labeling was performed on a light microscope. The immunostained sections were scanned using a 20× objective for the areas with the highest density of labeled tumor cells (hot spots). At least 1000 tumor cells, or alternatively 3 high power fields, were examined. Only immunoreactive tumor cell nuclei were counted. Necrotic areas and vascular endothelium were excluded. The Ki-67 index was defined as the percentage of immunoreactive tumor cell nuclei among the total number of cells.

The *MGMT* promoter methylation status was determined from formalin-fixed paraffin-embedded specimens taken during surgery using the MethyLight real-time polymerase chain reaction method as previously described.[17]

Isocitrate dehydrogenase mutation status was determined via Sanger sequencing. If not initially available, analysis was performed retrospectively.

Table 2. Linkage between Ki-67 Index and Patient Characteristics

	Total *P* Value*	Propensity Score–Matched *P* Value*
Sex	0.883	0.712
Age	0.111	0.383
Tumor volume	0.238	0.266
Edema volume	0.615	0.895
Necrosis volume	0.673	0.646
Edema tumor ratio	0.576	0.136
Necrosis tumor ratio	0.878	0.698

*Pearson χ^2 test.

Statistical Analysis

All data were stored and analyzed using SPSS version 22.0 software (IBM Corp., Armonk, New York, USA). Descriptive statistics were computed for continuous and categorical variables. The statistics computed included mean, median, standard deviation, minimum and maximum continuous variables (outlined as mean ± standard deviation), and frequencies and percentages of categorical factors. The linear relationship between 2 variables was evaluated by the most familiar measure of dependence between 2 not normally distributed quantities, the Spearman rank correlation coefficient rho (r_S). Survival was analyzed using the Kaplan-Meier product-limit method and Cox proportional hazards regression analysis in a univariate and multivariate model to determine statistical significance. First, univariate analyses were performed to show unadjusted significant associations between prognostic variables and OS. Thereafter, variables yielding P values <0.05 (as a whole) in the univariate analysis were entered in the multivariate model to highlight some adjusted associations between the outcome and covariates that were univariate of borderline significance.

All P values resulted from 2-sided statistical tests and values of $P < 0.05$ were considered to be statistically significant. A propensity score (PS) matching (1:1) was performed within the total cohort, resulting in a matched cohort of 118 patients. The cutoff value for matching was the Ki-67 index ≤20%. PS matching was performed to reduce the potential bias of confounding variables and adjustment of baseline imbalances. The same matching method was executed for the OS subgroup, resulting in a matched cohort of 84 individuals.

RESULTS

In our study, the mean age was 67 ± 10.6 years, with a male/female ratio of 1.14:1. The age distribution, with 71.7% in our cohort being >60 years of age at time of diagnosis, and the ratio of sexes correspond with previous studies.[8,18] Nearly half of all included patients had a low Charlson Comorbidity Index (<2) (68/152, 44.7%), corresponding with a higher performance status (KPS ≥70% in 94/152, 61.8%) (Table 1). The tumors were predominantly located within the temporal lobe (53/152, 34.9%), followed by a frontal (32/152, 21.1%) or parietal location (30/152, 19.7%). The distribution between both hemispheres was similar, with 54.6% of cases in the right hemisphere (83/152) and 10 tumors with a bilateral manifestation (10/152, 6,6%). The patients integrated into the OS subgroup ($n = 76$) showed a comparable distribution regarding sex, age and the Ki-67 index to the total cohort ($P \geq 0.211$). There was an apparent difference in measured KPS between both cohorts ($P = 0.006$), indicating that the surgically resected patients had a better initial performance status. The MGMT promoter methylation status was confirmed in 58 cases; 39 of these were unmethylated (67.2%). The characteristics of the PS-matched cohort, selected from the total cohort, are summarized in Supplementary Table 1.

Volumetric Results

The pretreatment volumetric assessment of the tumor compartments showed a median tumor volume of 30 ± 27.1 cm^3, which precisely matches the volume of a table tennis ball. The range of measured tumor volumes was wide, reaching from 0.36 cm^3 to a maximum of 158 cm^3, which nearly equals the volume of a Rubik cube (166 cm^3). The mean peritumoral edema size was 89.4 ± 62.5 cm^3, representing an average quadrupling of the tumor volume itself (mean edema/tumor ratio, 4.37 ± 7.71). The decayed inner core of the tumor, the necrosis, represents one quarter of the tumor volume on average (mean necrosis/tumor ratio, 0.25 ± 0.13). Like the clinical characteristics, the measured volumes and calculated ratios were comparably distributed within the total and the OS subgroup ($P \geq 0.245$). A correlation analysis between the measured compartments showed a strong dependency of all volumes toward each other ($P \leq 0.003$) (Supplementary Table 2). The strongest association was observed between the tumor volume and the necrosis ($r_S = 0.872$). RTV was 0 cm^3 in 38.2% of patients, between 0 and 0.3 cm^3 in 21.1%, and >0.3 cm^3 in 40.8%. The median extent of resection was 99.18%.

Ki-67 Labeling

The median Ki-67 labeling index was 20% in both groups (total cohort and OS subgroup) (ranging, 5%–50%). We could not observe any impact of patient characteristics on the Ki-67 index in the total and the PS-matched cohort (e.g., sex [$P = 0.883$ and 0.712, respectively] or age [$P = 0.111$ and 0.383, respectively]) (Table 2). In matters of the measured tumor compartments, the Ki-67 index had no influence on the derived volumes or the ratios ($P \geq 0.136$). These results were also evident within the correlation analysis ($P \geq 0.399$) (Supplementary Table 2).

Survival Analysis

For survival analysis, a total of 76 data sets contained all included variables. Most patients (57/76, 75%) received adjuvant radiotherapy and concomitant chemotherapy with temozolomide according to the Stupp protocol within the OS subgroup.[2] In some cases, individual deviations from the Stupp protocol were made according to patient age, MGMT methylation status, KPS, and patient preferences; 19 patients (25%) did not receive temozolomide but did receive radiation therapy, and 2 patients (2.6%) received neither radiation therapy nor temozolomide. The survival analysis showed significant influences of the patient's age and performance status (KPS) on OS in univariate analysis ($P = 0.024$ and 0.023, respectively) (Table 3 and Figure 2). However, in multivariate analyses, the effect of both variables lost statistical significance

Table 3. Univariate Survival Analysis*

	P Value	Hazard Ratio	95% Confidence Interval
Sex			
Female versus male†	0.511	1.18	0.72–1.91
Age (years)			
>70 versus ≤ 60†	**0.024**	1.95	1.09–3.48
Charlson Comorbidity Index			
≥5 versus ≤ 2†	0.060	2.14	0.97–4.71
Karnofsky Performance Status (%)			
<70 versus ≥70†	**0.023**	1.92	1.09–3.38
MGMT			
Unmethylated versus methylated†	0.356	1.33	0.73–2.44
Ki-67 (%)			
>20 versus ≤20†	**0.040**	1.70	1.03–2.80
>25 versus ≤25†	0.052	1.65	1.00–2.73
>30 versus ≤30†	**0.012**	2.59	1.24–5.42
Radiation therapy			
No versus yes†	**0.003**	9.89	2.22–43.93
Chemotherapy			
No versus yes†	**0.004**	2.26	1.30–3.94
Tumor volume (cm^3)			
>40 versus ≤16†	0.826	0.94	0.53–1.67
Edema volume (cm^3)			
>100 versus ≤50†	0.971	0.99	0.57–1.73
Necrosis volume (cm^3)			
>10 versus ≤3†	0.822	1.07	0.61–1.86
Edema tumor ratio			
≤2 versus >4†	0.569	0.84	0.47–1.51
Necrosis tumor ratio			
>0.33 versus ≤0.2†	0.231	1.51	0.77–2.95

*Cox proportional hazards regression.
†Reference category. Statistical significant values are presented in bold type (significant ≤0.05).

with 3 age groups and KPS threshold of 70% (Table 4). At a cutoff value of 90% for KPS, the initial performance status showed its significant influence on OS (Supplementary Table 3). The *MGMT* methylation status showed no significant impact on OS in our cohort. The Charlson Comorbidity Index also predicted a trend in survival analysis, with a hazard ratio (HR) of 2.14, for patients with a higher comorbidity index ($P = 0.060$). The measured pretreatment tumor compartment volumes and ratios showed no impact on survival ($P \geq 0.231$). Furthermore, the RTV showed no significant impact on survival ($P = 0.297$), which is not surprising because the OS subgroup consisted of only patients after a gross total resection. Adjuvant therapies after the surgical resection, both radiation and chemotherapy, showed a distinct effect on OS, confirming their significance in the treatment of glioblastoma ($P = 0.003$ and 0.004, respectively). In multivariate analysis, only radiation therapy still showed a statistical significance ($P = 0.027$; HR, 6.99 for Ki-67 cutoff 20%). The Ki-67 labeling index showed only a statistically significant effect on patients' OS with a cutoff value of 20% in multivariate analysis ($P = 0.043$). With a rise of the cutoff point to 30%, the HR also increased from 1.74 to 2.13 ($P = 0.086$).

DISCUSSION

Within the treatment of glioblastoma, prognostic markers play a pivotal role in clinical decision making. The aim of our study was not only to illuminate the prognostic strength of the Ki-67 index; we also wanted to link the histologic proliferation index to the pretreatment appearance of the tumor on MRI.

In our cohort, the diversity of glioblastoma on MRIs is well shown by the broad ranges of the 3 measured tumor volumes and the 2 derived ratios. Our data could not correlate the Ki-67 index with the volumetric measurements. In particular, we expected a relation between a higher necrosis volume and a corresponding increased proliferation index, which was not present in our cohort. This observation is perhaps allegeable, because the proliferation index cannot include an essential dimension of the tumor: its progression over time. Within a previous study by Chung et al.,[19] glioma cells with similar Ki-67 indices showed different progression rates. Therefore, a potential explanation lies within the time of acquisition of the MRI, usually with the onset of the first clinical symptoms. Smaller tumors with less necrosis that are situated within eloquent areas were possibly detected and treated earlier, eluding the potential for further growth of the tumor. Another explanation lies within the assessment of the index itself. The surgical specimen of the tumor often shows just a fragment of the whole tumor because of the surgical approach and the preparation of the tumor with suction and bipolar diathermy. The highest proliferation has been shown at the interface of the solid tumor and the surrounding tissue.[20,21] During the surgical resection, specimens for histologic examination are often taken from the tumor core and not exclusively from the margin. In addition, it is possible that the labeling index is adequate for the examined tumor area but underrated in relation to the whole tumor and not representative of its growth potential. This intratumoral heterogeneity of the Ki-67 index was previously described by Jakovlevs et al.,[22] ranging within the same specimen between 2% and 95%. Also, there is no clear consensus on how the index is best measured and in which areas, restricting its interlaboratory and the interstudy comparability, a problem not restricted only to the glioblastoma but also evident in breast cancer, for example.[23] A potential solution was proposed in 2000 by Shimizu et al.,[24] who showed a distinct correlation between choline levels measured by magnetic resonance spectroscopy and the Ki-67 index. However, limitations of magnetic resonance spectroscopy must be mentioned, such as restricted availability, distortion or signal degradation from artefacts, and, most importantly, a sampling error from choosing a representative tumor area for spectral evaluation. Hence, the last-mentioned restriction

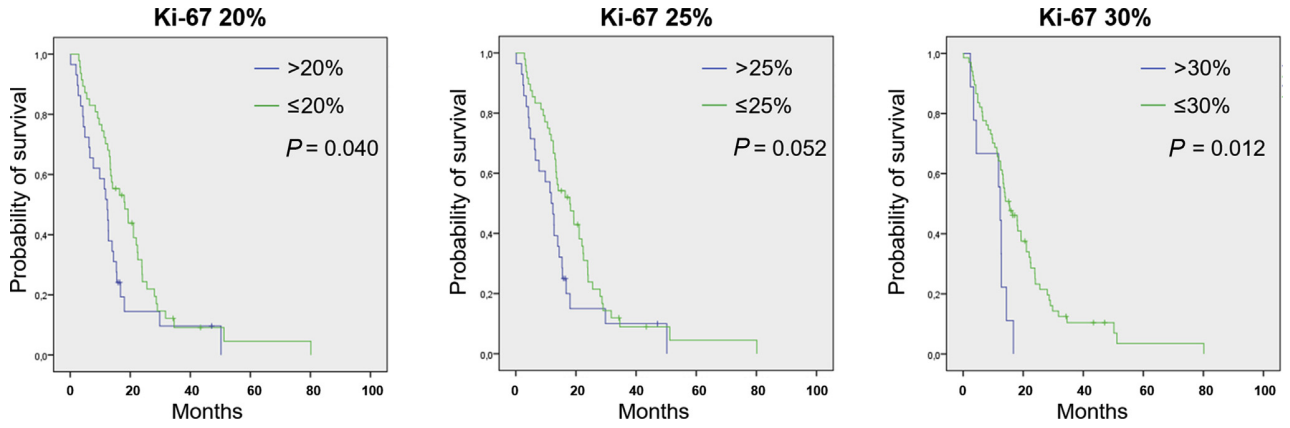

Figure 2. Kaplan-Meier curves and *P* values from Cox proportional hazards model. The survival curves from the overall survival subgroup show the influence of the Ki-67 index on patient survival in univariate analysis. Comparing the different cutoff values, 20% and 30% thresholds for Ki-67 showed significant *P* values.

applies not only to the Ki-67 index but also to magnetic resonance spectroscopy.

The advantage of our correlation analysis was that the Ki-67 index was analyzed as a continuous value rather than by evaluating specific cutoff values dichotomizing the index. Furthermore, our findings were strengthened by the PS matching. The advantage of this matching lies within its ability to partly overcome limitations from the retrospective setting of our cohort analyses. In particular, a potential bias from diverging patient characteristics can be reduced by matching the Ki-67 cohorts. For survival analysis, a threshold is mandatory. In our OS cohort, the Ki-67 index did reach statistical significance in multivariate analysis only at the 20% cutoff point. To our knowledge, no optimal threshold for the index within patients with glioblastoma has been defined. At its best, the cutoff value should accurately help to dichotomize patients with the poorest prognoses and those with a longer survival. Our initial cutoff value of 20% for the Ki-67 index was chosen before the statistical analysis, according to previous

Table 4. Multivariate Survival Analysis*

	Ki-67 20%		Ki-67 25%		Ki-67 30%	
	Adj. HR (CI)	*P* Value	Adj. HR (CI)	*P* Value	Adj. HR (CI)	*P* Value
Age (years)						
>70 versus ≤60†	1.50 (0.73–3.10)	0.269	1.49 (0.72–3.09)	0.283	1.52 (0.74–3.12)	0.257
Karnofsky Performance Status (%)						
<70 versus ≥70†	1.63 (0.84–3.17)	0.148	1.61 (0.83–3.13)	0.158	1.35 (0.67–2.74)	0.407
Ki-67 index						
High versus low†	1.74 (1.02–2.98)	**0.043**	1.69 (0.98–2.91)	0.060	2.13 (0.90–5.04)	0.086
Radiation therapy						
No versus yes†	6.99 (1.25–39.2)	**0.027**	6.87 (1.23–38.47)	**0.028**	7.19 (1.29–40.18)	**0.025**
Chemotherapy						
No versus yes†	1.56 (0.75–3.22)	0.233	1.56 (0.75–3.22)	0.231	1.75 (0.84–3.67)	0.137
Edema tumor ratio						
≤2 versus >4†	0.74 (0.40–1.36)	0.335	0.73 (0.40–1.35)	0.320	0.81 (0.44–1.48)	0.485

Adj. HR, adjusted hazard ratio; CI, confidence interval.
*Cox proportional hazards regression.
†Reference category. Statistical significant values are presented in bold type (significant ≤0.05).

studies.[25-28] Some studies used 10% or even lower as a cutoff value, showing in most cases significant results for the Ki-67 index as a predictor for OS.[13] In our opinion, this value is too low, especially because it is a more useful threshold for the discrimination between low-grade and high-grade gliomas.[11] For a further evaluation of a more accurate threshold within glioblastoma, we also tested 2 higher cutoffs (25% and 30%) within the OS subgroup. The 30% cutoff point showed the highest HRs within univariate and multivariate analysis of all tested cutoff points (HR, 2.59 and 2.13, respectively), but without reaching a statistical significance ($P = 0.086$). The *MGMT* methylation status showed no impact on OS in our cohort. As the Kaplan-Meier curve implicates, this effect seems to be more important at the second half of the survival curve. This observation might be because of an uneven distribution of the methylation status (19/58 methylated [32.8%] vs. 39/58 unmethylated [67.2%]). Furthermore, 19 patients did not receive temozolomide. According to a previous study,[29] *MGMT* methylation status does not influence patient outcome in solely irradiated glioblastoma.

One limitation of our study, besides its retrospective nature, lies within the not fully objectified assessment of the Ki-67 index by immunohistochemistry, including sampling errors, the chosen fields for counting of positive cells, and the counting procedure itself. In addition, the Ki-67 labeling was not performed within the setting of a study under similar conditions. On the other hand, this potential bias may strengthen our study results regarding their importance for the daily clinical routine. Within the scope of the existing literature, our results do confirm the prognostic value of the Ki-67 index within patients with glioblastoma. One advantage of our study is the homogenous structure of the patient cohort (only those with primary glioblastoma). Furthermore, only patients after a surgical resection with a very small remaining tumor burden (RTV) of <2 cm^3 were included. Most of the previously published results are from cohorts that have not been stratified for treatment characteristics.

CONCLUSIONS

In our opinion, the Ki-67 index is a valuable proliferation marker, especially for the discrimination between low-grade and high-grade tumors. It did not show a distinct correlation with the tumor appearance on pretreatment MRI in our cohort. The proliferation rate of the glioblastoma seems therefore not a sole explanation for the diverse appearance of the tumor in imaging studies. Moreover, we could strengthen its value as a prognostic marker for the OS of patients with glioblastoma. Yet, thresholds for a further subdivision of glioblastoma regarding the OS are not well defined. In our cohort, a cutoff value of 20% for the Ki-67 index seems to be an adequate threshold for the survival analysis of patients with glioblastoma. There is no consensus relating to the appropriate technique for the assessment of the Ki-67 index. All these issues should be considered in the scope of further investigations.

ACKNOWLEDGMENTS

The authors thank Prof. Günther Kundt for his valuable statistical suggestions and the patients who participated in this study.

REFERENCES

1. Ostrom QT, Gittleman H, Liao P, et al. CBTRUS Statistical Report: primary brain and other central nervous system tumors diagnosed in the United States in 2010-2014. *Neuro Oncol*. 2017;19(suppl 5):vi-v88.
2. Stupp R, Hegi ME, Mason WP, et al. Effects of radiotherapy with concomitant and adjuvant temozolomide versus radiotherapy alone on survival in glioblastoma in a randomised phase III study: 5-year analysis of the EORTC-NCIC trial. *Lancet Oncol*. 2009;10:459-466.
3. Brat DJ, Castellano-Sanchez AA, Hunter SB, et al. Pseudopalisades in glioblastoma are hypoxic, express extracellular matrix proteases, and are formed by an actively migrating cell population. *Cancer Res*. 2004;64:920-927.
4. Robbins SL. *Robbins Basic Pathology*. 10th ed. Philadelphia, PA: Elsevier; 2018.
5. Rong Y, Durden DL, van Meir EG, Brat DJ. 'Pseudopalisading' necrosis in glioblastoma: a familiar morphologic feature that links vascular pathology, hypoxia, and angiogenesis. *J Neuropathol Exp Neurol*. 2006;65:529-539.
6. Henker C, Kriesen T, Glass Ä, Schneider B, Piek J. Volumetric quantification of glioblastoma: experiences with different measurement techniques and impact on survival. *J Neurooncol*. 2017;135:391-402.
7. Hegi ME, Diserens A-C, Gorlia T, et al. MGMT gene silencing and benefit from temozolomide in glioblastoma. *N Engl J Med*. 2005;352:997-1003.
8. Bauchet L, Mathieu-Daudé H, Fabbro-Peray P, et al. Oncological patterns of care and outcome for 952 patients with newly diagnosed glioblastoma in 2004. *Neuro Oncol*. 2010;12:725-735.
9. Gerdes J, Schwab U, Lemke H, Stein H. Production of a mouse monoclonal antibody reactive with a human nuclear antigen associated with cell proliferation. *Int J Cancer*. 1983;31:13-20.
10. Scholzen T, Gerdes J. The Ki-67 protein: from the known and the unknown. *J Cell Physiol*. 2000;182:311-322.
11. Johannessen AL, Torp SH. The clinical value of Ki-67/MIB-1 labeling index in human astrocytomas. *Pathol Oncol Res*. 2006;12:143-147.
12. Hu X, Miao W, Zou Y, Zhang W, Zhang Y, Liu H. Expression of p53, epidermal growth factor receptor, Ki-67 and O6-methylguanine-DNA methyltransferase in human gliomas. *Oncol Lett*. 2013;6:130-134.
13. Chen W-J, He D-S, Tang R-X, Ren F-H, Chen G. Ki-67 is a valuable prognostic factor in gliomas: evidence from a systematic review and meta-analysis. *Asian Pac J Cancer Prev*. 2015;16:411-420.
14. Chen L, Voronovich Z, Clark K, et al. Predicting the likelihood of an isocitrate dehydrogenase 1 or 2 mutation in diagnoses of infiltrative glioma. *Neuro Oncol*. 2014;16:1478-1483.
15. Karnofsky DA, Abelmann WH, Craver LF, Burchenal JH. The use of the nitrogen mustards in the palliative treatment of carcinoma. With particular reference to bronchogenic carcinoma. *Cancer*. 1948;1:634-656.
16. Charlson M, Szatrowski TP, Peterson J, Gold J. Validation of a combined comorbidity index. *J Clin Epidemiol*. 1994;47:1245-1251.
17. Eads CA, Danenberg KD, Kawakami K, et al. MethyLight: a high-throughput assay to measure DNA methylation. *Nucleic Acids Res*. 2000;28:E32.
18. Lacroix M, Abi-Said D, Fourney DR, et al. A multivariate analysis of 416 patients with glioblastoma multiforme: prognosis, extent of resection, and survival. *J Neurosurg*. 2001;95:190-198.
19. Chung WJ, Lyons SA, Nelson GM, et al. Inhibition of cystine uptake disrupts the growth of primary brain tumors. *J Neurosci*. 2005;25:7101-7110.
20. Dalrymple SJ, Parisi JE, Roche PC, Ziesmer SC, Scheithauer BW, Kelly PJ. Changes in proliferating cell nuclear antigen expression in glioblastoma multiforme cells along a stereotactic biopsy trajectory. *Neurosurgery*. 1994;35:1036-1044 [discussion 1044-1045].
21. Eidel O, Burth S, Neumann J-O, et al. Tumor infiltration in enhancing and non-enhancing parts of glioblastoma: a correlation with histopathology. *PLoS One*. 2017;12:e0169292.

22. Jakovlevs A, Vanags A, Balodis D, Gardovskis J, Strumfa I. Heterogeneity of Ki-67 and p53 expression in glioblastoma. *Acta Chirurgica Latviensis*. 2014;14. https://doi.org/10.2478/chilat-2014-0102.

23. Inwald EC, Klinkhammer-Schalke M, Hofstädter F, et al. Ki-67 is a prognostic parameter in breast cancer patients: results of a large population-based cohort of a cancer registry. *Breast Cancer Res Treat*. 2013;139:539-552.

24. Shimizu H, Kumabe T, Shirane R, Yoshimoto T. Correlation between choline level measured by proton MR spectroscopy and Ki-67 labeling index in gliomas. *AJNR Am J Neuroradiol*. 2000;21:659-665.

25. Donato V, Papaleo A, Castrichino A, et al. Prognostic implication of clinical and pathologic features in patients with glioblastoma multiforme treated with concomitant radiation plus temozolomide. *Tumori*. 2007;93:248-256.

26. Yoshida Y, Nakada M, Harada T, et al. The expression level of sphingosine-1-phosphate receptor type 1 is related to MIB-1 labeling index and predicts survival of glioblastoma patients. *J Neurooncol*. 2010;98:41-47.

27. Yue Q, Zhang X, Ye H-X, et al. The prognostic value of Foxp3+ tumor-infiltrating lymphocytes in patients with glioblastoma. *J Neurooncol*. 2014;116:251-259.

28. Reavey-Cantwell JF, Haroun RI, Zahurak M, et al. The prognostic value of tumor markers in patients with glioblastoma multiforme: analysis of 32 patients and review of the literature. *J Neurooncol*. 2001;55:195-204.

29. Crinière E, Kaloshi G, Laigle-Donadey F, et al. MGMT prognostic impact on glioblastoma is dependent on therapeutic modalities. *J Neurooncol*. 2007;83:173-179.

Conflict of interest statement: The authors declare that the article content was composed in the absence of any commercial or financial relationships that could be construed as a potential conflict of interest.

Received 15 August 2018; accepted 1 February 2019

Citation: World Neurosurg. (2019). https://doi.org/10.1016/j.wneu.2019.02.006

Journal homepage: ***www.journals.elsevier.com/world-neurosurgery***

Available online: ***www.sciencedirect.com***

1878-8750/$ - see front matter © 2019 Elsevier Inc. All rights reserved.

SUPPLEMENTARY DATA

Supplementary Table 1. Characteristics of the Propensity Score–Matched Cohort

Variable	Propensity Score–Matched Sample (n = 118)
Sex, n (%)	
Male	64 (54.2)
Female	54 (45.8)
Age, n (%)	
≤60 years	35 (29.7)
>60–≤70 years	28 (23.7)
70 years	55 (46.6)
Charlson Comorbidity Index, n (%)	
1	54 (45.8)
2	39 (33.1)
3	25 (21.2)
Karnofsky Performance Status, n (%)	
≥70%	71 (60.2)
<70%	45 (38.1)
Ki-67 index (%), mean ± SD	24.2 ± 10.9
Tumor volume (cm^3), mean ± SD	36.1 ± 27.7
Edema volume (cm^3), mean ± SD	85.0 ± 60.0
Necrosis volume (cm^3), mean ± SD	10.4 ± 11.2
Edema tumor ratio, mean ± SD	3.65 ± 5.39
Necrosis tumor ratio, mean ± SD	0.26 ± 0.13

SD, standard deviation.

Supplementary Table 2. Correlation Analysis Between Tumor Compartments and Ki-67 Index*

	Ki-67	Tumor	Edema	Necrosis	Edema Tumor Ratio	Necrosis Tumor Ratio
Ki-67						
r_S	1	−0.051	−0.020	−0.014	0.069	0.056
P value	—	0.533	0.807	0.865	0.399	0.490
Tumor						
r_S	−0.051	1	0.601	0.872	−0.387	0.385
P value	0.533	—	**<0.001**	**<0.001**	**<0.001**	**<0.001**
Edema						
r_S	−0.020	0.601	1	0.526	0.380	0.241
P value	0.807	<0.001	—	<0.001	<0.001	0.003
Necrosis						
r_S	−0.014	0.872	0.526	1	−0.351	0.749
P value	0.865	<0.001	<0.001	—	<0.001	<0.001
Edema tumor ratio						
r_S	0.069	−0.387	0.380	−0.351	1	−0.154
P value	0.399	<0.001	<0.001	<0.001	—	0.058
Necrosis tumor ratio						
r_S	0.056	0.385	0.241	0.749	−0.154	1
P value	0.490	<0.001	0.003	<0.001	0.058	—

r_S, Spearman rho.
*Spearman rank correlation test. Statistical significant values are presented in bold type (significant ≤0.05).

Supplementary Table 3. Survival Analysis, Changed Cutoff Values

	P Value	Hazard Ratio	95% Confidence Interval
Univariate survival analysis*			
Age (years)			
>60 versus ≤60†	**0.110**	1.51	0.91–2.51
Karnofsky Performance Status (%)			
<90 versus ≥90†	**0.020**	1.812	1.10–2.99
Multivariate survival analysis (Ki-67 cutoff 20%)*			
Age (years)			
>60 versus ≤60†	0.267	1.38	0.78–2.42
Karnofsky Performance Status (%)			
<90 versus ≥90†	**0.046**	1.72	1.01–2.94
Ki-67 index (%)			
>20 versus ≥20†	**0.032**	1.79	1.05–3.03
Radiation therapy			
Yes versus no†	**0.010**	0.12	0.02–0.60
Chemotherapy			
Yes versus no†	0.196	0.66	0.35–1.24

*Cox proportional hazards regression.

†Reference category. Statistical significant values are presented in bold type (significant ≤0.05).

J Neurooncol (2016) 126:585–592
DOI 10.1007/s11060-015-2005-9

CLINICAL STUDY

Effect of 10 different polymorphisms on preoperative volumetric characteristics of glioblastoma multiforme

Christian Henker[1] · Thomas Kriesen[1] · Katharina Fürst[2] · Deborah Goody[2] · Änne Glass[3] · Brigitte M. Pützer[2] · Jürgen Piek[1]

Received: 26 August 2015 / Accepted: 19 November 2015 / Published online: 25 November 2015
© Springer Science+Business Media New York 2015

Abstract There is a distinct diversity between the appearance of every glioblastoma multiforme (GBM) on pretreatment magnetic resonance imaging (MRI) with a potential impact on clinical outcome and survival of the patients. The object of this study was to determine the impact of 10 different single nucleotide polymorphisms (SNPs) on various volumetric parameters in patients harboring a GBM. We prospectively analyzed 20 steroid-naïve adult patients who had been treated for newly diagnosed GBM. The volumetry was performed using MRI with the help of a semi-automated quantitative software measuring contrast enhancing tumor volume including necrosis, central necrosis alone and peritumoral edema (PTE). We calculated ratios between the tumor volume and edema (ETR), respectively necrosis (NTR). SNP analysis was done using genomic DNA extracted from peripheral blood genotyped via PCR and sequencing. There was a strong correlation between tumor volume and PTE ($p < 0.001$), necrosis ($p < 0.001$) and NTR ($p = 0.003$). Age and sex had no influence on volumetric data. The Aquaporin 4-31G > A SNP had a significant influence on the ETR ($p = 0.042$) by decreasing the measured edema compared with the tumor volume. The Interleukin 8-251A > T SNP was significantly correlated with an increased tumor ($p = 0.048$), PTE ($p = 0.033$) and necrosis volume ($p = 0.028$). We found two SNPs with a distinct impact on pretreatment tumor characteristics, presenting a potential explanation for the individual diversity of GBM appearance on MRI and influence on survival.

Keywords Glioblastoma · Volumetrics · Edema · Necrosis · Polymorphism

✉ Christian Henker
christian.henker@med.uni-rostock.de

[1] Department of Neurosurgery, University Hospital Rostock, Schillingallee 35, 18057 Rostock, Germany

[2] Institute of Experimental Gene Therapy and Cancer Research, Rostock University Medical Center, Schillingallee 69, 18057 Rostock, Germany

[3] Institute for Biostatistics and Informatics in Medicine, Rostock University Medical Center, Ernst-Heydemann-Str. 8, 18057 Rostock, Germany

Introduction

Glioblastoma multiforme (GBM) is the most common form of malignant glioma and still has the worst prognosis of all central nervous system tumors [1]. As the term itself multiforme implies the cellular appearance of the GBM varies, it comes to show that even when the patients are divided into homogenous groups with the same mode of therapy, they present with different clinical outcome and survival rate. The focus in previous studies was to preoperatively characterize the tumor itself, the central necrosis and the peritumoral edema (PTE) to predict the clinical behavior and therapy response using radiological imaging. The identification and evaluation of such prognostic factors can be vital for further treatments and future researches.

The results of previously published studies concerning the potential impact of morphometric data are inconsistent, due to mixed patient-populations (e.g. GBM and WHO grade II glioma), mixed treatment plans (biopsy, subtotal and total resection, concomitant radiotherapy and/or chemotherapy) and different measuring techniques [2–5]. Beside these technical issues, there are interpersonal diversities among patients with GBM showing a variety of alterations in morphometric values. The imaging patterns or hallmarks of GBMs on MRI consist of three different presentations in appearance: the contrast-enhancing tumor

itself, the central necrosis, and the PTE. Thus we can state that the appearance of each GBM on MRI is unique und every pattern is individually different. Previous studies have shown that many physiological appearing proteins and their gene expression are linked to these imaging patterns. For our investigation we chose six different and commonly occurring proteins: Aquaporin-1, -4 and-5 (AQP), Interleukin-8 (IL-8), Apolioprotein E (ApoE), and endothelial nitric oxide synthase (eNOS). The expressions of these proteins that can potential affect the imaging patterns have partly been investigated in other types of diseases.

GBM is a highly vascularized tumor with an altered vascular permeability and is characterized by a breakdown of the blood–brain barrier (BBB) [6] that results in a PTE. Some proteins have already been described to have an impact on the magnitude of the PTE, for example AQP4 [7]. It has been shown that the family of Aquaporins (AQP), which are transmembrane water channel proteins, and their expression correlates positively with the histological tumor grading in astrocytomas [8–10]. AQP1 was also associated with the formation of vasogenic edema and glioma cell invasion [7, 11]. Although AQP5 plays a crucial role in water hemostasis of the cerebrospinal fluid (CSF), the inner ear and salivary and lacrimal glands under neurohormonal control [12], up till now it has only been detected in the choroid plexus. Another essential proteins of tumor permeability, invasiveness and PTE are the nitric oxide synthases (NOS) [13] and the inflammatory cytokine Interleukin-8 (IL-8), which especially had been linked to the proliferation of GBM [14, 15]. A key protein for GBM metabolism is ApoE which coordinates the intracranial lipid transport via the bloodstream [16]. The possession of the ApoE ε4 allele is a risk factor for Alzheimeŕs disease and severe brain swelling after trauma [17]. Despite these findings, an influence on the clinical outcome of GBM patients in relation to ApoE has not yet been linked [18].

Beside these well-known investigations there are big interpersonal differences between individuals and the anatomical appearance of the GBM they suffer from. One factor of influence could be the concomitance of commonly occurring single nucleotide polymorphisms (SNPs). These variations of the DNA-sequence may change the amount of produced protein or its expression and manifest a pathological condition. The current study was conducted to analyze the association between the different genotypes of ten SNPs and their impact on the preoperative volumetric data of patients with GBM.

Materials and methods

In this prospective single-center study we analyzed preoperative MRI scans of steroid-naïve patients with the diagnosis of primary GBM (n = 20). Institutional review board approval by the Ethics Committee of the University of Rostock, Germany was obtained prior to the start of this study (Nr. A2014-0035). Written consent was obtained from all patients.

Patient selection

20 adult patients (age > 18 years) of Caucasian ethnicity who had been treated between 2012 and 2014 in our institution with a newly diagnosed intracranial GBM were included. Determination of a GBM was made according to the World Health Organization (WHO) classification system [19]. Patients with previous low-grade gliomas, steroid intake at the time of preoperative MRI scan, insufficient or missing preoperative MRI-data were excluded.

The clinical records of all included patients were reviewed, and collected information included demographics, presenting symptoms, medication at time of preoperative MRI scan and comorbidities.

Volumetric measurement

Preoperative volumes were measured using T1-weighted (T1-W) gadolinium-enhanced MRI (0.9 mm axial cuts) and T2-Fluid Attenuated Inversion Recovery sequences (FLAIR) (3–6 mm axial cuts) obtained on 1,5-T and 3-T scanners. Tumor volume was considered to be the contrast-enhancing area including central necrosis on contrast-enhanced T1-W images. The central necrosis was defined as regions with low signal on T1-W images within the tumor border defined on contrast enhanced T1-W images. PTE was defined as bright T2-FLAIR signal surrounding the tumor.

Using Brainlabs iPlan software (version 3.0; Brainlab, Feldkirchen, Germany), the Region of Interest (ROI)—respectively tumor, necrosis and PTE—was quantitatively measured and analyzed by the included volumetric software. Therefore the ROI was manually marked with the support of the semi-automated software.

The two volume-ratios (Edema/Tumor-Ratio = ETR, Necrosis/Tumor-Ratio = NTR) were calculated using the PTE volume or necrosis volume divided by tumor volume. A functional grading was performed as described by Sawaya et al. [20] to characterize the tumor location with regard to proximity to eloquent areas (I = non eloquent, II = near eloquent, III = eloquent). All volumes were measured and assessed by the same neurosurgeon.

Genetic analysis

A 5 ml venous whole blood sample was taken from every patient and stored in an EDTA-buffered tube at −4 °C refrigerator till further use. For genetic analysis and

identification of SNPs, genomic DNA was first isolated from patient blood using DNeasy Blood & Tissue Kit (Qiagen) following phenol–chloroform extraction. PCR amplification of specific DNA fragments was performed using peqGOLD Master-Mix (Peqlab). Samples were sequenced with the following specific primers: eNOS-786T > C fwd 5′-TGGAGAGTGCTGGTGTACCCCA-3′ and rev 5′-GCCTCCACCCCCACCCTGTC-3′; eNOS-894G > T fwd 5′-CTGGAGATGAAGGCAGGAGAC-3′ and rev 5′-CTCCATCCCACCCAGTCAATC-3′; IL-8-251 A > T fwd 5′-CTTATCTTCACCATCATGATAGCATCTG-3′ and rev 5′-GGCTGCCAAGAGAGCCACGGCCA-3′; AQP1-783G/C fwd 5′-GCCTGCCCTCAAATCATTGG-3′ and rev 5′-CCGAGCTAGGCAGAGCTGTTAGA-3′; AQP4-131G > A fwd 5′-CCTCATTTTCAAAAATTACTGTCTC-3′ and rev 5′-TTGCTGTGGGTCTGTCACTCAT-3′; AQP4 22C > T fwd 5′-TCCTCATTTTCAAAAATTACTGTCTCA-3′ and rev 5′-TTGCTGTGGGTCTGTCACTCAT-3′; AQP4-1478A/G fwd 5′-CATAGCCTGTATTCCTTCTATC-3′ and rev 5′-GCCCCACAATGAGCTTTGAA-3′; AQP4 9898G > A fwd 5′-GCCTGACAGAACTCAAAGACAC-3′ and rev 5′-GCTAATGCTCTTTTGCCAAGGT-3′; AQP5-1364A/C fwd 5′-CAGCACCTTCCAATGCCAGGTG-3′ and rev 5′-TTTTGGTCTCTGACCTCTTC-3′; ApoE fwd 5′-ACGCGGGCACGGCTGTCCAAGGA-3′ and rev 5′-GCCCCGGCCTGGTACACTGCCA-3′, and SNPs were analyzed.

Statistical analysis

All data were stored and analysed using the SPSS 22.0 software (SPSS, Chicago, IL, USA). Descriptive statistics were computed for continuous and categorical variables. The statistics computed included mean, median, standard deviations, minimum and maximum of continuous variables, frequencies and percentages of categorical factors. Testing for differences of continuous variables between study groups was accomplished by the 2-sample *t* test and ANOVA respectively or the Mann–Whitney U test and Kruskal–Wallis-test respectively, as appropriate. Test selection was based on evaluating the variables for normal distribution employing the Kolmogorov–Smirnov-test. All *p* values resulted from two-sided statistical tests and values of $p < 0.05$ were considered to be statistically significant.

Linear relationship between two variables was evaluated by the most familiar measure of dependence between two quantities, the "Pearson correlation coefficient". The impact of the SNPs on volumetric data was testes under the assumption of a dominant (wildtype vs. heterozygote+homozygote allele carrier) or recessive (wildtype+heterozygote allele carrier vs. homozygote allele carrier) genetic model for each SNP. All SNPs were tested for accordance with the Hardy–Weinberg-equilibrium (HWE). Pearsońs Chi squared test was used testing deviation from HWP, significant if the value of 3.84 was exceeded or values of $p < 0.05$.

Results

The patientś characteristics are shown in Table 1, along with the preoperative volumetric data. A total of 20 patients met the inclusion criteria for our study. Median age was 63 years which is in accordance with other tumor databases [21]. Tumor localization and functional grading were similar to larger series of GBM patients [22], showing that most of the tumors were located closely to (45 %) or within (30 %) eloquent areas. The volumetric characteristics showed comparable results with other series [2, 23]. The ETR showed that the median volume of PTE was two times higher than the tumor volume itself and the necrosis (NTR) reflects approximately a quarter of the whole tumor volume.

Figure 1 combines the measured volumetric data for every patient and reflects the individual diverseness between the tumor volume and PTE, respectively necrosis.

Table 1 Patient characteristics and volumetric data

Patient characteristics	n (%)
Age (years) [median (range)]	63 (48–82)
Sex	
Male	9 (45)
Female	11 (65)
Tumor location	
Temporal	10 (50)
Frontal	6 (30)
Parietal	2 (10)
Other	2 (10)
Tumor side	
Left	9 (45)
Right	11 (65)
Functional grading	
I (noneloquent area)	5 (25)
II (near eloquent area)	9 (45)
III (eloquent area)	6 (30)
Volumetric data	**Median cm^3 (range)**
Tumor	34.9 (2.047–82.4)
PTE	77.4 (0.467–192.6)
Necrosis	5.35 (0.018–45.9)
ETR	2.37 (0.228–4.69)
NTR	0.247 (0.022–0.605)

PTE peritumoral edema, *ETR* Edema/Tumor-Ratio, *NTR* Necrosis/Tumor-Ratio

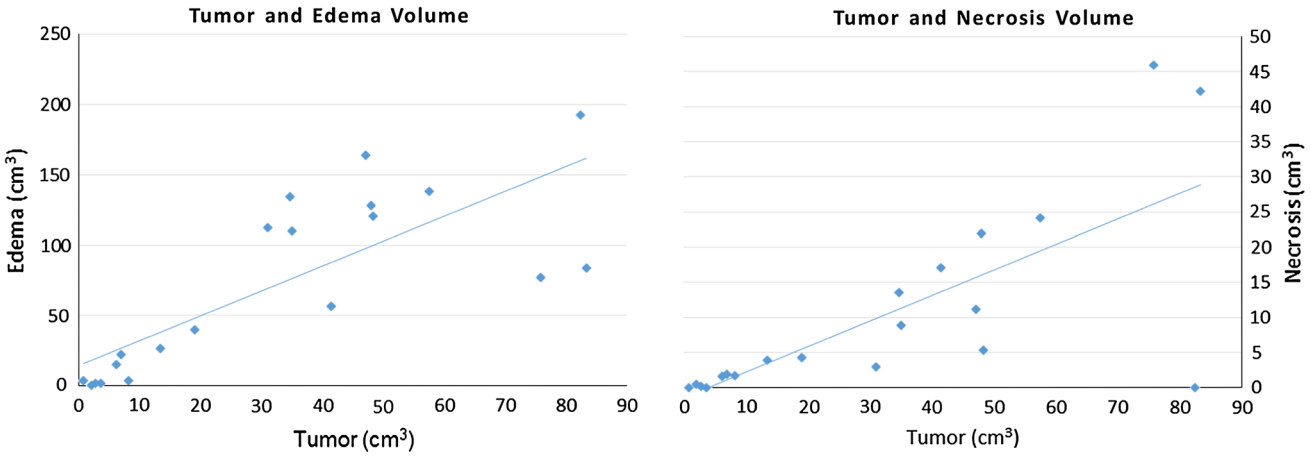

Fig. 1 Individual volumetric data with integrated trendline

Table 2 Correlations between volumetric data and potential influence factors

	Tumor		PTE		Necrosis		ETR		NTR		Sex	Age
	r value	*p* value	r value	*p* value	r value	*p* value	r value	*p* value	r value	*p* value	*p* value	*p* value
Tumor	–	–	**0.788**	**<0.001**	**0.870**	**<0.001**	0.025	0.915	**0.628**	**0.003**	0.308	0.721
PTE	**0.788**	**<0.001**	–	–	**0.472**	**0.036**	0.427	0.061	0.311	0.182	0.219	0.488
Necrosis	**0.870**	**<0.001**	**0.472**	**0.036**	–	–	−0.155	0.515	**0.848**	**<0.001**	0.710	0.988
ETR	0.025	0.915	0.427	0.061	-0.155	0.515	–	–	-0.180	0.449	0.592	0.619
NTR	**0.628**	**0.003**	0.311	0.182	**0.848**	**<0.001**	−0.180	0.449	–	–	0.666	0.994

PTE peritumoral edema, *ETR* Edema/Tumor-Ratio, *NTR* Necrosis/Tumor-Ratio

Statistical significant values are presented in boldtype

Table 2 shows that age and sex had no significant effect on the volumetric data and displays the correlations among the different variables with a significant coherency between the tumor volume and PTE, necrosis and NTR. The PTE itself is also related to the necrosis volume. These interdependence have been partly predictable, especially the connection between tumor volume and PTE and amount of necrosis respectively the NTR. ETR was not correlated with any other volume possibly reflecting the interpersonal diversity of the magnitude of PTE. This findings are also visualized by Fig. 1, showing a closer correlation of necrosis volume towards the tumor volume then the PTE volume.

The SNP-Analysis (Table 3) showed one deviation from Hardy–Weinberg-equilibrium (eNOS-786T > C) caused either by the small sample size or the selection of patients. Distribution of the three isoforms of ApoE have been described previously and our sample population is comparable to these results [24], both ApoE SNPs (rs429358 and rs7412) are within the HWE. The AQP5-SNP was detected in only 19 of 20 patients.

The evaluation of the impact of the ten SNPs (Table 4) on the volumetric characteristics showed a significant association of the IL-8-251A > T-SNP and all three anatomical tumor characteristics (tumor volume, PTE and central necrosis). ETR and NTR were not affected by the IL-8 SNP, which appears just logical according to the influence of the SNP on both datasets in the same way. The ETR was significantly influenced by the appearance of the AQP4-131G > A SNP. A recessive model could not be generated for AQP4-131G > A, AQP 22C > T and AQP5-1364A/C due to missing homozygote genotypes in our study population.

In Table 5 the mean and median volumetric data is shown for the IL-8 and AQP4-131G > A SNPs. The IL-8 SNP homozygote allele carriers do have a significant smaller tumor volume combined with a smaller PTE and amount of necrosis—according to the correlations shown in Table 3. As described above no homozygote allele carriers (AA) for the AQP4-131G > A SNP have been in our study population. The result show a more then bisected ETR of the GA allele carriers compared to G allele carriers.

Discussion

The current study examined the influence of ten different SNPs on the considerable variability of anatomical volumes among individuals harboring a GBM.

Table 3 SNP-Analysis

SNP	Rs2070744 (eNOS-786T > C)			HWE	SNP	Rs162008 (AQP4 22C > T)			HWE
Genot	TT	TC	CC	*p* value	Genot	CC	CT	TT	*p* value
	5 (25 %)	14 (70 %)	1 (5 %)	0.040		14 (70 %)	6 (30 %)	0 (0 %)	0.430
SNP	rs1799983 (eNOS 894G > T)			HWE	SNP	rs9951307 (AQP4-1478A/G)			HWE
Genot	GG	GT	TT	*p* value	Genot	AA	AG	GG	*p* value
	9 (45 %)	9 (45 %)	2 (10 %)	0.909		9 (45 %)	7 (35 %)	4 (20 %)	0.257
SNP	rs4073 (IL-8-251A > T)			HWE	SNP	rs3763043 (AQP4 9898G > A)			HWE
Genot	TT	AT	AA	*p* value	Genot	GG	GA	AA	*p* value
	7 (35 %)	10 (50 %)	3 (15 %)	0.852		7 (35 %)	11 (55 %)	2 (10 %)	0.438
SNP	rs1476597 (AQP1-783G/C)			HWE	SNP	rs3759129 (AQP5-1364A/C)			HWE
Genot	GG	GC	CC	*p-value*	Genot	AA	AC	CC	*p* value
	7 (35 %)	10 (50 %)	3 (15 %)	0.852		13 (68 %)	6 (32 %)	0 (0 %)	0.414
SNP	rs162007 (AQP4-131G > A)			HWE	SNP	rs429358, rs7412 (ApoE)			HWE
Genot	GG	GA	AA	*p* value	Genot	ApoE2	ApoE3	ApoE4	*p* value
	15 (75 %)	5 (25 %)	0 (0 %)	0.523		4 (20 %)	8 (40 %)	8 (40 %)	0.436

SNP single nucleotide polymorphism, *Genot* Genotype, *HWE* Hardy–Weinberg-equilibrium

Table 4 Influence of the analyzed SNPs on volumetric data

SNPs	Tumor *p* value		PTE *p* value		Necrosis *p* value		ETR *p* value		NTR *p* value	
	Recessive	Dominant	Recessive	Dominant	Recessive	Dominant	Recessive	Dominant	Recessive	Dominant
eNOS-786T > C	0.271	0.507	0.250	0.674	0.400	0.612	0.116	0.780	0.854	0.561
eNOS 894G > T	0.993	0.324	0.843	0.261	0.674	0.230	0.468	0.990	0.467	0.520
IL-8-251A > T	**0.048**	0.193	**0.033**	0.472	**0.028**	0.485	0.579	0.600	0.175	0.813
AQP1-783G/C	0.508	0.524	0.942	0.947	0.416	0.438	0.256	0.078	0.147	0.128
AQP4-31G > A	–	0.690	–	0.460	–	1.000	–	**0.042**	–	0.825
AQP4 22C > T	–	0.946	–	0.254	–	0.718	–	0.071	–	0.818
AQP4-478A/G	0.447	0.138	0.496	0.187	0.750	0.152	0.298	0.471	0.676	0.296
AQP4 9898G > A	0.471	0.884	0.702	0.495	0.589	0.877	0.565	0.987	0.831	0.629
AQP5-364A/C	–	0.923	–	0.69	–	0.831	–	0.287	–	0.788
ApoE	0.272		0.570		0.273		0.400		0.486	

PTE peritumoral edema, *ETR* Edema/Tumor-Ratio, *NTR* Necrosis/Tumor-Ratio

Statistical significant values are presented in boldtype

Table 5 Detailed volumetric data itemized for corresponding genotypes

SNP	Genot	Tumor		PTE		Necrosis		ETR		NTR	
		Median	Mean	Median	Mean	Median	Mean	Median	Mean	Median	Mean
IL-8-251A > T	TT	36.2	37.0	70.2	68.0	10.0	14.7	2.34	1.98	0.263	0.282
	AT	41.1	39.4	110	91.5	8.87	13.0	2.58	2.45	0.266	0.297
	AA	**5.10**	**5.10**	**2.18**	**2.18**	**1.08**	**1.08**	0.477	1.80	0.205	0.156
AQP4-131G > A	GG	34.7	33.0	93.6	80.8	6.7	11.7	2.44	2.52	0.253	0.275
	GA	41.4	36.8	56.6	53.3	5.3	13.3	**1.01**	1.20	0.205	0.256

PTE peritumoral edema, *ETR* Edema/Tumor-Ratio, *NTR* Necrosis/Tumor-Ratio

Statistical significant values are presented in boldtype

We found one genetic marker, the AQP4-131G > A SNP, which influenced the individual magnitude of the PTE. AQP4 is the most abundant water channel in the human brain [25] and essential for the physiological function of the BBB. *In vivo* studies showed that AQP4-knockout mice develop a smaller cytotoxic edema under certain pathological conditions like cerebral water intoxication, cerebral ischemia or meningitis [26, 27]. The AQP4 gene contains a promoter binding site for the hypoxia-inducible factor 1-alpha (HIF 1α), which is a very important transcriptional regulator for the cellular response to hypoxia [28]. Pathognomonic features of GBM are necrotic areas surrounded by pseudopalisading cells and intravascular thrombosis. Pseudopalisades show increased HIF 1α expression resulting in high levels of vascular endothelial growth factor (VEGF), AQP4, tissue factor (TF) and IL-8 as an angiogenic response [29–31]. An in vivo study showed a direct correlation between the expression levels of HIF 1α, AQP4 and the PTE; whereby AQP4 was upregulated within the PTE [32].

The AQP4-131G > A SNP is located in the promoter region of the AQP4 gene and an alteration of the expression can thereby lead to a decreased water accumulation and a smaller PTE. This connection had been proven previously by Sorani and coworkers, demonstrating that gene variants of AQP4 lead to a reduction in cellular water permeability [33]. Another study group revealed a reduction of the postischemic brain edema, caused by another AQP4 SNP [34]. Hence our results explain the individual difference of the volumetric data concerning the magnitude of the PTE and particularly the ETR volume.

Our study acknowledges for the first time the ratio between the PTE and the tumor volume to illustrate the individual differences of the PTE appearance. The effect of PTE on survival of patients with GBM is still controversial and most studies focused on the preoperative tumor volume, amount of necrosis or the extent of resection [5, 35] while it is unquestioned that a larger PTE affects the clinical signs and symptoms of patients with a GBM. It is also important to be aware of the relevance of the PTE not only as a side effect of the tumor itself but as an active infiltration zone that already harbors microscopic invasion of cancer cells [36]—recurrence of GBM typically occurs within the PTE. Other authors refer to these areas "T2 hyperintense signal change" to underline the complicacy to distinguish between edema, inflammation, gliosis, and active tumor invasion. Thus it is important to consider the PTE especially when planning a tumor resection.

Another finding of our study was the significant effect of the IL-8-251A > T SNP on all volumetric measured anatomical features of GBM, which were considerably smaller in the homozygote AA group compared to T-Allele carriers. The chemokine IL-8 is a crucial factor in astrocytoma progression and angiogenesis, invasiveness and tumor growth in GBM [14]. The tumor cells secrete IL-8 to promote their growth in an autocrine manner in vitro [37]. As been described above IL-8 expression and secretion is promoted by HIF 1α and TF. *In vitro* studies showed that the expression of TF signaling pathways also correlates with the production of IL-8 [15]. TF is the primary initiator of the coagulation cascade and is upregulated depending on the malignancy grade of tumors [38]. The amount of IL-8 also correlates with the TF gene expression causing intravascular thrombosis, a pathognomonic characteristic of GBM. Previous studies showed an decreased IL-8 production of AA allele carriers in vivo and a 2- to 5-fold stronger transcriptional activity of the TT counterpart in vitro [39, 40]. Our results are in accordance with these findings giving a plausible explanation why all volumetric characters of AA allele carriers are smaller. The smaller tumor volume is concordant with the results from Sun and coworkers, showing the direct linkage between tumor growth and IL-8 levels [37]. The correlation between IL-8 expression, TF and the amount of necrosis can be a coherent explanation why in our study sample the IL-8-251A > T SNP is associated with a smaller amount of necrosis. Given that tumor and necrosis volumes correlate with the PTE, representing partly the active tumor, it is not surprising that the IL-8 SNP influences the PTE volume as well.

A previous study proved the negative effect of the volumetrically measured necrosis on survival [2], showing that it is not only a pathological feature and imaging hallmark of GBM, but also represents the grade of invasiveness and specific activity of the tumor. Thus our findings thereby underline the importance of IL-8 regarding tumor growth and aggressiveness.

The limitation towards the potential effect of volumetric data on survival of GBM patients is certainly the heterogeneous data. There are numerous other studies showing a lack of prognostic importance of tumor volume, PTE or amount of necrosis [3, 22, 41]. A few explanations to this are, populations of most studies are not uniform, measurement techniques are partly descriptive analyses rather than real volumetric measurements, inclusion of maybe steroid treated patients and mixing different treatment regimes.

One true drawback of the current study is the limited sample size, for which reason a haplotype analysis was not performed. The impact of the measured volumetric data on survival was also not reviewed due to the sample size and non-uniform therapy regimes followed the initial MRI (e.g. biopsy, subtotal and gross-total resection). To overcome these restrictions a multi-center follow-up study has already been designed and has been initialized.

Conclusion

Our study is the first one showing a significant effect of SNPs on pretreatment MRI volumetric parameters in GBM patients. The AQP4 131G > A SNP is associated with a distinct smaller PTE volume probably due to a decreased transcription and expression of the AQP4 water channel. Because PTE volume potentially represents an infiltration zone of the tumor rather than a simple water accumulation as a side-effect of the tumor, the AQP4 131G > A SNP may hold a benefit on the survival of GBM patients.

The IL-8-251A > T SNP had a remarkable effect on each measured volumes by decreasing them. These findings underline the importance of the cytokine IL-8 as a driver of GBM proliferation, invasiveness and tumor growth. There is a need of further studies to support our findings and evaluate potential targets for potential therapies.

Acknowledgments We thank Dr. Maryam Sherman for her kind help in editing our draft.

Funding No financial support was provided for this study.

Compliance with ethical standards

Conflict of interest No conflicts of interest to disclose.

Ethical approval All procedures performed in studies involving human participants were in accordance with the ethical standards of the institutional and national research committee and with the 1964 Helsinki declaration and its later amendments or comparable ethical standards.

References

1. Ostrom QT, Bauchet L, Davis FG et al (2014) The epidemiology of glioma in adults: a "state of the science" review. Neuro Oncol 16(7):896–913
2. Iliadis G, Kotoula V, Chatzisotiriou A et al (2012) Volumetric and MGMT parameters in glioblastoma patients: survival analysis. BMC Cancer 12(3):3
3. Crawford FW, Khayal IS, McGue C et al (2009) Relationship of pre-surgery metabolic and physiological MR imaging parameters to survival for patients with untreated GBM. J Neurooncol 91(3):337–351
4. Nestler U, Lutz K, Pichlmeier U, Stummer W et al (2015) Anatomic features of glioblastoma and their potential impact on survival. Acta Neurochir (Wien) 157(2):179–186
5. Liu SY, Mei WZ, Lin ZX (2013) Pre-operative peritumoral edema and survival rate in glioblastoma multiforme. Onkologie 36(11):679–684
6. Dubois LG, Campanati L, Righy C et al (2014) Gliomas and the vascular fragility of the blood brain barrier. Front Cell Neurosci 8:418
7. Nico B, Ribatti D (2011) Role of aquaporins in cell migration and edema formation in human brain tumors. Exp Cell Res 317(17):2391–2396
8. Saadoun S, Papadopoulos MC, Davies DC, Bell BA, Krishna S (2002) Increased aquaporin 1 water channel expression in human brain tumours. Br J Cancer 87(6):621–623
9. Saadoun S, Papadopoulos MC, Davies DC, Krishna S, Bell BA (2002) Aquaporin-4 expression is increased in oedematous human brain tumours. J Neurol Neurosurg Psychiatry 72(2):262–265
10. Warth A, Simon P, Capper D et al (2007) Expression pattern of the water channel aquaporin-4 in human gliomas is associated with blood-brain barrier disturbance but not with patient survival. J Neurosci Res 85(6):1336–1346
11. Kim J, Jung Y (2011) Different expressions of AQP1, AQP4, eNOS, and VEGF proteins in ischemic versus non-ischemic cerebropathy in rats: potential roles of AQP1 and eNOS in hydrocephalic and vasogenic edema formation. Anat Cell Biol 44(4):295–303
12. Lee MD, Bhakta KY, Raina S et al (1996) The human Aquaporin-5 gene. Molecular characterization and chromosomal localization. J Biol Chem 271(15):8599–8604
13. Weyerbrock A, Walbridge S, Saavedra JE, Keefer LK, Oldfield EH (2011) Differential effects of nitric oxide on blood-brain barrier integrity and cerebral blood flow in intracerebral C6 gliomas. Neuro Oncol 13(2):203–211
14. Yeung YT, McDonald KL, Grewal T, Munoz L (2013) Interleukins in glioblastoma pathophysiology: implications for therapy. Br J Pharmacol 168(3):591–606
15. Carneiro-Lobo TC, Lima MT, Mariano-Oliveira A et al (2014) Expression of tissue factor signaling pathway elements correlates with the production of vascular endothelial growth factor and interleukin-8 in human astrocytoma patients. Oncol Rep 31(2):679–686
16. Poirier J, Miron J, Picard C et al (2014) Apolipoprotein E and lipid homeostasis in the etiology and treatment of sporadic Alzheimer's disease. Neurobiol Aging 35(suppl 2):S3–S10
17. Horsburgh K, McCarron MO, White F, Nicoll JA (2000) The role of apolipoprotein E in Alzheimer's disease, acute brain injury and cerebrovascular disease: evidence of common mechanisms and utility of animal models. Neurobiol Aging 21(2):245–255
18. Nicoll JA, Zunarelli E, Rampling R, Murray LS, Papanastassiou V, Stewart J (2003) Involvement of apolipoprotein E in glioblastoma: immunohistochemistry and clinical outcome. NeuroReport 14(15):1923–1926
19. Louis DN, Ohgaki H, Wiestler OD et al (2007) The 2007 WHO classification of tumours of the central nervous system. Acta Neuropathol 114(2):97–109
20. Sawaya R, Hammoud M, Schoppa D et al (1998) Neurosurgical outcomes in a modern series of 400 craniotomies for treatment of parenchymal tumors. Neurosurgery 42(5):1044–1055
21. Rigau V, Zouaoui S, Mathieu-Daudé H et al (2011) French brain tumor database: 5-year histological results on 25 756 cases. Brain Pathol 21(6):633–644
22. Lacroix M, Abi-Said D, Fourney DR et al (2001) A multivariate analysis of 416 patients with glioblastoma multiforme: prognosis, extent of resection, and survival. J Neurosurg 95(2):190–198
23. Grabowski MM, Recinos PF, Nowacki AS et al (2014) Residual tumor volume versus extent of resection: predictors of survival after surgery for glioblastoma. J Neurosurg 121(5):1115–1123
24. Bennet AM, Di Angelantonio E, Ye Z, Wensley F, Dahlin A, Ahlbom A, Keavney B, Collins R, Wiman B, de Faire U, Danesh J (2007) Association of apolipoprotein E genotypes with lipid levels and coronary risk. JAMA 298(11):1300–1311
25. Papadopoulos MC, Verkman AS (2013) Aquaporin water channels in the nervous system. Nat Rev Neurosci 14(4):265–277
26. Papadopoulos MC, Verkman AS (2005) Aquaporin-4 gene disruption in mice reduces brain swelling and mortality in pneumococcal meningitis. J Biol Chem 280(14):13906–13912
27. Zador Z, Stiver S, Wang V, Manley GT (2009) Role of aquaporin-4 in cerebral edema and stroke. Handb Exp Pharmacol 190:159–170

28. Abreu-Rodríguez I, Sánchez Silva R, Martins AP et al (2011) Functional and transcriptional induction of aquaporin-1 gene by hypoxia; analysis of promoter and role of Hif-1α. PLoS One 6(12):e28385
29. Brat DJ, Bellail AC, Van Meir EG (2005) The role of interleukin-8 and its receptors in gliomagenesis and tumoral angiogenesis. Neuro Oncol 7(2):122–133
30. Cooper LA, Gutman DA, Chisolm C et al (2012) The tumor microenvironment strongly impacts master transcriptional regulators and gene expression class of glioblastoma. Am J Pathol 180(5):2108–2119
31. Anand M, Brat DJ (2012) Oncogenic regulation of tissue factor and thrombosis in cancer. Thromb Res 129(suppl 1):S46–S49
32. Mou K, Chen M, Mao Q et al (2010) AQP-4 in peritumoral edematous tissue is correlated with the degree of glioma and with expression of VEGF and HIF-alpha. J Neurooncol 100(3):375–383
33. Sorani MD, Zador Z, Hurowitz E, Yan D, Giacomini KM, Manley GT (2008) Novel variants in human Aquaporin-4 reduce cellular water permeability. Hum Mol Genet 17(15):2379–2389
34. Kleffner I, Bungeroth M, Schiffbauer H, Schäbitz WR, Ringelstein EB, Kuhlenbäumer G (2008) The role of aquaporin-4 polymorphisms in the development of brain edema after middle cerebral artery occlusion. Stroke 39(4):1333–1335
35. Chaichana KL, Cabrera-Aldana EE, Jusue-Torres I et al (2014) When gross total resection of a glioblastoma is possible, how much resection should be achieved? World Neurosurg 82(1–2):257–265
36. Kelly PJ, Daumas-Duport C, Kispert DB, Kall BA, Scheithauer BW, Illig JJ (1987) Imaging-based stereotaxic serial biopsies in untreated intracranial glial neoplasms. J Neurosurg 66(6):865–874
37. Sun S, Wang Q, Giang A et al (2011) Knockdown of CypA inhibits interleukin-8 (IL-8) and IL-8-mediated proliferation and tumor growth of glioblastoma cells through down-regulated NF-κB. J Neurooncol 101(1):1–14
38. Rak J, Milsom C, Magnus N, Yu J (2009) Tissue factor in tumour progression. Best Pract Res Clin Haematol 22(1):71–83
39. Ahn MH, Park BL, Lee SH et al (2011) A promoter SNP rs4073T > A in the common allele of the interleukin 8 gene is associated with the development of idiopathic pulmonary fibrosis via the IL-8 protein enhancing mode. Respir Res 12:73
40. Lee WP, Tai DI, Lan KH et al (2005) The -251T allele of the interleukin-8 promoter is associated with increased risk of gastric carcinoma featuring diffuse-type histopathology in Chinese population. Clin Cancer Res 11(18):6431–6441
41. Hammoud MA, Sawaya R, Shi W, Thall PF, Leeds NE (1996) Prognostic significance of preoperative MRI scans in glioblastoma multiforme. J Neurooncol 27(1):65–73

Association Between Tumor Compartment Volumes, the Incidence of Pretreatment Seizures, and Statin-Mediated Protective Effects in Glioblastoma

Christian Henker, MD [*]
Thomas Kriesen, MD [*]
Moritz Scherer, MD [‡]
Änne Glass, PhD [§]
Andreas von Deimling, MD [¶]
Martin Bendszus, MD, PhD [‖]
Marc-André Weber, MD, PhD [#]
Christel Herold-Mende, PhD [‡]
Andreas Unterberg, MD, PhD [‡]
Jürgen Piek, MD, PhD [*]

[*]Department of Neurosurgery, University Medicine of Rostock, Rostock, Germany; [‡]Department of Neurosurgery, Heidelberg University Hospital, Heidelberg, Germany; [§]Institute for Biostatistics and Informatics in Medicine, University Medicine of Rostock, Rostock, Germany; [¶]Department of Neuropathology, Institute of Pathology, University Hospital, and, CCU Neuropathology German Cancer Research Center (DKFZ), and DKTK, Heidelberg, Germany; [‖]Department of Neuroradiology, Heidelberg University Hospital, Heidelberg, Germany; [#]Institute of Diagnostic and Interventional Radiology, University Medicine of Rostock, Rostock, Germany

Correspondence:
Christian Henker, MD,
Department of Neurosurgery,
University Medicine of Rostock,
Rostock, Germany.
E-mail:
Christian.Henker@med.uni-rostock.de

Received, April 20, 2018.
Accepted, February 14, 2019.
Published Online, March 19, 2019.

Copyright © 2019 by the
Congress of Neurological Surgeons

BACKGROUND: Seizures are a common initial symptom of malignant brain tumors such as glioblastoma (GBM). However, why some of these tumors are epileptogenic and others never trigger seizures remains controversial.

OBJECTIVE: To identify potential clinical and radiological features of epileptogenic tumors and the effect of initial seizures on survival.

METHODS: The analyzed patient cohort was retrospectively compiled (bicentric), only isocitrate dehydrogenase wild-type GBMs were included. Volumetric assessment was performed on pretreatment magnetic resonance imaging with the aid of a semi-automated 3D measurement (tumor, necrosis, and edema volume). Two ratios were calculated, reflecting the proportion of peritumoral edema and necrosis (NTR) toward the tumor volume. For overall survival analyses, only patients after a surgical resection (residual tumor volume <2 cm^3) followed by standard radiation and chemotherapy were included.

RESULTS: Pretreatment seizures occurred in 33% of cases (n = 224), younger patients ($\leq$60 yr) were predominantly affected ($P = .022$). All measured volumes were inversely correlated with the onset of seizures ($P = .001$). In multivariate analyses, the total tumor volume and the NTR were considerably smaller within epileptogenic GBMs ($P = .050$, $P = .019$, respectively). A positive statin intake was associated with significantly lesser seizure ($P = .007$, odds ratio 4.94). Neither the occurrence of seizures nor the intake of statins had an impact on OS ($P = .357$, $P = .507$, respectively).

CONCLUSION: The size and amount of necrosis was significantly smaller in epileptogenic GBMs, maybe owed to the fact that these tumors were clinically detected at an earlier stage of their growth. Furthermore, the intake of statins was associated with a decreased occurrence of pretreatment seizures.

KEY WORDS: Glioblastoma, Necrosis, Neuroimaging, Oncology, Prognostic markers, Seizures

Neurosurgery 85:E722–E729, 2019 DOI:10.1093/neuros/nyz079 www.neurosurgery-online.com

Glioblastoma (GBM) is the most malignant and most frequently occurring type of glioma in adult patients.[1] The prognosis of patients harboring a GBM still remains poor, with a median overall survival (OS) of only 18.8 mo after a complete surgical resection followed by concomitant radiation and chemotherapy.[2] Seizures occur as a presenting symptom in 40 to 60% of GBM patients.[3] Tumor-related seizures can manifest as simple or complex partial seizures with the potential of a secondary generalization in 40% of patients.[4] Seizures are far more prevalent in low-grade tumors, with a risk of 60 to 100%.[3] The tumor localization seems to be important for the development of seizures: the involvement of the temporal lobe and a cortical manifestation are associated with a higher risk of seizures.[4,5] In tumor-related seizures, the focus of epileptic activity is often situated within the tumor

ABBREVIATIONS: EOR, extent of resection; **ETR,** edema tumor ratio; **FLAIR,** fluid-attenuated inversion-recovery; **GBM,** glioblastoma; **IDH,** isocitrate dehydrogenase; **KPS,** Karnofsky performance status; **NTR,** necrosis tumor ratio; **MRI,** magnetic resonance imaging; **OR,** odds ratio; **OS,** overall survival

Supplemental digital content is available for this article at www.neurosurgery-online.com.

Downloaded from https://academic.oup.com/neurosurgery/article-abstract/85/4/E722/5386559 by Universitaetsbibliothek Rostock user on 28 November 2019

margins, where the tumor cells have already invaded the surrounding tissue and disturbed the functional network.[6-8] The pathogenesis of tumor-related seizures is still not fully understood. In low-grade gliomas, the data from previous studies indicate a survival benefit for patients with initial seizures.[9,10] For GBMs, the available data also tend to point toward an increased survival associated with pretreatment seizures.[11-13]

Statins are inhibitors of the 3-hydroxy-3-methylglutaryl-coenzyme A reductase and are widely used to lower cholesterol. Statins also exhibit a variety of pleiotropic effects beyond their lipid-lowering abilities. Neuroprotective effects result from anti-inflammatory properties and vascular protection via an upregulation of the endothelial nitric oxide synthases, an increased expression of the vascular endothelial growth factor receptor-2, and a reduction in proinflammatory cytokines.[14-17] In vitro and animal studies showed the anti-seizure and anti-excitotoxic effects of statins, which act via the inhibition of inflammatory signaling cascades and regulation of gene expression and neurosteroid synthesis.[16,18] In some animal studies, statins demonstrated anticonvulsant effects, but not all statins showed these effects and some results are antidromic.[18]

The aim of this study was to shed some light on the scant results provided by other studies regarding seizures and their potential impact on GBM patient survival. Additionally, we wanted to investigate whether the occurrence of seizures can be linked to the unique appearance of every GBM on magnetic resonance imaging (MRI). With the aid of a very accurate measurement technique, a 3D volumetric assessment, we tried to correlate the different tumor compartments to the incidence of pretreatment seizures. Furthermore, we wanted to evaluate the potential impact of a statin intake onto the occurrence of seizures within GBM patients and their potential neuroprotective effects.

METHODS

Study Design

The study was conducted at 2 neurosurgical departments. The protocol was approved by both Institutional Review Boards and Ethic Committees according to the Declaration of Helsinki. Informed consent was obtained from all participants.

In this bi-institutional retrospective study, a total of 224 adult patients (>18 yr of age) with a histologically proven primary GBM were included. All patients had been treated at 2 neurosurgical departments between January 2009 and December 2016. Definition of *IDH* wild-type GBM was based on *IDH-1 R132* status, according to the WHO guidelines.[19,20] Only unifocal, supratentorial lesions were included. All patients were steroid naive at the time of presurgical MRI scans, excluding the potential bias of steroids on the peritumoral edema. Seizures were defined and classified according to the 2010 criteria of the International League Against Epilepsy.[21] Seizures were only recorded if they occurred at the first time and if they were related to the tumor diagnosis. All preoperative seizures were subsumed as one positive event, patients with known epilepsy or with seizures with a different known cause were excluded. Additionally, the Karnofsky performance status (KPS) at admission and the age-adjusted Charlson comorbidity index score were measured.[22,23] For statistical analysis, data were partly grouped as follows: age (<60 yr, 60-70 yr, >70 yr), Charlson comorbidity index (≤2, 3-4, ≥5), and KPS (≥80%, 70-50%, ≤40%). The *MGMT* promoter methylation status was determined using the MethyLight real-time PCR method as previously described.[24]

For OS analysis, a subpopulation was filtered from the initial patient cohort. Only patients were included after a surgical resection with a residual tumor burden <2 cm^3, as proven by postoperative volumetric analysis (see the next section). All patients received radiation and concomitant chemotherapy with temozolomide.[2] The primary endpoint for this subgroup was the OS (difference between time point of surgery and date of tumor-related death of the patient or study end (January 2018)). A total of 99 patients were included within this subgroup. The STrengthening the Reporting of OBservational studies in Epidemiology (STROBE) statement checklist for cohort studies was used as a reporting guideline.

Volumetric Analyses of MRI Scans

Preoperative MRI scans were obtained at least 1 wk before surgery, and postoperative scans were obtained within 48 h after surgery. For image analysis, contrast-enhanced T1-weighted 3D datasets with 1 mm isotropic voxels and 2D T2-weighted fluid-attenuated inversion-recovery (FLAIR) sequences were evaluated. Volumetric measurement was performed, using a contour-expansion algorithm (SmartBrush®, Brainlab AG, Feldkirchen, Germany). Volumes measured on preoperative MRI included:

Tumor: Enhancing volume on postcontrast T1 including the central necrosis.

Necrosis: Nonenhancing region within the tumor on postcontrast T1.

Peritumoral edema: Hyperintensive volume on T2/FLAIR surrounding the lesion, excluding the tumor volume.

Cystic lesions: Bright T2 signal within the tumor, well-circumscribed and corresponding to a low T1 signal. The cystic volumes were measured and subtracted from the total tumor volume, not confounding the "vital" tumor volume by secreted fluids.

Residual tumor volume was measured on postoperative 3D pre- and postcontrast T1 sequences, subtracting the precontrast T1 signals within the resection cavity (reflecting blood) from the postcontrast T1 enhancement (reflecting vital tumor). Subsequently, 2 ratios were calculated reflecting the relationships between the different proportions of the measured tumor compartments toward each other: edema tumor ratio (ETR; edema divided by the tumor volume) and necrosis tumor ratio (NTR; necrosis divided by the tumor volume). The used measurement technique was previously validated, and has been shown to be superior than other tumor assessments.[25] According to this preliminary work, we used the validated cut-off values for a division of the cohorts into 3 groups for ETR and NTR.

Statistical Analyses

Statistical analysis was carried out using SPSS 22.0 software (IBM Inc, Armonk, New York). Descriptive statistics have been applied for continuous and categorical variables. Survival rates were analyzed using the Kaplan-Meier product-limit method, and the Cox proportional hazards regression model was used to assess the independence of OS from categorial prognostic variables. Logistic regression analyses were utilized for investigation of variables associated with seizure occurrence. First, in both cases univariate analyses were performed to reveal unadjusted significant associations between variables and seizure occurrence. Thereafter,

Downloaded from https://academic.oup.com/neurosurgery/article-abstract/85/4/E722/5386559 by Universitaetsbibliothek Rostock user on 28 November 2019

TABLE 1. Patient Characterization

		Total sample (n = 224)	OS subgroup (n = 99)	*P*-value[α]
Sex	Male	123 (54.9%)	64 (64.6%)	.103
	Female	101 (45.1%)	35 (35.4%)	
Age	≤60 yr	75 (33.5%)	47 (47.5%)	.001
	>60 to ≤ 70 yr	66 (29.5%)	37 (37.4%)	
	>70 yr	83 (37.1%)	15 (15.2%)	
Charlson Index	Mean (±SD)	2.84 (2.0)	2.19 (1.57)	.005
KPS	Mean (±SD), %	73.8 (18.11)	81.5 (13.13)	< .001
Seizure incidents	n	74 (33%)	41 (41.4%)	.148
Statin intake	n	40 (17.9%)	16 (16.2%)	.712
Tumor volume	Mean (±SD), cm^3	32.1 (26.73)	28.0 (25.78)	.190
Edema volume	Mean (±SD), cm^3	83.5 (58.84)	71.9 (56.41)	.102
Necrosis volume	Mean (±SD), cm^3	10.4 (12.28)	8.83 (10.98)	.282
ETR	Mean (±SD)	4.46 (7.00)	4.11 (4.83)	.672
NTR	Median (Q1, Q3)	0.259 (0.161, 0.365)	0.250 (0.150, 0.326)	.881

ETR = edema tumor ratio; KPS = Karnofsky performance status; NTR = necrosis tumor ratio; Q1 = first quartile; Q3 = third quartile; SD = standard deviation.
Student's *t*-test. Mann-Whitney U test. Chi-square test.

variables yielding *P*-values ≤ .200 (as a whole) in the univariate analyses were entered in the multivariable model to highlight some adjusted associations between outcome and covariates which were univariate of borderline significance. All *P*-values resulted from 2-sided statistical tests, and values of $P \leq .05$ were considered statistically significant.

The degree to which the relationship between 2 variables is monotonic was evaluated by the most familiar measure of dependence between 2 not normally distributed quantities, Spearman's rank correlation coefficient rho (r_S). The respective 95% confidence intervals are given.

RESULTS

Patient Characterization

In our cohort, the average age was 65.8 ± 10.6 yr (range 31-92 yr) with a male-to-female ratio of 1.2:1 (Table 1). The KPS was 73.8 ± 18.3% with a median of 80%. The Charlson comorbidity index was generally low, being ≤ 2 points in 46.9% of cases. 17.9% of patients (40/224) had a positive anamnesis for statin intake. The most prevalent statin was simvastatin (34/40, 85%), followed by pravastatin (4/40, 10%) and atorvastatin (2/40, 5%). Simvastatin dosages were mostly 20 mg or higher (88%).

Pretreatment MRI scans were of high quality, with a mean slice thickness of 1.91 mm. Distribution of the lesions was equal within both brain hemispheres (105/224 (46.9%) on the left vs 119/224 (53.1%) on the right side). Most of the tumors were situated within the temporal lobe (87/224, 38.8%), followed by the frontal (69/224, 30.8%), parietal (46/224, 20.5%), and the occipital lobe (12/224, 5.4%). Mean tumor volume was 32.1 ± 26.7 cm^3, ranging from 0.36 to 157.7cm^3, which nearly equals the volume of a table tennis ball (33.5 cm^3). Approximately one quarter of the tumor itself consisted of necrosis, reflected by the NTR (median 0.259, range 0.0-0.83). The edema

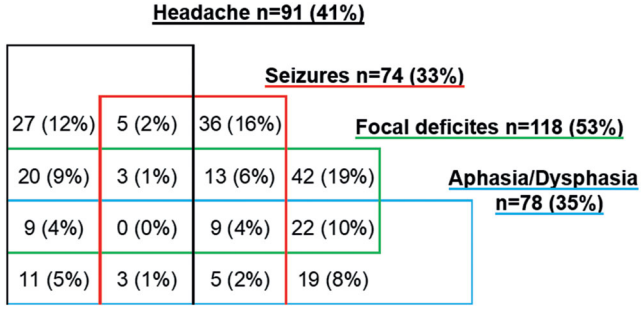

FIGURE 1. *Venn diagram of clinical signs and symptoms. The diagram displays the initial clinical appearance of the total study cohort (n = 224). Every panel is encompassed by the associated frame according to a color-coded symptom. Intersections, representing patients with 2 or more symptoms at initial admission, are gridded by 2 or more colored frames. The total frequency of the individual symptoms was specified following the underlined description. Most prevalent initial symptoms were focal deficits alone (19%), commonly combination of signs were focal deficits and aphasia/dysphasia (10%).*

surrounding the tumor was in most cases 4 times larger than the lesion itself (mean ETR 4.46 ± 7.0, range 0.0-74.9). All tumor volumes were significantly correlated with each other ($P = .001$; **Table**, **Supplemental Digital Content 1**). The strongest correlation between the tumor compartments was among the tumor and necrosis volumes ($r_S = 0.879$). The age of the patients had no effect on all measured volumes and the 2 derived ratios ($P \geq .252$).

Prevalent symptoms as first manifestation of the tumor disease were focal deficits (118/224, 53%), followed by headaches (91/224, 41%), dysphasia or aphasia (78/224, 35%), and seizures (74/224, 33%; Figure 1). The most frequent combination of

Downloaded from https://academic.oup.com/neurosurgery/article-abstract/85/4/E722/5386559 by Universitaetsbibliothek Rostock user on 28 November 2019

TABLE 2. Analysis of the Influence of Clinical and Radiological Data on Seizure Incidence

	Variable	Univariate analysis[b]			Multivariable analysis[b]		
		OR	95% CI	*P*-value	adj. OR	95% CI	*P*-value
Sex	Male vs female[a]	1.43	0.813-2.52	.213	-	-	-
Age	≤ 60 yr vs > 70 yr[a]	2.18	1.12-4.25	.022	1.37	0.552-3.42	.495
Charlson Index	≤2 vs ≥ 5[a]	1.78	0.757-4.18	.187	-	-	-
KPS	≥80% vs ≤ 40%[a]	1.71	0.622-4.72	.298	0.485	0.204-1.15	.102
Statin intake	No vs yes[a]	2.70	1.13-6.44	.025	4.94	1.56-15.7	.007
Tumor location	Side (left vs right[a])	1.21	0.690-2.11	.511	-	-	-
	Lobe (temporal vs frontal[a])	0.987	0.508-1.92	.969	-	-	-
Tumor volume	≤ 16 cm^3 vs > 40 cm^3[a]	18.8	7.51-46.9	.001	6.42	1.00-41.2	.050
Edema volume	≤50 cm^3 vs > 100 cm^3[a]	6.59	3.07-14.1	.001	2.71	0.762-9.64	.123
Necrosis volume	≤3 cm^3 vs > 10 cm^3[a]	10.4	4.64-23.4	.001	8.50	0.773-93.4	.080
ETR	≤2 vs > 4[a]	0.402	0.203-0.797	.009	0.631	0.178-2.25	.447
NTR	≤0.2 vs 0.33[a]	2.26	1.08-4.70	.030	0.122	0.878-4.22	.019

Adj. = adjusted; CI = confidence interval; ETR = edema tumor ratio; KPS = Karnofsky performance status; NTR = necrosis tumor ratio; OR = odds ratio.
[a]Reference category.
[b]Logistic regression analysis.

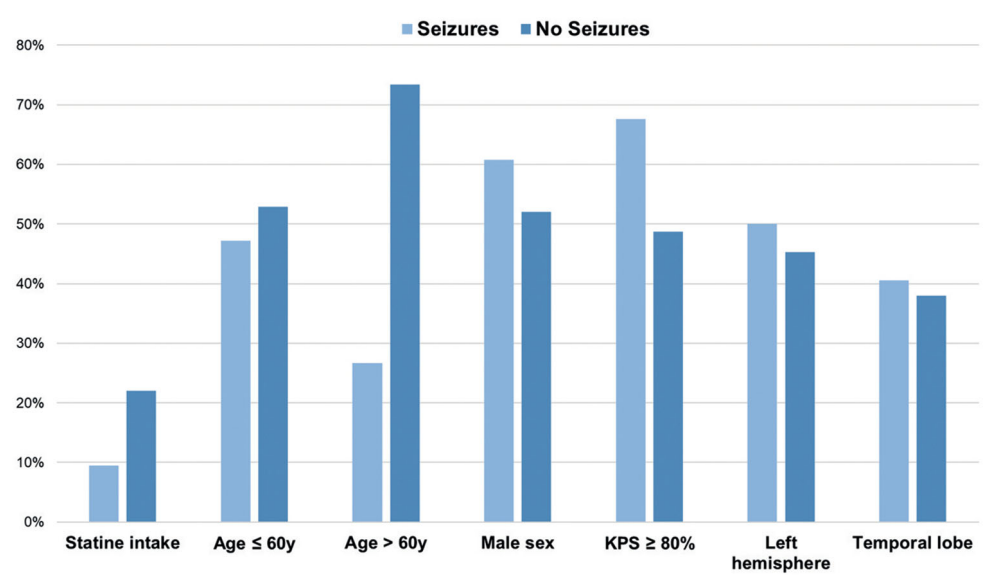

FIGURE 2. *Comparison between patients with and without initial seizures and their clinical and MRI-morphologic tumor appearance. The bar graph illustrates side by side the different frequencies of patients' data subdivided by the appearance of pretreatment seizures. The bars in lighter blue on the left side of every pair of bars are representing the patients with initial seizures. Apart, the darker blue ones are standing for patients without pretreatment seizures. The patients suffering from seizures are altogether younger, with a better KPS result (higher value) and lesser intake of statins. Distribution of the tumors is comparable between both groups. KPS = Karnofsky performance status.*

symptoms was focal deficits and seizures, observed in 19% of all cases. Seizures primarily occurred within temporal GBMs (30/74, 40.5%), followed by frontal and parietal tumors (32.4 and 21.6%, respectively). The left hemisphere and the temporal lobe were slightly more often affected by GBM within the population of patients with initial seizures compared to nonictogenic GBMs ($P = .513$, $P = .715$, respectively). *MGMT* status was available for 109 patients, being mostly unmethylated (68/109, 62.4%). Table 2, Figure 2, and **Table, Supplemental Digital Content 2** illustrate the clinical and MRI-morphological characteristics for the patients with initial seizures compared to ones without tumor-related seizures. The patients experiencing seizures were younger

Downloaded from https://academic.oup.com/neurosurgery/article-abstract/85/4/E722/5386559 by Universitaetsbibliothek Rostock user on 28 November 2019

TABLE 3. Variables of Overall Survival in Univariate Analyses

	Variable	HR	95% CI	*P*-value[b]
Sex	Male vs female[a]	1.02	0.664-1.56	.937
Age	> 70 yr vs ≤ 60 yr[a]	2.18	1.191-4.01	.012
Charlson Index	≥ 5 vs ≤ 2[a]	1.14	0.725-1.79	.571
KPS	≥ 80% vs ≤ 40%[a]	1.18	0.162-8.52	.873
Seizure	No vs yes[a]	1.22	0.801-1.85	.357
Statin intake	Yes vs no[a]	1.20	0.700-2.06	.507
Cystic tumor	Yes vs no[a]	1.03	0.560-1.89	.928

CI = confidence interval; HR = hazard ratio; KPS = Karnofsky performance status.
[a]Reference category.
[b]Cox's proportional hazards regression.

($P = .006$), and the initial KPS was also higher ($P < .001$). The intake of statins was more than doubled within the subgroup of patients without initial seizures ($P = .011$). The median volumes of tumor and necrosis were clearly higher in epileptogenic GBMs ($P < .001$, $P < .001$, respectively). Interestingly, the relation of the peritumoral edema toward the tumor was considerably increased in patients with pretreatment seizures ($P = .014$). Regarding the different distributions of measured volumes and derived ratios, there was no significant difference between the subgroups of patients with and without a positive intake of statins ($P \geq .125$; **Table**, **Supplemental Digital Content 3**).

Potential Triggers of Seizure Occurrence

One-third of all patients sustained seizures before treatment as a single symptom or in combination with others. In univariate analysis, we observed a significant accumulation of seizures within the subgroup of patients who were 60 yr old or younger ($P = .022$; **Table**, **Supplemental Digital Content 2**). The affected lobe and hemisphere had no impact on seizures incidence ($P = .969$, $P = .511$ respectively; Table 2). The univariate volumetric analysis showed a very strong association between seizures and all measured volumes and their resultant ratios ($P \leq .030$). Interestingly, the highest risk for seizures was observed in patients with smaller tumors, an increased ETR, and a reduced necrotic core (NTR). The incidence of seizures was distinctively reduced within patients with a positive intake of statins ($P = .025$, odds ratio [OR] 2.70). In multivariable analysis, only the statin intake and smaller tumor volume with a reduced NTR were significant variables influencing the occurrence of seizures ($P = .007$, $P = .050$, and $P = .019$, respectively). Looking at the ORs, patients with a tumor volume smaller or equal to 16 cm^3 had a nearly 7 times higher odds for seizures as an initial symptom of their tumor disease relative to those with larger tumor volumes (>40 cm^3). A reduced amount of necrosis within the tumor, smaller than the regular observed correlation between tumor and necrosis volume (smaller NTR), also decreased the odds for seizures (OR 0.122). A lack of preoperative statin intake was associated with 5-fold increased odds of having a seizure (OR 4.94). Clinical data showed a difference between patients with and without a documented statin intake regarding their age and Charlson index ($P = .001$, $P = .003$, respectively). All these findings could also be confirmed within a single institute analysis as an internal validation (**Table**, **Supplemental Digital Content 4**).

Survival Analysis

A total of 99 were included in our subpopulation analysis. Reasons for exclusion from the OS subgroup were mainly a larger residual tumor volume, if only biopsies were taken and a lack of adjuvant therapies after surgery. In general, patients within the OS subgroup were younger ($P = .001$), the sexes were equally distributed ($P = .103$), and the average KPS was higher compared to the total study population ($P = .001$; Tables 1 and 3). The incidence of seizures was comparable among both cohorts ($P = .148$), just like the statin intake ($P = .712$). Measured tumor compartments were similar to those of the total cohort ($P \geq .102$). The age of the patients at initial diagnosis and resection of the tumor significantly influenced the survival of the patients ($P = .041$) (Figure 3). The occurrence of pretreatment seizures had no impact on OS in our subpopulation ($P = .357$), just as the intake of statins ($P = .507$).

DISCUSSION

Seizures are a common initial symptom of malignant brain tumors such as GBM. They can dramatically reduce the quality of life of the patient.[26,27] Seizure histories are highly variable among GBM patients, and specific predictors for their occurrence remain controversial. Our results suggest that the initial tumor size, inversely correlated with the incidence of seizures, is a strong ictogenic variable ($P = .050$, OR 6.42), in concordance with previous studies.[5,11] Furthermore, the tumor location, regarding the affected lobe and hemisphere, did not influence the occurrence of seizures in our cohort ($P = .969$, $P = .511$,

Downloaded from https://academic.oup.com/neurosurgery/article-abstract/85/4/E722/5386559 by Universitaetsbibliothek Rostock user on 28 November 2019

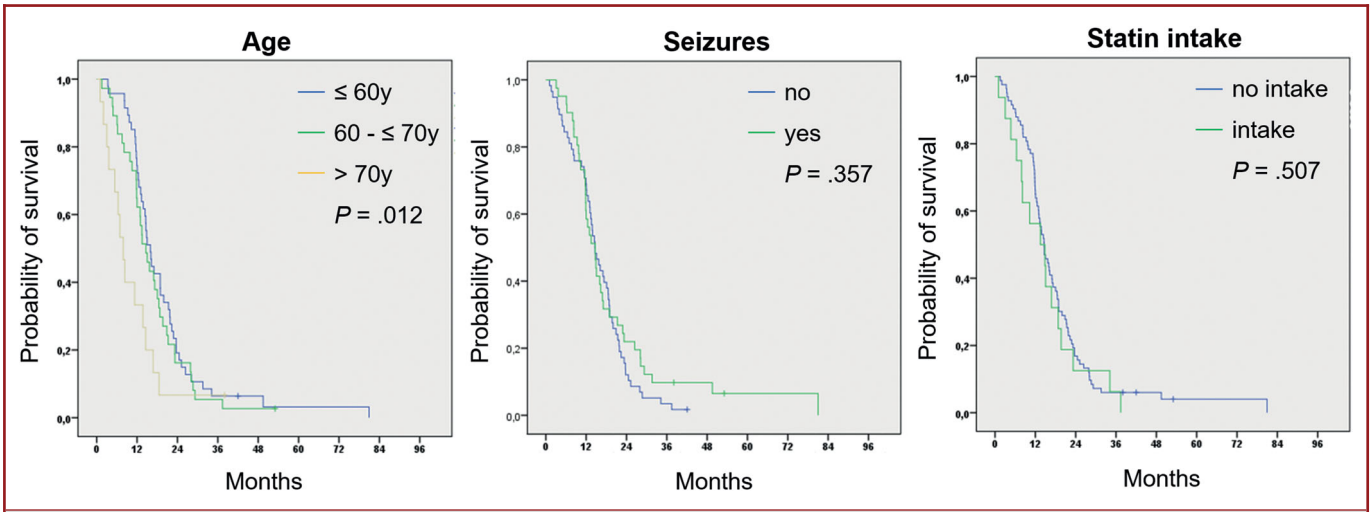

FIGURE 3. *Kaplan-Meier curves and P-values from Cox's proportional hazards model. The survival curves from the OS subgroup are showing a significant influence of the patients age at the time of diagnosis on OS (P = .012). Neither the pretreatment occurrence of seizures affected the OS (P = .357) nor a statin intake (P = .507).*

respectively). Another volumetric predictor for potentially epileptogenic tumors in our cohort is the amount of necrosis in relation to the total tumor volume, the NTR ($P = .019$; OR 0.122).

The third compartment of every GBM is the peritumoral edema, which should not be underestimated as a simple side effect of the tumor, rather serving as a niche for a further invasion of the tumor.[28] Clinically, the edema plays a major role in determining the initial symptoms of a yet unknown tumor beside its location.[29] Our data showed a general correlation between the tumor volume and the size of its surrounding edema ($P = .001$). Comparing the single volumes between the 2 groups of patients with and without pretreatment seizures, tumor and edema volume were both decreased for patients with seizures ($P < .001$). Interestingly, the ETR of the patients with seizures was significantly increased ($P = .014$). Apparently, more ictogenic tumors not only appear smaller on MRI comprising less necrosis, they also exhibit a relatively larger peritumoral edema compared to nonepileptogenic GBMs. To our knowledge, this inverse relation was observed for the first time in vivo. In multivariate comparison of the 2 ETR classes (≤2 vs >4), this effect could not be reproduced with the same impact. One reason for this missing multivariate correlation might be wide distribution of the ratio, ranging from 0.0 to 74.9. The age of the patient did not affect these findings, as there was no correlation found between age and the measured volumes and ratio ($P \geq .303$), according to other studies.[30]

Toledo and colleagues[31] observed a significant correlation of a prolonged survival in GBM patients younger than 60 yr of age with initial seizures. However, that study did not stratify their patients considering the surgical "extent of resection" (EOR) or the subsequent neuro-oncological treatment as we did. Berendsen et al[32] also reported an association between initial seizures and a prolonged survival within a very large patient cohort with GBMs. Likewise, the EOR was not measured. As our data indicate, seizures may serve as a surrogate parameter for a better outcome of GBM patients, because they were closely linked to other clinical characteristics, like a younger age and a better performance status, in combination with an easier resectable (smaller) tumor—all being strong predictors for the OS of GBM patients.[33] Furthermore, the moment of clinical presentation with seizures is maybe so early that these GBMs lack the typical radiological hallmarks like an extensive necrosis, as previously suggested by Rossi and colleagues.[34] Within their presented case series, all patients with initial minor abnormalities on MRI will develop the typical radiological hallmarks of a malignant brain tumor over time.

The second main finding in our study was an observed protective effect of statins against pretreatment seizures within our cohort of GBM patients. This effect was not biased through an unbalanced distribution of the measured volumes and ratios between patients with and without a confirmed statin intake ($P \geq .125$). The potential neuroprotective properties of statins, beyond their lipid reduction effects, have been known within the scientific community for years. However, clinically relevant effects proven within in vivo studies are rare, especially regarding anticonvulsant properties of statins.[18] The distinct seizure-protective effect of statins, beside the tumor volume and NTR, was the only predictor being significant in multivariate analysis within our cohort and is the only one that can be modulated. In 85% of documented statin intake, simvastatin was likely the prescribed statin in our cohort with the greatest ability to cross the blood brain barrier.[35] However, it must be noted that the recording of a positive or negative statin intake was made from anamnestic data, not being the most reliable source of data.

Our results showed no impact of a positive statin intake on the OS of GBM patients. A potential explanation for the lack of further neuroprotective effects is the vast and invasive growth of

Downloaded from https://academic.oup.com/neurosurgery/article-abstract/85/4/E722/5386559 by Universitaetsbibliothek Rostock user on 28 November 2019

GBMs within the brain and a devastating OS, despite the known treatments. Furthermore, the total number of patients with a known statin intake was small within the OS subgroup (16/99, 16.2%), besides being comparable to the intake rate of the total cohort ($P = .712$).

Limitations

A limitation of our current study lies within its retrospective nature. Therefore, via inclusion criteria and by filtering the OS subgroup from our overall cohort, a selection bias must be considered. Additionally, a potential recall bias for the anamnestic data acquisition of seizures and statin intake can affect the quality of our source data. Nevertheless, selection criteria were clearly defined, and the patient population was considerably large given the bicentric approach. Another confounding factor are the various variables analyzed in this study.

Furthermore, we cannot completely rule out that the statin intake serves as a proxy for a higher age of GBM patients with a decreased seizure risk.

CONCLUSION

In terms of volumetric predictors for patient survival, the phrase "the less the better" seems to be mirror inverted regarding the incidence of seizure in patients harboring a GBM. In our cohort, the strongest predictors for the occurrence of pretreatment seizures were a small tumor volume and a lesser amount of necrosis within the tumor (NTR). Younger patients harboring a GBM are more often affected by seizures, but the initial age cannot per se be related to a small, epileptogenic tumor. The occurrence of seizures did not increase the OS within our cohort, rather being a surrogate parameter for a subset of patients possibly being symptomatic at an earlier stage of their tumor progression. Statins are believed to impart neuroprotective abilities, which were observed in our cohort via a distinct reduction in seizure occurrence. Since the underlying mechanism is not fully elucidated, this observed effect may be evoked by a higher patient age and the statin intake itself serves as a surrogate for older patients with less pretreatment seizures.

Disclosures

The authors have no personal, financial, or institutional interest in any of the drugs, materials, or devices described in this article.

REFERENCES

1. Ostrom QT, Gittleman H, Liao P, et al. CBTRUS Statistical Report: primary brain and other central nervous system tumors diagnosed in the United States in 2010-2014. *Neuro Oncol.* 2017;19(suppl_5):v1-v88.
2. Stupp R, Hegi ME, Mason WP, et al. Effects of radiotherapy with concomitant and adjuvant temozolomide versus radiotherapy alone on survival in glioblastoma in a randomised phase III study: 5-year analysis of the EORTC-NCIC trial. *Lancet Oncol.* 2009;10(5):459-466.
3. Vecht CJ, Kerkhof M, Duran-Pena A. Seizure prognosis in brain tumors: new insights and evidence-based management. *Oncologist.* 2014;19(7):751-759.
4. Kerkhof M, Vecht CJ. Seizure characteristics and prognostic factors of gliomas. *Epilepsia.* 2013;54(suppl 9):12-17.
5. Chaichana KL, Parker SL, Olivi A, Quiñones-Hinojosa A. Long-term seizure outcomes in adult patients undergoing primary resection of malignant brain astrocytomas. Clinical article. *J Neurosurg.* 2009;111(2):282-292.
6. Buckingham SC, Robel S. Glutamate and tumor-associated epilepsy: glial cell dysfunction in the peritumoral environment. *Neurochem Int.* 2013;63(7):696-701.
7. Pallud J, van Quyen M, Bielle F, et al. Cortical GABAergic excitation contributes to epileptic activities around human glioma. *Sci Transl Med.* 2014;6(244):244ra89.
8. Gerin C, Pallud J, Deroulers C, et al. Quantitative characterization of the imaging limits of diffuse low-grade oligodendrogliomas. *Neuro Oncol.* 2013;15(10):1379-1388.
9. Pallud J, Audureau E, Blonski M, et al. Epileptic seizures in diffuse low-grade gliomas in adults. *Brain.* 2014;137(2):449-462.
10. Chang EF, Potts MB, Keles GE, et al. Seizure characteristics and control following resection in 332 patients with low-grade gliomas. *J Neurosurg.* 2008;108(2):227-235.
11. Lee JW, Norden AD, Ligon KL, et al. Tumor associated seizures in glioblastomas are influenced by survival gene expression in a region-specific manner: a gene expression imaging study. *Epilepsy Res.* 2014;108(5):843-852.
12. Okumus NO, Gursel B, Meydan D, Ozdemir O, Odabas E, Gonullu G. Prognostic significance of concomitant radiotherapy in newly diagnosed glioblastoma multiforme: a multivariate analysis of 116 patients. *Ann Saudi Med.* 2012;32(3):250-255.
13. Stark AM, van de Bergh J, Hedderich J, Mehdorn HM, Nabavi A. Glioblastoma: clinical characteristics, prognostic factors and survival in 492 patients. *Clin Neurol Neurosurg.* 2012;114(7):840-845.
14. Wu H, Jiang H, Lu D, et al. Induction of angiogenesis and modulation of vascular endothelial growth factor receptor-2 by simvastatin after traumatic brain injury. *Neurosurgery.* 2011;68(5):1363-1371; discussion 1371.
15. Laufs U, Liao JK. Post-transcriptional regulation of endothelial nitric oxide synthase mRNA stability by Rho GTPase. *J Biol Chem.* 1998;273(37):24266-24271.
16. Lee J-K, Won J-S, Singh AK, Singh I. Statin inhibits kainic acid-induced seizure and associated inflammation and hippocampal cell death. *Neurosci Lett.* 2008;440(3):260-264.
17. van der Most PJ, Dolga AM, Nijholt IM, Luiten PGM, Eisel ULM. Statins: mechanisms of neuroprotection. *Prog Neurobiol.* 2009;88(1):64-75.
18. Banach M, Czuczwar SJ, Borowicz KK. Statins - Are they anticonvulsant? *Pharmacol Rep*. 2014;66(4):521-528.
19. Louis DN, Perry A, Reifenberger G, et al. The 2016 World Health Organization classification of tumors of the central nervous system: a summary. *Acta Neuropathol.* 2016;131(6):803-820.
20. Chen L, Voronovich Z, Clark K, et al. Predicting the likelihood of an isocitrate dehydrogenase 1 or 2 mutation in diagnoses of infiltrative glioma. *Neuro Oncol* 2014;16(11):1478-1483.
21. Berg AT, Berkovic SF, Brodie MJ, et al. Revised terminology and concepts for organization of seizures and epilepsies: report of the ILAE Commission on Classification and Terminology, 2005-2009. *Epilepsia.* 2010;51(4):676-685.
22. Karnofsky DA, Abelmann WH, Craver LF, Burchenal JH. The use of the nitrogen mustards in the palliative treatment of carcinoma. With particular reference to bronchogenic carcinoma. *Cancer.* 1948;1(4):634-656.
23. Charlson M, Szatrowski TP, Peterson J, Gold J. Validation of a combined comorbidity index. *J Clin Epidemiol.* 1994;47(11):1245-1251.
24. Eads CA, Danenberg KD, Kawakami K, et al. MethyLight: a high-throughput assay to measure DNA methylation. *Nucleic Acids Res.* 2000;28(8):32e.
25. Henker C, Kriesen T, Ä Glass, Schneider B, Piek J. Volumetric quantification of glioblastoma: experiences with different measurement techniques and impact on survival. *J Neurooncol.* 2017;135(2):391-402.
26. Jacoby A, Wang W, Vu TD, et al. Meanings of epilepsy in its sociocultural context and implications for stigma: findings from ethnographic studies in local communities in China and Vietnam. *Epilepsy Behav.* 2008;12(2):286-297.
27. Klein M, Engelberts NHJ, van der Ploeg HM, et al. Epilepsy in low-grade gliomas: the impact on cognitive function and quality of life. *Ann Neurol.* 2003;54(4):514-520.
28. Eidel O, Burth S, Neumann J-O, et al. Tumor infiltration in enhancing and non-enhancing parts of glioblastoma: a correlation with histopathology. *PLoS One* 2017;12(1):e0169292.

Downloaded from https://academic.oup.com/neurosurgery/article-abstract/85/4/E722/5386559 by Universitaetsbibliothek Rostock user on 28 November 2019

29. Aaslid R, Gröger U, Patlak CS, Fenstermacher JD, Huber P, Reulen H-J. Fluid flow rates in human peritumoural oedema. In: Reulen H-J, Baethmann A, Fenstermacher J, eds. *Brain Edema 8: Proceedings of the Eighth International Symposium, Bern*, June 17–20, 1990. N. Vienna: Springer; 1990;152-154.
30. Seidel C, Dörner N, Osswald M, et al. Does age matter? - A MRI study on peritumoral edema in newly diagnosed primary glioblastoma. *BMC Cancer.* 2011;11(1):127.
31. Toledo M, Sarria-Estrada S, Quintana M, et al. Epileptic features and survival in glioblastomas presenting with seizures. *Epilepsy Res.* 2017;130:1-6.
32. Berendsen S, Varkila M, Kroonen J, et al. Prognostic relevance of epilepsy at presentation in glioblastoma patients. *Neuro Oncol.* 2016;18(5):700-706.
33. Grabowski MM, Recinos PF, Nowacki AS, et al. Residual tumor volume versus extent of resection: predictors of survival after surgery for glioblastoma. *J Neurosurg.* 2014;121(5):1115-1123.
34. Rossi R, Figus A, Corraine S. Early presentation of de novo high grade glioma with epileptic seizures: electroclinical and neuroimaging findings. *Seizure* 2010;19(8):470-474.
35. Sierra S, Ramos MC, Molina P, Esteo C, Vázquez JA, Burgos JS. Statins as neuroprotectants: a comparative in vitro study of lipophilicity, blood-brain-barrier penetration, lowering of brain cholesterol, and decrease of neuron cell death. *J Alzheimers Dis.* 2011;23(2):307-318.

Acknowledgments

The authors thank Prof Günther Kundt for his valuable statistical suggestions and the patients who participated in this study.

Supplemental digital content *is available for this article at www.neurosurgery-online.com.*

Supplemental Digital Content 1. Table. Correlation analyses between tumor compartments and age.
Supplemental Digital Content 2. Table. Patient cohort subdivided by the occurrence of seizures.
Supplemental Digital Content 3. Table. Patient cohort subdivided by the intake of statins.
Supplemental Digital Content 4. Table. Single institute analysis of the influence of clinical and radiological data on seizure incidence.

COMMENTS

This is a retrospective review of 224 IDH wild-type GBMs treated at 2 institutions. This paper correlates various radiographic preoperative tumor characteristics with the likelihood of seizure at diagnosis. In summary, it finds that young patients with smaller tumors that have relatively small areas of central necrosis were more likely to have a seizure as their initial presenting symptom. Interestingly, it also demonstrates a direct correlation between the extent of peritumoral edema and the likelihood of seizure at presentation. These findings in younger patients may help explain the prior association between GBM, seizures, and increased overall survival that has been previously described. Finally, it also postulates that patient statin intake may help prevent seizures due to their downstream systemic anti-inflammatory effects. This can further inform clinicians to make prompt prognostic and treatment decisions based on patient demographics, presentation, and tumor radiographic characteristics.

Joseph Quillin
Jeffrey J. Olson
Atlanta, Georgia

This is an important and well-done retrospective study demonstrating the inverse relationship between the incidence of preoperative seizures in GBM and such variables as patient age and tumor volume at time of diagnosis. Peritumoral edema around small tumors rather than large areas of tumor necrosis correlates with seizure activity because edema represents microscopic invasion rather than gross destruction of tissue and functional nervous tissue is required for seizure activity, ie, the brain seizes and not the tumor. The inverse relationship between seizure incidence and statin intake is an interesting observation of, at present, unknown significance. I would have wanted to see statistical comparisons at the extremes of patient age using 40 or 45 years as the breakpoint in addition to 60 years. Differences in OS between patients in their sixties and those older than seventy are unlikely to be revelatory but the use of statins in patients under 40 or 45 is bound to be much different from that found in older patients. It would be very interesting to know whether statins confer any additional advantage in younger patients with GBM above and beyond the advantages due to the biology of the tumor alone.

Michael Salcman
Baltimore, Maryland

Downloaded from https://academic.oup.com/neurosurgery/article-abstract/85/4/E722/5386559 by Universitaetsbibliothek Rostock user on 28 November 2019